PTB mitteilungen 2 2015

Traceable Dynamic Measurement of Mechanical Quantities



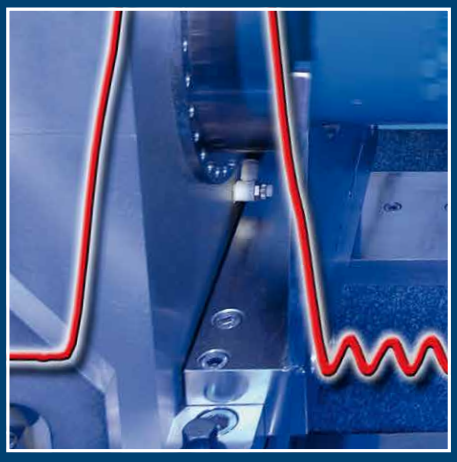
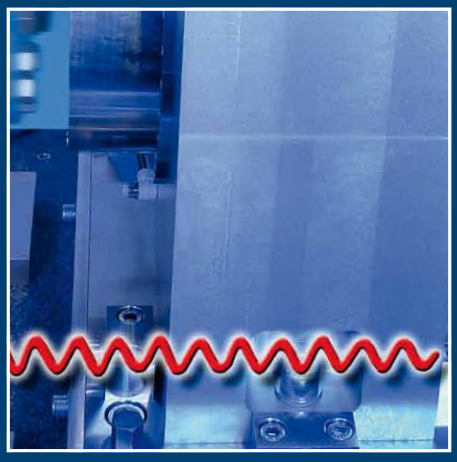
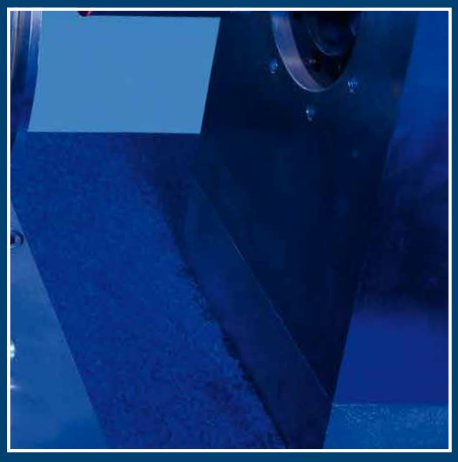

Physikalisch-Technische Bundesanstalt ■ Braunschweig and Berlin

National Metrology Institute

PTB mitteilungen

Traceable Dynamic Measurement of Mechanical Quantities

Cover picture:
The cover picture shows a measuring device of PTB for the shock calibration of force transducers, and a measured force signal. (Source of picture: PTB)

PTB mitteilungen

Special Journal for the Economy and Science
Official Information Bulletin of the Physikalisch-Technische Bundesanstalt
Braunschweig and Berlin

Volume 125 (2015), No. 2

Contents

Dynamic Measurement of Mechanical Quantities

Vorwort des Herausgebers

Die Physikalisch-Technische Bundesanstalt spielt auf sehr unterschiedlichen Bühnen: auf der nationalen, der europäischen und der weltweiten Bühne. Da die Metrologie eine weltumspannende Angelegenheit ist, ist dies auch nur folgerichtig. Für ein Fachjournal wie die PTB-Mitteilungen, das sich metrologische Themen als Schwerpunkte setzt, bedeutet dies zwangsläufig auch eine Internationalisierung. Eben davon zeugt diese Ausgabe, die Fachaufsätze als Ergebnisse des europäischen Forschungsprojekts *Traceable Dynamic Measurement of Mechanical Quantities* versammelt. Dieses Projekt wurde von der EU im Rahmen des Europäischen Metrologieforschungsprogramms (EMRP) gefördert und startete im September 2011. Vier Jahre später liegt nun ein ganzer Strauß von Ergebnissen vor, die hier erstmals an einem Ort zusammengetragen sind.

In zwei Fällen sind die Aufsätze bereits in anderen Fachjournalen publiziert – die entsprechenden Zitate sind bei den Beiträgen angegeben. Diese PTB-Mitteilungen versuchen einen Mehrwert in Form dieser Zusammenschau zu generieren. Und da dieser Mehrwert keine nationale Größe, sondern eine europäische Größe sein soll (zu erkennen an den Beiträgen der Gastautoren des NPL und der Firma HBM), ist die Publikationssprache in dieser Ausgabe durchweg Englisch. Da solche EMRP-Projekte zahlreich sind und die PTB als das größte Nationale Metrologieinstitut Europas bei fast allen dieser Projekte eine wichtige Rolle spielt, werden die PTB-Mitteilungen in Zukunft sicher immer mal wieder als englischsprachiges Journal erscheinen. Es würde mich freuen, wenn Sie die PTB-Mitteilungen auf diesen gelegentlichen Wegen der Europäisierung weiterhin mit Interesse begleiten.

Jens Simon, Pressesprecher PTB

Foreword by the Editor

The Physikalisch-Technische Bundesanstalt is a player on the most diverse fronts: on the national, the European and the global front. This is only logical – seeing that metrology (PTB's field of work) is of global concern. For a scientific journal such as the PTB-Mitteilungen, which focuses on topics of metrology, this inevitably calls for internationalization. Precisely this has been taken into account with this issue which has collected scientific papers as the findings of the European research project *Traceable Dynamic Measurement of Mechanical Quantities*. This project was funded by the EU within the framework of the European Metrology Research Programme (EMRP) and was launched in September 2011. Now, four years later, there is a full spectrum of findings which have been compiled here at one place for the first time.

In two cases, the articles have already been published in other scientific journals – the corresponding quotes have been stated in the articles. This edition of PTB-Mitteilungen tries to generate additional value in the form of this synopsis. And since this additional value is not to be of national importance, but rather of European importance (seen by the articles by the guest authors from NPL and the HBM company), the issue was published throughout in English. Since such EMRP projects are numerous and PTB, as the largest national metrology institute in Europe, plays an important role in almost all of these projects, PTB-Mitteilungen will in future certainly be published as an English-language journal every now and then. I would be pleased if you would continue to show interest in PTB-Mitteilungen along these occasional paths of Europeanization.

Jens Simon, Press Officer of PTB

European Research Project for the Dynamic Measurement of Mechanical Quantities

Michael Kobusch*, Thomas Bruns

* Dr. Michael Kobusch, Working Group "Impact Dynamics", PTB, e-mail: michael.kobusch@ptb.de

Abstract

This first article of this issue of PTB-Mitteilungen presents an overview of the research project IND09 *Traceable Dynamic Measurement of Mechanical Quantities*, in which a total of nine national metrology institutes participated to provide traceability to the dynamic measurement of the three mechanical quantities, force, pressure and torque. The work was focused on developing traceable dynamic calibration methods, mathematical modelling, and evaluation of measurement uncertainty, considering both mechanical sensors as well as the complementary electrical amplifiers. This project began in September 2011 and lasted three years, and was supported by the European Metrology Research Programme of the European Union.

1 Introduction

In many industries such as automotive, aerospace, wind power plants, manufacturing, medicine, industrial automation and control, dynamic measurements of mechanical quantities are tasks consistently applied today. Moreover, together with an increased number of dynamic measurement applications, the quality of the measurements is a very important aspect.

Although many measurements of the three magnitudes force, pressure and torque are performed under dynamic conditions, current transducers and amplifiers are calibrated statically. There are still no specific standards or guidelines for the dynamic calibration of these quantities.

It is well known that various mechanical transducers have a specific dynamic behaviour where the sensitivity under dynamic input load deviates from the static value. Also, the various electrical components of the measuring chain may have an additional frequency response that has to be taken into account for accurate and reliable measurements.

To advance the dynamic metrology, nine European national metrology institutes participated in a research project dedicated to traceable dynamic measurement. This project IND09 was entitled *Traceable Dynamic Measurement of Mechanical Quantities* and was funded by the European Metrology Research Programme (EMRP) in the European Union with 46 % of a total volume of nearly 3.6 million euros. The project started in September 2011 and lasted three years.

The project aimed to develop and provide the future basis of traceability for dynamic measurements. To achieve this goal, it was necessary to develop and investigate various dynamic calibration facilities, their mechanical and electrical components, to develop the corresponding mathematical model and to estimate the associated measurement uncertainty.

The investigations were focused on the traceability of the dynamic responses of different transducers, as well as the corresponding electrical instrumentation for conditioning, amplification and data acquisition. With respect to the dynamic calibration, excitations with sinusoidal signals and shocks have been investigated to study wide ranges of amplitude and frequency.

2 Work Packages

The project was structured into seven work packages (WPs), of which four were technical, one was interdisciplinary and two were administrative in nature:

- WP 1: Dynamic force
- WP 2: Dynamic pressure
- WP 3: Dynamic torque
- WP 4: Amplifiers
- WP 5: Mathematics and statistics
- WP 6: Impact
- WP 7: Coordination

The coordination and interaction among the various work packages are illustrated in figure 1.

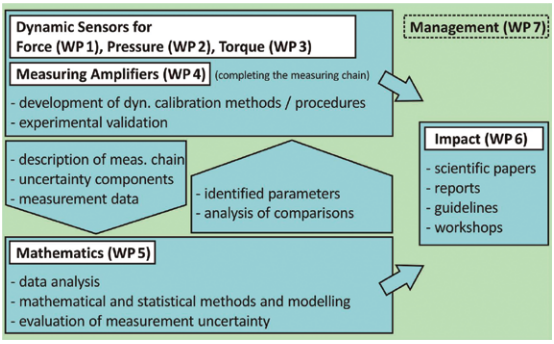

Figure 1:
Interaction between work packages [1].

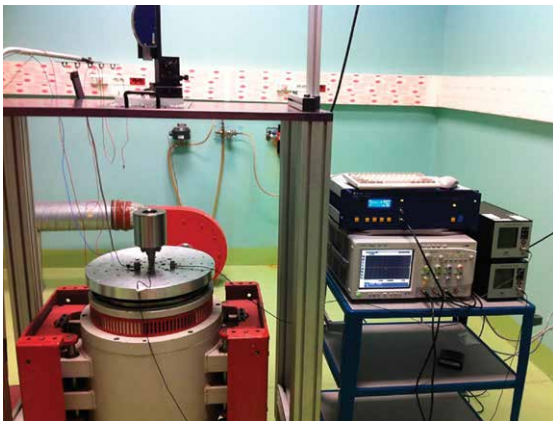

Figure 2:
Calibration device for sinusoidal forces at CEM.

The following sections provide a brief summary of the issues and activities in the work packages, with special emphasis on the dynamic force as an example.

2.1 Dynamic force (WP 1)

This work package focused on measuring the dynamic force using two types of excitation, sinusoidal excitation tests in the institutes PTB (Germany), LNE (France) and CEM (Spain), and with shocks (PTB). WP 1 was coordinated by PTB.

Several transducers of different designs and physical principles were selected for the tests: resistive sensors (based on strain gauges) and piezoelectric sensors, measuring ranges from 1 kN to 30 kN, suitable for tensile and compressive forces.

For the calibration with sinusoidal forces [2, 3], each of the participants used their own device employing an electrodynamic shaker and a load mass mounted on top of the transducer under calibration. As an example, the corresponding device of the Spanish metrology institute CEM is presented in figure 2.

When this mechanical system vibrates, the mass loading generates a dynamic force according to Newton's second law: force is the product of mass and acceleration. The measurement of this inertial force acting on the top of the transducer provides the reference for the dynamic calibration. This measurement is based on the determination of the mass and the acceleration measurement using laser vibrometers or accelerometers. Thus traceability is achieved by a primary method [4].

The result of the sinusoidal calibration is the frequency response of the complex sensitivity (magnitude and phase) defined as the ratio between the output signals of the transducer under calibration and the reference force (proportional to the acceleration).

This mechanical system, into which the sinusoidal excitation is introduced at the base of the force transducer, has a characteristic resonance because of the elastically coupled load mass. The elasticity may be considered as an inherent property of the force transducer, assuming that the two couplings on each side of the transducer, that is, to the loading mass and the vibrating platform, are rigid. This is reasonable as the components are firmly screwed.

As an example, figure 3 shows the measurement of the resonance of the force transducer HBM U9B / 1 kN which is coupled to a load mass of 1 kg. It is noted that the ratio of accelerations of the load mass and the vibrating platform can exceed the value of 400, which means that the damping of this system is considerably small.

This dynamic behaviour can be described by a mass-spring-damper system of one degree of freedom (linear displacement x). Figure 4 illustrates the basic model of a force transducer with a rigidly mounted load mass m. The transducer consists of two point masses (m_H and m_B) connected by an elastic spring (stiffness k) and a viscous damper (constant d). The masses designate the top and bottom part of the force transducer, i.e. the head and base. The transducer output signal is considered to be proportional to the elongation of the measuring spring. The base of the transducer is fixed to the top of the shaker's vibrating armature.

Calibration with shock excitation has been another objective of the theoretical and experimental investigations [5–8]. This method offers the advantage of the easy generation of larger forces and spectral contents at higher frequencies. Of course, the peak force should never exceed the specified working range of the transducer under

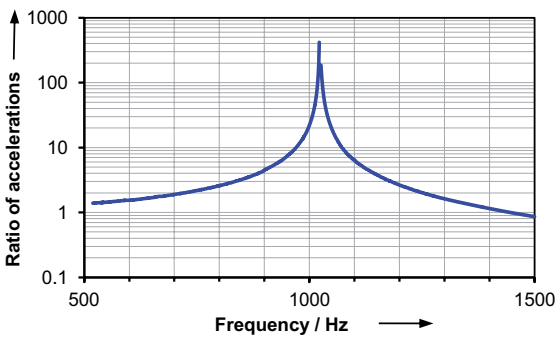

Figure 3:
Mechanical resonance of the transducer HBM U9B / 1 kN loaded with 1 kg.

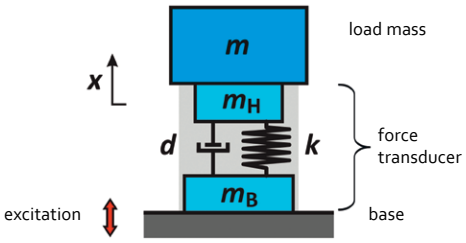

Figure 4:
Model of a force transducer applied in the sinusoidal calibration device.

calibration. Calibration devices for shock forces only exist at PTB, so far. A shock calibration device using two cubic mass bodies of 10 kg is depicted in figure 5. Its working principle is illustrated in figure 6.

The mass body on the right side of the figure is impacting onto the transducer under calibration which is mounted at the mass body on the left. A linear air bearing is used to guide the mass bodies in order to minimize friction. Again, the traceability of the dynamic force is achieved by means of laser vibrometers measuring the acceleration of the two mass bodies in the direction of the common axis of movement.

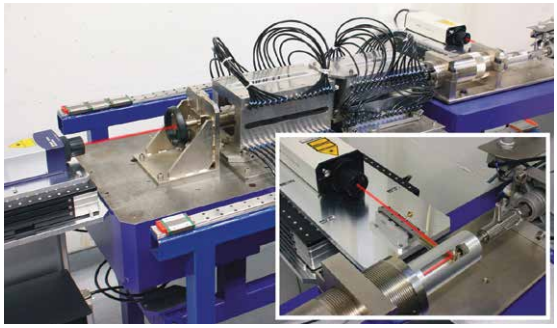

Figure 5:
Calibration device for shock forces up to 20 kN at PTB.

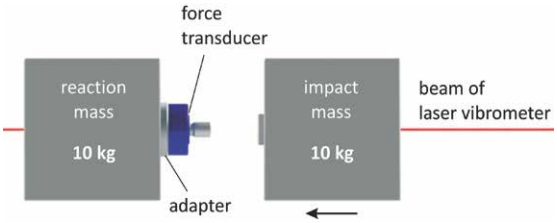

Figure 6:
Schematic drawing of the primary shock force calibration.

Typical examples of shock force signals measured with two resistive transducers of different design are shown in figure 7. The left signal was obtained with a transducer of a total mass (including the adapter) of 1.5 kg. The impact of the mass of 10 kg resulted in a pulse width of 0.7 ms followed by a strong oscillation. The main pulse shows superposed vibrations during the time of the actual contact.

The identification of the force transducer's parameters was performed using an expanded model [6], which also takes into account the potential elastic couplings. The results show that the strong vibration is caused by the inner mass m_H acting on the measuring spring of stiffness k.

In contrast to this response, the second example (figure 7b) obtained with a transducer of only

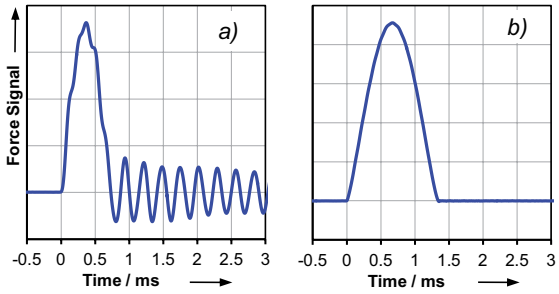

Figure 7:
Measured shock forces:
a) Interface 1610 / 2.2 kN, b) HBM U9B / 1 kN.

0.063 kg shows a smooth pulse of 1.3 ms without noticeable superposed vibration. Obviously, the impact obtained with a mass of 10 kg is not able to excite the resonance of the transducer. Theoretical studies show that the parameter identification requires the excitation of resonances to provide the key information for the determination of the system's dynamic behaviour. A method to increase the spectral content at higher frequencies and to excite the transducer's resonance modes is the use of a smaller impact mass which generates shorter pulses. Various experimental tests have shown that a pulse of 0.1 ms is sufficiently short to excite resonances even of the small transducer [7].

To facilitate the transfer of the various dynamic calibration results, the method of the model-based calibration is proposed. The dynamic response of a transducer under calibration is described by a model, and its characteristic parameters are identified using the measured data. With respect to the model above, the transducer is characterized by the four parameters m_H, m_B, k, d. If the elasticity of the coupling to its mechanical environment cannot be neglected, the model will present additional parameters.

In general, models of more complex structures can be derived from the basic model in order to describe the various devices and mechanical couplings. For this purpose, the appropriate secondary conditions such as external excitations have to be applied, e.g. the vibration of the transducer base to generate sine forces, and other mass-spring-damper components might be added to have more degrees of freedom, if necessary.

At the end, the results obtained with different devices and different excitation methods [9] are compared. The dynamic behaviour of a transducer under calibration can be considered understood correctly if the respective models result in consistent parameters even under different measurement conditions (different load masses, accelerations and frequencies, amplitudes and pulse widths, etc.). This knowledge is required to assess the uncertainty associated with the dynamic measurement. Preliminary results show that further research is needed to understand the dynamic

behaviour of the various mechanical designs of the force transducers and their coupling to the calibration devices.

2.2 Dynamic pressure (WP 2)

This work package, which was led by NPL, was dedicated to the measurement of dynamic pressure investigating the following two methods:

A. Shock tube:
NPL (UK), SP (Sweden)

B. Drop weight:
PTB, MIKES (Finland), UME (Turkey)

The first method uses a shock tube to generate pressure steps in a tube filled with gas at low pressure. The device consists of a closed system of two tubes which are connected by a thin membrane (figure 8). To generate a step with a short rise time, the pressure is built up in the first section until the membrane breaks, causing a compression wave front which propagates along the second section with hypersonic speeds. The high speed results in a rapid increase in pressure in less than a microsecond. This resulting step is the input signal to the device under calibration which is located at the far end of the low pressure section.

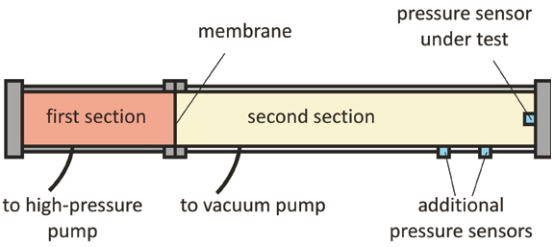

Figure 8:
Schematic drawing of a shock tube.

Figure 9 shows a shock tube made of plastic tubes used for the tests at NPL. The first section (high pressure) measures 0.7 m in length and the second (low pressure) 2 m.

The shock tubes within the project have been investigated in various aspects [10, 11], among them the characterization of the devices, the influence of the material onto which the sensor under calibration is mounted, the modelling of the gas shock and the sensor, and the measurement of the reference signal by means of a laser vibrometer.

The second method for the dynamic calibration of pressure transducers uses a drop weight system to generate pressure pulses in the range of a few hundred megapascals and a few milliseconds duration. For this purpose, a mass body is dropped from a given height to impact onto the piston of a high-pressure chamber. The impact force drives the piston into to a small internal cavity filled with a hydraulic fluid and thus generates a pressure pulse. The sensors under calibration are connected to this cavity through thin holes.

Figure 9:
Shock tube at NPL.

The collaborating NMIs pursue different procedures for measurement traceability. While UME uses its device only for secondary calibrations, PTB and MIKES made some progress in establishing traceability with primary methods.

The metrologists at MIKES have investigated the device illustrated in figure 10, where traceability is obtained by measuring the dynamic motion of the piston using an accelerometer or a laser vibrometer.

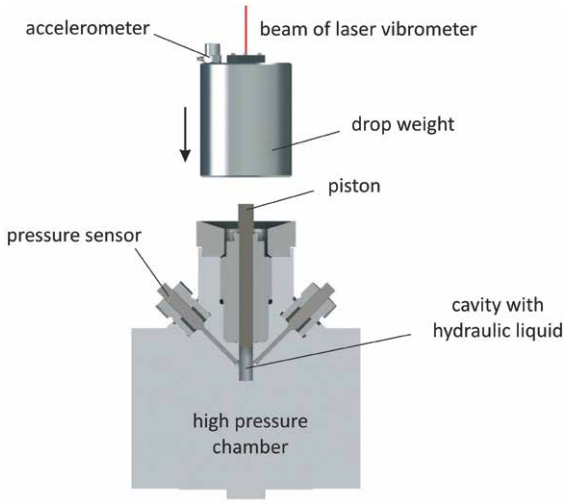

Figure 10:
Schematic drawing of the dynamic pressure calibration device at MIKES.

Figure 11 shows the device that has been developed at PTB [12]. The beam of a laser vibrometer passes through the cavity with the hydraulic fluid and is retro-reflected. The dynamic pressure instantaneously affects the density of the liquid resulting in a change of its refractive index, which means that the laser vibrometer detects a variation of displacement. By means of a static calibration to determine the relationship between pressure and refractive index, this optical method may provide traceability to dynamic pressure using primary methods.

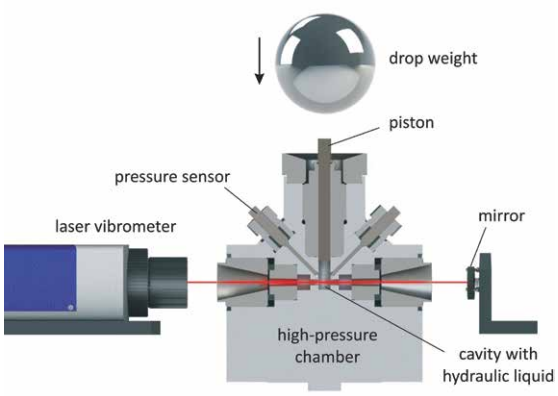

Figure 11:
Schematic drawing of the dynamic pressure calibration device at PTB.

2.3 Dynamic torque (WP 3)

The third work package involved only CMI (Czech Republic) and PTB. The German institute coordinated and performed the majority of the activities.

The work focused on the investigation of methods and procedures for the calibration of torque transducers with sinusoidal torque. The metrologists at PTB developed a device with a rotary vibration exciter to excite torsional oscillations up to 500 Hz and a maximum range of 20 N·m (figure 12).

Figure 12:
Device for dynamic torque calibration at PTB.

Dynamic traceability is achieved with a primary method in the same way as explained above for sinusoidal force applying Newton's second law for rotation, wherein the torque is defined as the product of moment of inertia and angular acceleration.

The torque transducer under calibration is coupled to the rotational exciter (below) and the moment of inertia (above) by means of clamping sleeves. The angular accelerations at both sides were measured by means of a rotational vibrometer and the built-in angular acceleration sensor of the exciter.

Similar to the procedures in dynamic force, the modelling of the rotational device and the torque transducer is performed with a corresponding rotational mass-spring-damper system [13]. To determine the parameters of the various mechanical components which are included in this model, three dedicated devices were developed to measure the moment of inertia, rotational stiffness and damping [14, 15].

2.4 Amplifiers (WP 4)

The institutes PTB (coordination) and NPL were involved in this work package.

In general, it is required to know the dynamic behaviour of the various electrical components of the measuring chain in addition to those of the sole transducer. Assuming a minimum range of 10 kHz which is desired for the dynamic measurement of the considered mechanical magnitudes, the typical instrumentation may have a frequency response that should not be neglected. The activities in this WP have focused on the dynamic characterization of the following components.

A. Bridge amplifiers for resistive sensors like strain gauges.

B. Charge amplifiers for piezoelectric sensors.

For the dynamic calibration of bridge amplifiers, both institutes developed their own dynamic calibration standard that is able to provide an adequate reference input signal.

The operation principle of PTB's dynamic bridge calibration standard is illustrated in the simplified scheme of figure 13. Like a strain gauge transducer, the instrument provides a ratiometric output signal U_0 with respect to the supply voltage U_i of the bridge amplifier. It is capable of generating arbitrary dynamic signals from zero to more than 10 kHz using two MDACs (multiplying digital-to-analogue converter). More detailed information about this device is found in [16, 17].

Figure 14 shows the result of a dynamic calibration of a bridge amplifier showing the frequency response in magnitude and phase.

Further research within the project on the calibration of charge amplifiers has shown that

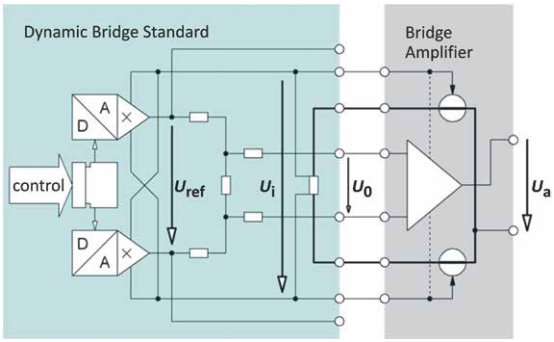

Figure 13:
Schematic diagram of PTB's dynamic bridge standard.

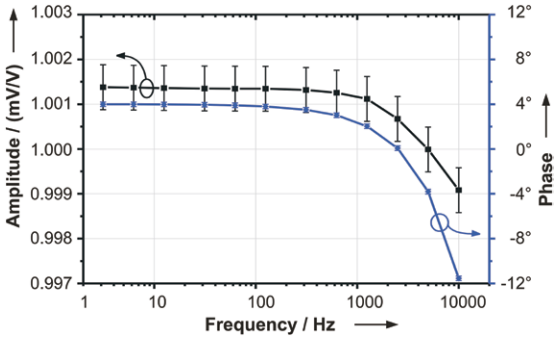

Figure 14:
Frequency response (magnitude and phase) of a bridge amplifier.

significant errors can occur at high frequencies because of the difference of the source impedances of the piezoelectric sensor under calibration and the charge standard [18].

2.5 Mathematics and statistics (WP 5)

Four national institutes participated in this interdisciplinary work package: PTB, NPL, LNE and INRIM (Italy). The work was coordinated by PTB and NPL, depending on the tasks.

Previous work [19–21] on the calibration of accelerometers already paved the way for the proposed dynamic calibration method using a model-based calibration, which is applied to the mechanical parameters of this project.

The math work package supported the four technical packages WP 1–4 in analysing the data, modelling the mechanical systems, identifying and determining the parameters of the dynamic models, and developing methods of measurement uncertainty evaluation. Several studies with emphasis on mathematics have been developed, e.g. [22–25], considering the mathematical description, identification procedures, fitting methods, statistical analysis, filtering or the deconvolution of data [26].

Figures 15 and 16 show two examples of collaboration in the field of shock force calibration. In the context of the identification of the parameters of a force transducer, the first example compares the measured force signal to the calculated responses using three models of different degrees of freedom. The second example displays a spectral analysis of shock-excited vibrations in order to elaborate suitable models.

2.6 Impact (WP 6)

The dissemination of the results produced in a JRP is an important task within the EMRP and, therefore, was dedicated to an extra work package led by LNE.

The work of this joint research project has been presented at metrology conferences, particularly those of IMEKO and the Workshop on Analysis of Dynamic Measurements, and in journals and reports. In addition, participation in committees and working groups, e.g. [27, 28], has already provided progress in developing future standards in the dynamic measurement of mechanical quantities.

The project website [29] and the web repositories of the EMRP and the conferences offer free access to most of the work.

3 Conclusions

With the support of the research programme EMRP of the European Union, the joint project made extensive progress in the field of dynamic measurement of the three quantities force, pressure and torque.

For the first time in this field of metrology, joint international research has been conducted in dynamic measurement. New devices and methods for the dynamic calibration with primary traceability methods have been developed in several national institutes, which are the key requirements for future dynamic calibrations. In addition, first comparisons have been performed in dynamic force and dynamic pressure. To understand the dynamic behaviour, the method of model-based calibration is proposed in this project.

The work has given great impetus to the European metrology community to continue the chosen way, which finally will result in specific rules and guidelines to disseminate the dynamic procedures to the industrial users.

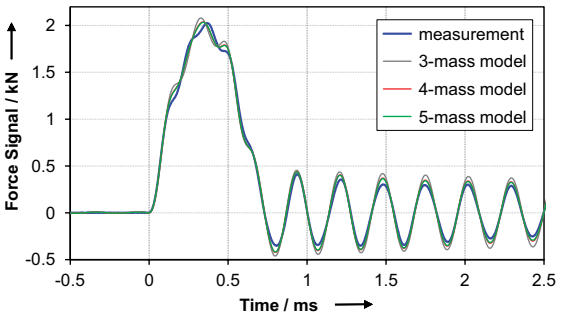

Figure 15:
Comparison of measured and modelled shock force responses.

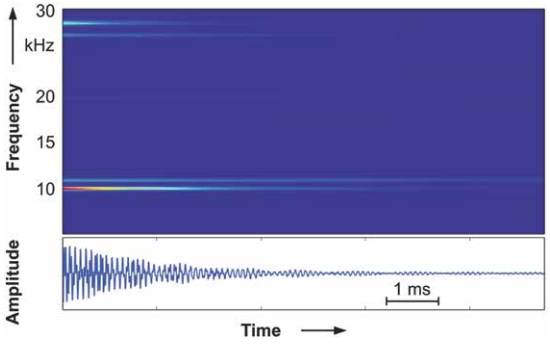

Figure 16:
Spectrogram of excited vibrations in shock force calibration.

Acknowledgements

This work was supported by the European Metrology Research Programme (EMRP). The EMRP is jointly funded by the EMRP participating countries within EURAMET and the European Union.

References

[1] C. Bartoli, M. F. Beug, T. Bruns, C. Elster, T. Esward, L. Klaus, A. Knott, M. Kobusch, S. Saxholm and C. Schlegel, *Traceable Dynamic Measurement of Mechanical Quantities: Objectives and First Results of this European Project*, International Journal of Metrology and Quality Engineering, 3, pp. 127–135, 2012.

[2] C. Schlegel, G. Kieckenap, B. Glöckner, A. Buß and R. Kumme, *Traceable Periodic Force Measurement*, Metrologia, 49, pp. 224–235, 2012.

[3] N. Medina, J. L. Robles and J. de Vicente, *Realization of Sinusoidal Forces at CEM*, IMEKO TC3, TC5 and TC22 International Conference, Cape Town, South Africa, 2014.

[4] *International Vocabulary of Metrology – Basic and General Concepts and Associated Terms* (*VIM*), 3rd edition, JCGM, 2008.

[5] M. Kobusch, L. Klaus and T. Bruns, *Model-based Analysis of the Dynamic Behaviour of a 250 kN Shock Force Calibration Device*, XX IMEKO World Congress, Busan, Republic of Korea, 2012.

[6] M. Kobusch, *Influence of Mounting Torque on Stiffness and Damping Parameters of the Dynamic Model of a 250 kN Shock Force Calibration Device*, 7th Workshop on Analysis of Dynamic Measurement, Paris, France, 2012.

[7] M. Kobusch, S. Eichstädt, L. Klaus and T. Bruns, *Investigations for the Model-based Dynamic Calibration of Force Transducers by Using Shock Excitation*, ACTA IMEKO, 4 (2), pp. 45–51, 2015.

[8] M. Kobusch, S. Eichstädt, L. Klaus and T. Bruns, *Analysis of Shock Force Measurements for the Model-based Dynamic Calibration*, 8th Workshop on Analysis of Dynamic Measurement, Turin, Italy, 2014.

[9] M. Kobusch, A. Link, A. Buss and T. Bruns, *Comparison of Shock and Sine Force Calibration Methods*, IMEKO TC3, TC16 and TC22 International Conference, Mérida, Mexico, 2007.

[10] S. Downes, A. Knott and I. Robinson, *Determination of Pressure Transducer Sensitivity to High Frequency Vibration*, IMEKO TC3, TC5 and TC22 International Conference, Cape Town, South Africa, 2014.

[11] S. Downes, A. Knott and I. Robinson, *Towards a Shock Tube Method for the Dynamic Calibration of Pressure Sensors,* Hopkinson Centenary Conference, Philosophical Transactions A, 4, 2014.

[12] T. Bruns, E. Franke and M. Kobusch, *Linking Dynamic to Static Pressure by Laser Interferometry*, Metrologia, 50, pp. 580–585, 2013.

[13] L. Klaus, B. Arendacká, M. Kobusch and T. Bruns, *Dynamic Torque Calibration by Means of Model Parameter Identification*, ACTA IMEKO, 4 (2), pp. 39–44, 2015.

[14] L. Klaus, T. Bruns and M. Kobusch, *Modelling of a Dynamic Torque Calibration Device and Determination of Model Parameters*, ACTA IMEKO, 3 (2), pp. 14–18, 2014.

[15] L. Klaus and M. Kobusch, *Experimental Method for the Non-Contact Measurement of Rotational Damping*, IMEKO TC3, TC5 and TC22 International Conference, Cape Town, South Africa, 2014.

[16] M. F. Beug, H. Moser and G. Ramm, *Dynamic Bridge Standard for Strain Gauge Bridge Amplifier Calibration*, Conference on Precision Electromagnetic Measurements (CPEM), 568–569, 2012.

[17] C. Bartoli, M. F. Beug, T. Bruns, S. Eichstädt, T. Esward, L. Klaus, A. Knott, M. Kobusch and C. Schlegel, *Dynamic Calibration of Force, Torque and Pressure Sensors*, IMEKO TC3, TC5 and TC22 International Conference, Cape Town, South Africa, 2014.

[18] H. Volkers and T. Bruns, *The Influence of Source Impedance on Charge Amplifiers*, ACTA IMEKO, 2 (2), pp. 56–60, 2013.

[19] A. Link, A. Täubner, W. Wabinski, T. Bruns and C. Elster, *Calibration of Accelerometers: Determination of Amplitude and Phase Response upon Shock Excitation*, Measurement Science and Technology, 17, pp. 1888–1894, 2006.

[20] A. Link, A. Täubner, W. Wabinski, T. Bruns and C. Elster, *Modelling Accelerometers for Transient Signals Using Calibration Measurements upon Sinusoidal Excitation*, Measurement, 40, pp. 928–935, 2007.

[21] C. Elster and A. Link, *Uncertainty Evaluation for Dynamic Measurements Modelled by a Linear Time-invariant System*, Metrologia, 45, pp. 464–473, 2008.

[22] C. Matthews, F. Pennecchi, S. Eichstädt, A. Malengo, T. Esward, I. Smith, C. Elster, A. Knott, F. Arrhen and A. Lakka, *Mathematical Modelling to Support Traceable Dynamic Calibration of Pressure Sensors*, Metrologia, 51, pp. 326–338, 2014.

[23] A. Malengo and F. Pennecchi, *A Weighted Total Least Squares Algorithm for any Fitting Model with Correlated Variables*, Metrologia, 50, pp. 654–662, 2013.

[24] B. Arendacká, A. Täubner, S. Eichstädt, T. Bruns and C. Elster, *Linear Mixed Models: GUM and Beyond, Measurement Science Review*, 14 (2), pp. 52–61, 2014.

[25] S. Eichstädt, A. Link, P. Harris and C. Elster, *Efficient Implementation of a Monte Carlo Method for Uncertainty Evaluation in Dynamic Measurements*, Metrologia, 49, pp. 401–410, 2012.

[26] S. Eichstädt, C. Elster, T. J. Esward and J. P. Hessling, *Deconvolution Filters for the Analysis of Dynamic Measurement Processes: A Tutorial*, Metrologia, 47, pp. 522–533, 2010.

[27] T. Eswards, *Current and Future Challenges in Modelling and Simulation of Measuring Systems*, VDI/VDE-GMA FA 1.10 Grundlagen der Messsysteme, Frankfurt, Germany, 2012.
[28] A. Schäfer, *Challenges in Dynamic Torque and Force Measurement with Special Regard to Industrial Demands*, BIPM Workshop on Challenges in Metrology for Dynamic Measurement, 2012.
[29] http://projects.ptb.de/emrp/279.html. (Retrieved: 2015-08-11).

Dynamic Torque Calibration

Leonard Klaus*

* Leonard Klaus, Working Group "Impact Dynamics", PTB, e-mail: leonard.klaus@ptb.de

1 Introduction

The demand from industry for dynamic torque calibration has significantly increased over the past years. However, dynamic torque calibrations are not available at present and the respective research activities have started only a few years ago. As part of the European Metrology Research Programme (EMRP), research in dynamic torque calibration took part in work package 3 *Dynamic Torque* of the joint research project IND09 *Traceable Dynamic Measurement of Mechanical Quantities*.

2 Definition of the Unit Torque

The International System of Units (SI) [1] defines the torque M as a derived unit given by the cross product of the position vector $\vec{r}$ and the force vector $\vec{F}$:

$$\vec{M} = \vec{r} \cdot \vec{F} . \quad (1)$$

Maybe easier to understand is the simplified scalar representation as a force F acting on a lever arm of length l, which leads to

$$M = l \cdot F . \quad (2)$$

The unit of torque is newton metres (N·m).

3 Design of Torque Transducers

The vast majority of torque transducers used in dynamic applications and for high-precision measurements are based on strain gauges. Strain gauge torque transducers have a specific mechanical design consisting of rigid components and of compliant measuring elements at which the strain gauges are located. In case of a change of the applied torque load, the measuring element's deflection will change and the strain gauges will detect a change in the surface strain. The mechanical elongation of a strain gauge proportionally changes its electrical resistance. Usually, four strain gauges are electrically connected to a full Wheatstone bridge circuit in order to compensate for temperature drift and to obtain an output signal with a good signal-to-noise ratio, which is proportional to the applied load. The output voltage of such a bridge circuit is conditioned by a bridge amplifier. Based on the transducer, this amplifier can be included in integrated electronics. The traceable dynamic calibration of bridge amplifiers is described in a dedicated contribution in this issue [pp. 52–61].

In general, two easily distinguishable structural designs of strain gauge torque transducers can be found: shaft-type transducers and flange-type transducers. The two types are depicted in figure 1.

The classic shaft-type transducer consists of a cylindrical shaft with specific structural parts of reduced stiffness used for the strain measurement. The measuring elements can be carried out as a tapered solid shaft, a hollow shaft or as a cage shaft as displayed in the figure.

Flange type transducers have a much shorter design with larger diameters. They possess a significantly higher torsional stiffness and mass moment of inertia than shaft-type transducers. The shear elements at which the strain is picked up are positioned between the two flanges, and are exposed to radial or axial strain.

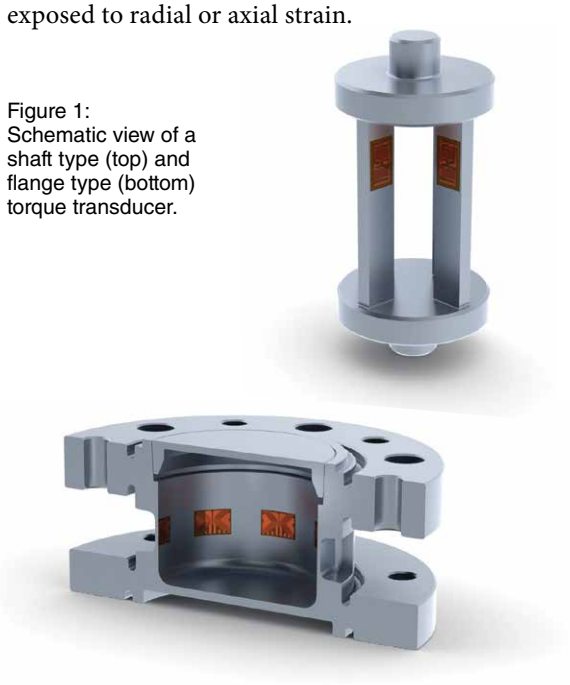

Figure 1: Schematic view of a shaft type (top) and flange type (bottom) torque transducer.

4 Applications with Dynamic Torque Excitation

The demand for research on the traceable dynamic calibration of torque transducers comes from two main applications with dynamic torque signals.

4.1 Impulse wrenches

Screw connections in industrial assembly lines are often fastened by impulse wrenches. For safety-relevant screw connections, the traceable measurement of the fastening torque is required.

Impact wrenches fasten the screw connection by applying a sequence of short impulses generated by the release of a pressurized hydraulic fluid. The operator's exposition to the high fastening torque is limited due to the steepness of the pulses and the tools' inertia. The measurement of a typical torque pulse is shown in figure 2. The pulse duration of impulse wrenches is in the range of milliseconds which results in an associated frequency content of several hundred hertz. The fastening torque can amount up to one kilonewton metre.

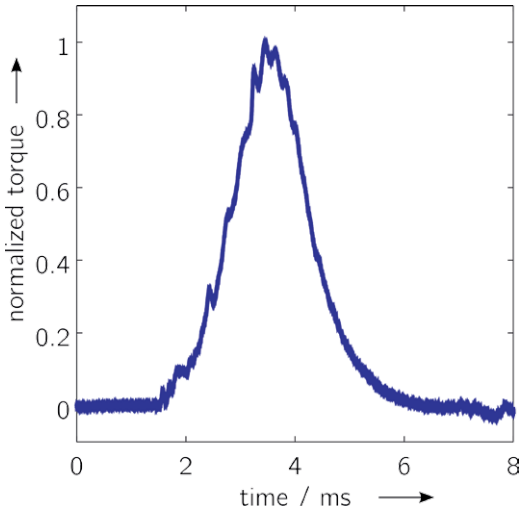

Figure 2:
Torque output of an impulse wrench.

4.2 Motor test rigs

The output of electric motors and internal combustion engines (ICE) is analyzed in research and development, but for type-approval as well. The mechanical power P transferred by a rotating shaft can be measured by means of the rotational speed n and the torque M as

$$P = n \cdot M \,. \qquad (3)$$

This relationship is often used for the mechanical output power measurement of the aforementioned electric motors as well as of ICEs. The output torque level of both types does not only contain static components. ICEs rather generate a highly fluctuating torque output due to their working principle with several strokes and combustion processes, where the dynamic torque components can range in the same magnitude as the mean torque level.

Figure 3:
Test bench for electric motors.

The frequency content of the dynamic torque components can be up to the kilohertz range, and the respective torque amplitude can be up to some kilonewton metres. In the case of electric drives, strong dynamic components in the torque output can be caused by the electronic frequency converters, which are used to control the rotational speed and the torque output of synchronous and asynchronous electric motors. The dynamic components are usually smaller than those of ICEs, however, they can be in the range of several per cent of the mean torque. Both frequency content and mean torque level are comparable to ICEs. A typical test rig for electric motors is shown in figure 3. The measured torque output of a synchronous electric motor is depicted in figure 4.

5 State of the Art in Torque Calibration

At present, commonly accepted methods for a dynamic calibration of torque transducers, or even documentary standards, do not exist. All torque transducers that are used in the above-mentioned

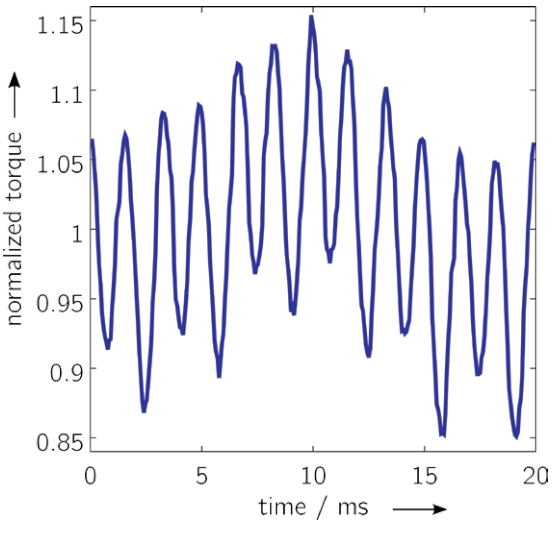

Figure 4:
Torque output of a synchronous electric motor (courtesy of Working Group 3.52 of PTB).

applications with dynamic torque signals are calibrated only statically.

Static torque calibrations can be carried out in a wide torque range and with small measurement uncertainties. For a precise primary static torque calibration, deadweight facilities are used. A deadweight with the mass m is connected to a lever arm of a known length l. With the known local gravitational acceleration g_{loc}, equation 2 leads to

$$M = l \cdot m \cdot g_{loc} . \quad (4)$$

However, in reality, the air density has to be compensated and many more influences have to be taken into account. A detailed overview of the realization of the static torque can be found in [2].

6 Measurement Principle for the Dynamic Torque Calibration

The primary dynamic calibration is based on Newton's second law. The generated dynamic torque $M(t)$ equals the mass moment of inertia J times the time-dependent angular acceleration $\ddot{\varphi}(t)$, and it holds

$$M(t) = J \cdot \ddot{\varphi}(t) . \quad (5)$$

A dedicated dynamic torque measuring device based on this principle was developed and commissioned at PTB [3]. At the beginning of the joint research project, the dynamic torque device was improved by installing a new exciter and a larger air bearing with higher capacity.

The design and the components of the measuring device are depicted in figure 5. The device consists of a freely rotatable vertical drive shaft at which all components are arranged in series. At the bottom, a rotational exciter is mounted on a platform which can be moved vertically. Attached to the exciter is the transducer under test (device under test, DUT), which is mounted between two single cardanic couplings on both sides. These couplings are torsionally stiff, but compliant for bending to reduce parasitic lateral forces and bending moments. At the top end of the drive shaft, an arrangement is mounted of a radial grating disk (which is used for the incremental angle measurement) and of an air bearing (which enables low-friction support of the components). The angle position at the top is measured by interferometric methods and afterwards converted to the angular acceleration. The two laser beams of a rotational vibrometer pass through the radial grating disk at diametrically opposed positions and get diffracted. The first order of diffraction of the beam is coupled back into the vibrometer. When a grating line passes the beam, a phase shift of 2π will be detected.

The angular acceleration at the bottom of the drive shaft is measured by an angular accelerometer which is embedded in the rotor of the rotational exciter. For the dynamic calibration measurement, the rotational exciter generates monofrequent sinusoidal excitations. The angular acceleration at the bottom, the output signal of the transducer, and the angle position at the top are acquired simultaneously by a data acquisition system.

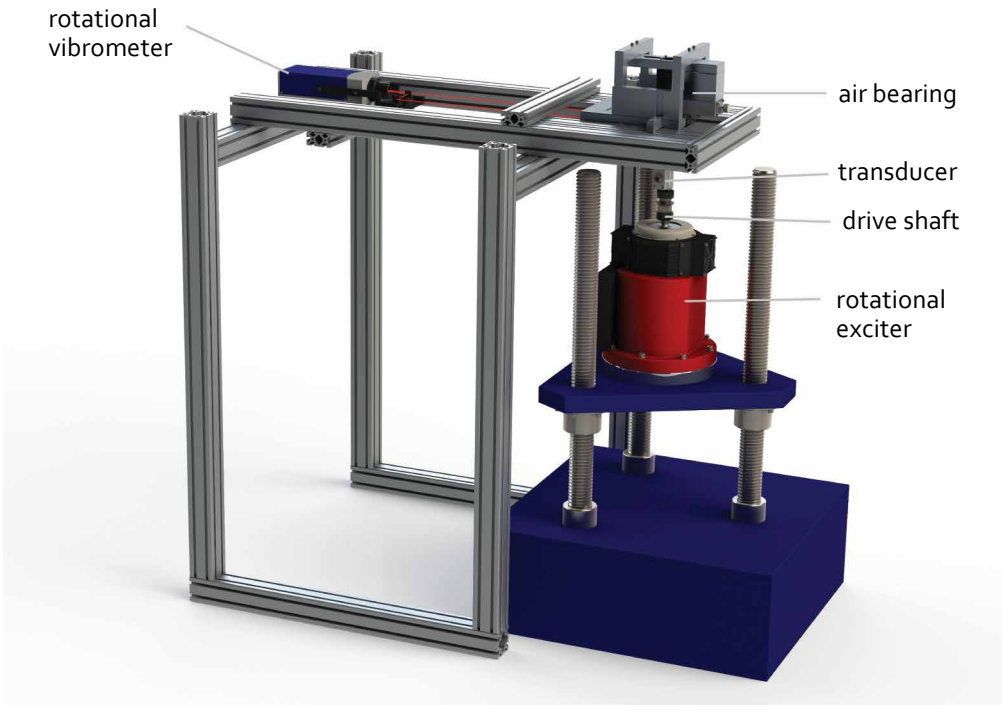

Figure 5: Dynamic torque measuring device and its components.

7 Physical Model

Torque transducers are always coupled to their mechanical environment on both sides when used for measurements. The mechanical environment may have influence on the transducer's dynamic behaviour, and vice versa. To understand this influence, the mechanical system of torque transducer and measuring device can be described by model calculations.

The model uses a system consisting of two elements of mass moment of inertia J_H, J_B connected by a torsional spring c_T and damper d_T in parallel, which represent the transducer under test, and an additional rigidly coupled mass moment of inertia J_0 at the top. The dynamic behaviour is described by the magnitude response which is the ratio of the magnitudes of the angular accelerations $\ddot{\varphi}_0$ and $\ddot{\varphi}_B$ at the top and the bottom, respectively. The model and the magnitude response are depicted in figure 6 and figure 7.

Different mass moments of inertia J_0 (which represent different mechanical environment properties connected to the torque transducer) lead to a change in the magnitude response of the system, as illustrated in figure 7. Marked in red is the sensitivity value which would have been obtained by a static calibration. The dynamic behaviour of such a system is obviously dependent on both the properties of the coupled components and of those of the transducer. Deviations from the static calibration value can occur even if the excitation frequency is significantly below the resonance frequency (illustrated by the grey box).

To properly describe such an interaction of transducer and environment and to be able to determine these influences, it is necessary to describe the transducer by a proper physical model. For this purpose, a model similar to that of the simulation calculation was developed.

The model approach is linear and time-invariant (LTI). These assumptions are valid, because transducers are designed to be linear and to not change their properties over time significantly (time invariance).

The model is based on the mechanical design of torque transducers. As described in section 3, these transducers have a characteristic mechanical design consisting of torsionally compliant measuring elements, which are modelled as a torsional spring and a damper in parallel, and of rigid components, which are modelled as coupled mass moments of inertia. The model components of the transducer are marked in red in figure 6.

To be able to identify the torque transducer's model properties, the model needs to be extended to include the measuring device, which is the mechanical environment in the case of the calibration.

The chosen model represents the mechanical design of the components in the drive train. The coupling elements are assumed to be the components with the lowest torsional stiffness and, therefore, are represented by a mass-spring-damper element, whereas all other components are assumed to be rigidly coupled mass moment of inertia elements. The model and the corresponding components of the drive train are shown in figure 8.

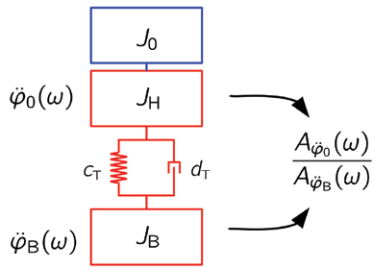

Figure 6:
System of torque transducer (red) and a rigidly coupled mass moment of inertia (blue).

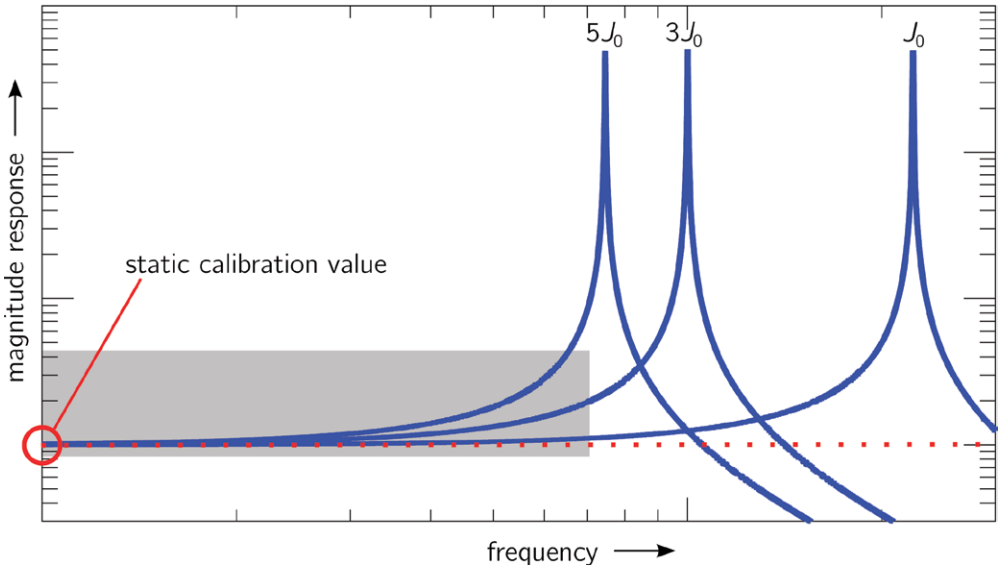

Figure 7:
Magnitude response of the modelled system with different mass moments of inertia.

The modelled measuring device can be described mathematically as an inhomogeneous ordinary differential equation (ODE) system

$$\boldsymbol{J}\,\ddot{\boldsymbol{\varphi}} + \boldsymbol{D}\,\dot{\boldsymbol{\varphi}} + \boldsymbol{C}\,\boldsymbol{\varphi} = \boldsymbol{M}\,. \qquad (6)$$

$\boldsymbol{J}$ denotes the mass moment of inertia matrix, $\boldsymbol{D}$ the damping matrix, and $\boldsymbol{C}$ the stiffness matrix. The angle vector $\boldsymbol{\varphi}$ describes the angle values at the different positions as depicted in figure 8, and $\dot{\boldsymbol{\varphi}}$ and $\ddot{\boldsymbol{\varphi}}$ denote the vectors of the corresponding derivatives. The forced excitation of the rotational exciter is given in the load vector $\boldsymbol{M}$.

8 Model Parameter Identification

The model parameters of the transducer under test are going to be identified by means of measurement data. For this purpose, all angle positions, angular velocities and angular accelerations at the four positions marked in figure 8 would have to be measured. Due to the fact that the excitation is sinusoidal, it is possible to calculate the angular acceleration or the angular velocity from the angle position, and vice versa. Technically, it is not possible to measure the torsion angles directly above and below the device under test (φ_H, φ_B) with sufficient precision.

The output voltage signal of the transducer $U_{DUT}(t)$ is assumed to be proportional to the torsion of the transducer $\Delta\varphi_{HB} = \varphi_H - \varphi_B$ giving

$$U_{DUT}(t) = \rho \cdot \Delta\varphi_{HB}(t)\,. \qquad (7)$$

The proportionality factor ρ has to be identified by the model parameter identification as well, in order to use the transducer's voltage output instead of two angular positions.

Prior to the identification, the model properties of the measuring device need to be identified. For this purpose, three dedicated auxiliary measurement set-ups were developed to determine mass moment of inertia, torsional stiffness [4], and damping [5]. Based on the measurement results of the three set-ups, all necessary model parameters could be determined.

With this knowledge of the model parameters of the dynamic torque measuring device, it is now possible to identify the unknown parameters of the device under test from measurement data. A summary of all known and unknown model parameters is given in table 1.

Table 1:
Model parameters of the measuring device and of the device under test.

	known parameters of the measuring device	unknown parameters of the DUT
MMOI	J_{M2}, J_{M1}, J_{E2}	J_H, J_B
torsional stiffness	c_M, c_E	c_T
damping	d_M, d_E	d_T
proportionality factor		ρ

The simultaneously acquired data samples of the three measurement channels (transducer signal, angular acceleration at the bottom, angular acceleration at the top) are processed applying a sine fit to identify magnitude and phase of each signal. All three signals are fitted in a combined process, applying a common frequency [7]. As the corresponding

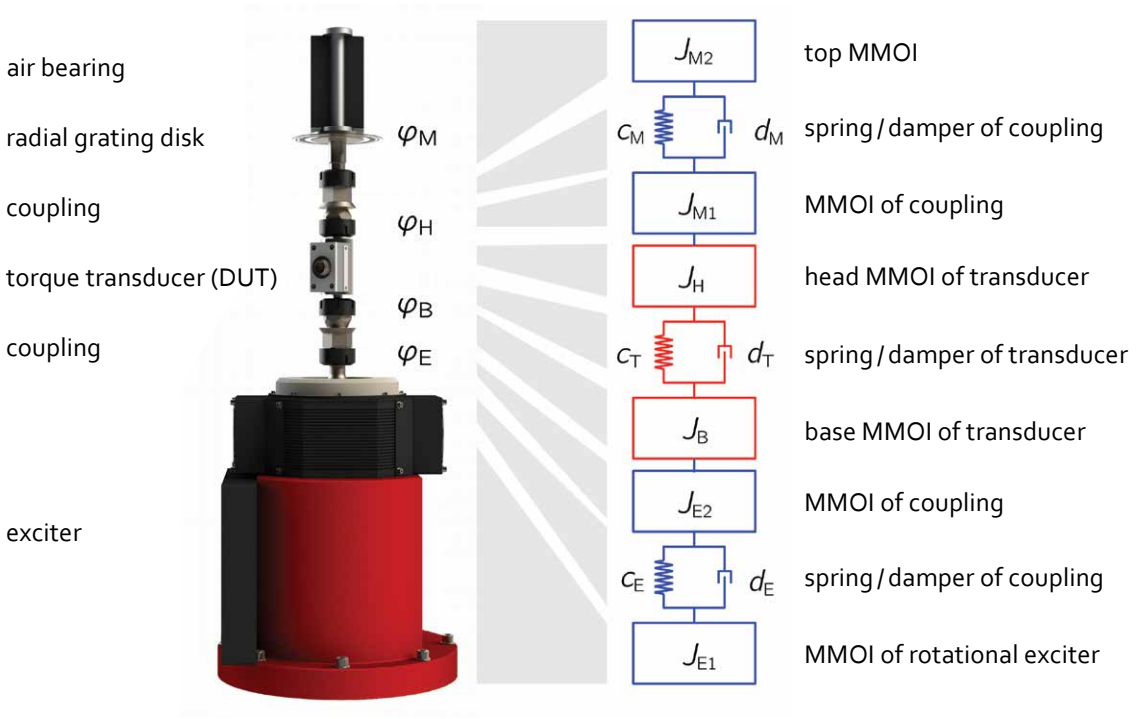

Figure 8:
Extended model of the measuring device and corresponding components of the drive shaft. The different angle positions of the model are displayed to the right of the drive shaft.

equations are non-linear in their parameters, an iterative fitting algorithm is required.

Based on the results from the three measurement channels, two complex frequency response functions can be calculated (see figure 9). The response function $H_{\mathrm{top}}(\mathrm{i}\omega)$ represents the top part of the measuring device and consists of the angular acceleration at the top and the output voltage of the transducer under test

$$H_{\mathrm{top}}(\mathrm{i}\omega) = \frac{\rho \cdot \Delta\varphi_{\mathrm{HB}}(\mathrm{i}\omega)}{\ddot{\varphi}_{\mathrm{M}}(\mathrm{i}\omega)}, \tag{8}$$

the other response function $H_{\mathrm{bott}}(\mathrm{i}\omega)$ represents the dynamic behaviour of the bottom part of the device under test giving

$$H_{\mathrm{bott}}(\mathrm{i}\omega) = \frac{\rho \cdot \Delta\varphi_{\mathrm{HB}}(\mathrm{i}\omega)}{\ddot{\varphi}_{\mathrm{E}}(\mathrm{i}\omega)}. \tag{9}$$

The model parameters of the transducer under test can be determined from the two transfer functions derived from the ODE system of equation 6. For more details, cf. [7].

$H_{\mathrm{top}}(\mathrm{i}\omega)$ comprises the parameters J_{H}, d_{T}, c_{T}, and ρ, whereas $H_{\mathrm{bott}}(\mathrm{i}\omega)$ comprises all parameters of the DUT J_{H}, J_{B}, d_{T}, c_{T}, as well as ρ. Consequently, parameter identification is carried out that applies to both transfer functions at once.

The parameter identification can be carried out as a one-step non-linear regression using the frequency response functions, where some of the parameters are linear. Alternatively, it is possible to identify these linear parameters by a linear regression algorithm followed by a consecutive approximation of the non-linear parameters using non-linear methods [7].

9 Summary

Several industrial applications with highly dynamic torque excitation call for dynamic torque calibrations procedures. For this reason, research in this field was carried out as part of the joint research project IND09 of the EMRP. An existing dynamic torque measuring device was improved with a new exciter and a more capable air bearing. A mechanical model of the transducer and an extended model of the measuring device were developed. Three auxiliary measuring set-ups for the determination of the measuring device's characteristics were developed, and the model parameters of the dynamic torque calibration device were determined. Based on measurement data, the model parameters of the transducer under test can now be determined in the next step. The paper briefly presents the procedures that will be applied to this model parameter identification and the data analysis which is involved.

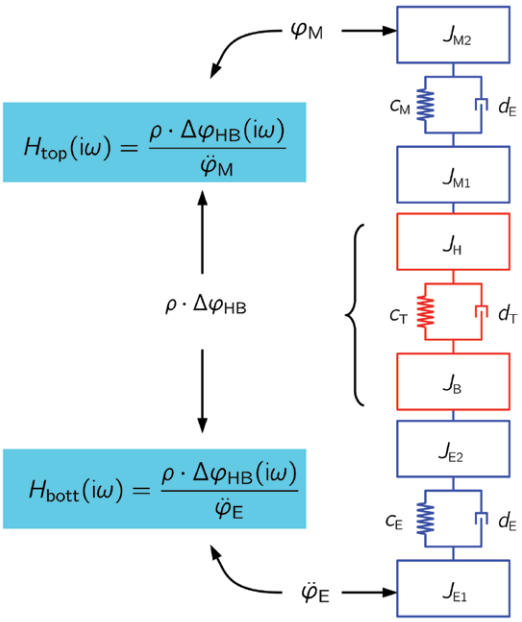

Figure 9: Transfer functions based on the three acquired measurement channels.

Acknowledgements

The author would like to thank his colleagues Oliver Slanina (PTB) for the illustrations of the measuring device and the transducers and Barbora Arendacká (PTB) for the helpful recommendations and the support with system simulation and model parameter identification issues.

This work was part of the joint research project IND09 *Traceable Dynamic Measurement of Mechanical Quantities* of the *European Metrology Research Programme* (EMRP). The EMRP is jointly funded by the EMRP participating countries within EURAMET and the European Union.

References

[1] Bureau International des Poids et Mesures: *Le Système International d'Unités (SI) – The International System of Units (SI)*, 2006.

[2] D. Röske, *Torque Measurement: From a Screw to a Turbine*, PTB-Mitteilungen 118 (2, 3), pp. 48–55, 2008.

[3] T. Bruns, *Sinusoidal Torque Calibration: A Design for Traceability in Dynamic Torque Calibration*, XVII IMEKO World Congress. Dubrovnik, Croatia, 2003.

[5] L. Klaus, T. Bruns and M. Kobusch, *Determination of Model Parameters for a Dynamic Torque Calibration Device*, XX IMEKO World Congress, Busan, Republic of Korea, 2012.

[6] L. Klaus and M. Kobusch, *Experimental Method for the Non-Contact Measurement of Rotational Damping*, IMEKO International TC3, TC5 and TC 22 Conference, Cape Town, South Africa, 2014.

[7] L. Klaus, B. Arendacká, M. Kobusch and T. Bruns, *Dynamic Torque Calibration by Means of Model Parameter Identification*, ACTA IMEKO, 4 (2), pp. 39–44, 2015.

Parameter Identification and Measurement Uncertainty for Dynamic Measurement Systems

Sascha Eichstädt*

* Dr. Sascha Eichstädt, Working Group "Data Analysis and Measurement Uncertainty" e-mail: sascha.eichstaedt@ptb.de

1 Introduction

The analysis of dynamic measurements requires new approaches to the estimation of the value of the measurand as well as for the evaluation of measurement uncertainty. In static measurements the value of the measurand is represented by a single value or a tuple of values, and estimation of the measurand typically requires solving algebraic equations. In dynamic measurements the value of the measurand varies with time. In addition, the response of the measurement device depends on the frequency content in the measured time series.

A typical workflow in the analysis of a dynamic measurement is shown in figure 1. The measurand is the system input signal and the available data the corresponding output signal. Estimation of the measurand requires a mathematical model for the dynamic system which covers its frequency-dependent response in the relevant frequency range. This cannot be accomplished by algebraic equations.

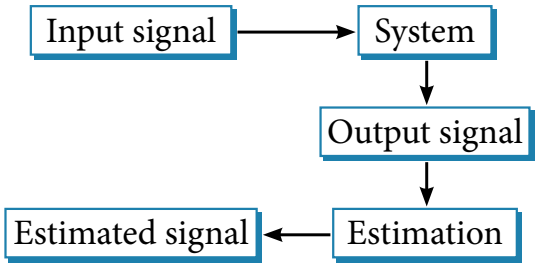

Figure 1: Work flow in the analysis of dynamic measurements.

An appropriate mathematical model for most dynamic systems is given by the state-space system model

$$\dot{z}(t) = f(z(t), y(t), t) \tag{1}$$

$$x(t) = g(z(t), y(t), t)\,, \tag{2}$$

with (1) being the state equation modelling the dynamics of the system, and (2) the observation equation modelling the data acquisition [1]. Such state-space system models cover single sensors [2] as well as complex measurement set-ups [3] or sensor networks. Sometimes the system model can be determined based on physical reasoning and the calibrated parameters then give insights into the physical properties of the measurement system. For instance, in a shock-force calibration experiment the measurement system may be modelled by means of coupled mass-spring-damper elements such that estimated spring stiffness values correspond to the stiffness of the coupling of the measurement system components [4].

The goal of dynamic calibration is to provide a characterization of the system dynamics and the influence of the measurement itself. Both can be achieved by means of parameterization of the functions f and g in (1)–(2). A parametric characterization has the benefit that it allows versatile application of the calibration result. For instance, a calibrated parametric model of a force transducer can be applied as part of a model of a fatigue testing machine [3], or a model of a torque sensor can be incorporated into a model of an engine test stand [5].

For the state-space model (1)–(2), special cases exist which allow a simplified treatment in certain scenarios. For instance, if the complete measurement system can be modelled by a linear time-invariant (LTI) system with single input and single output, then equations (1)–(2) can be transformed to a transfer function model in the Laplace domain [1]

$$H(s) = \frac{\sum_{k=0}^{K} b_k s^k}{\sum_{l=0}^{L} a_l s^l}\,. \tag{3}$$

The relation between input and output of the dynamic system is then given by

$$L\{x(t)\} = H(s) L\{y(t)\}\,, \tag{4}$$

where $L\{x(t)\}$ denotes the Laplace transform of the time signal $x(t)$. In order to emphasize the dependence of the transfer function on its parameters we write $H(s; \boldsymbol{\theta})$ with $\boldsymbol{\theta} = (b_0, \ldots, b_K, a_0, \ldots, a_L)^{\mathrm{T}}$ as the vector of parameters.

In the following, the task of calibrating a linear time-invariant dynamic system by means of identification of the transfer function model parameters (3) is considered. In section 2 generic methods for parameter estimation are discussed. In section 3 and 4, estimation is addressed for calibration data available in the frequency and time domain, respectively. The evaluation of uncertainty for parameter estimation in line with GUM [6] is discussed in section 5.

2 Generic Parameter Identification

An important step in the process of parameter identification is to set up the statistical measurement model

$$H(s_k; \boldsymbol{\theta}) = H_0(s_k; \boldsymbol{\theta}) + \varepsilon_k \,, \tag{5}$$

where H_0 denotes the (unavailable) error-free value and the ε_k denote statistical measurement errors. The statistical model takes into account all sources of uncertainties in the calibration experiment, (cf. [7]) for an example, in the field of acceleration using sophisticated statistical modelling.

The aim of parameter identification is to determine the parameter vector $\boldsymbol{\theta}$ which provides the best explanation of the data given the statistical model (5). One possibility to achieve that goal is to carry out a maximum likelihood estimation [9]. In this approach the statistical model (5) is employed to define the likelihood function $l(\boldsymbol{\theta}, \boldsymbol{H})$ as a probabilistic expression of the likelihood of the data $\boldsymbol{H}$ for a given parameter vector $\boldsymbol{\theta}$. Parameter estimation in this context corresponds to determining the solution of

$$\hat{\boldsymbol{\theta}} = \arg\max_{\boldsymbol{\theta}} l(\boldsymbol{\theta}, \boldsymbol{H}) \,. \tag{6}$$

Consider, for instance, the case which the measurement errors ε_k in (5) follow a normal distribution with zero mean and known covariance $\boldsymbol{\Sigma}$. In this case, the likelihood function is proportional to $\exp(-0.5\|\boldsymbol{H} - H(s; \boldsymbol{\theta})\|_{\boldsymbol{\Sigma}}^2)$ and the application of the maximum likelihood method becomes the weighted least squares estimation [8]

$$\hat{\boldsymbol{\theta}} = \arg\min_{\boldsymbol{\theta}} \|\boldsymbol{H} - H(s; \boldsymbol{\theta})\|_{\boldsymbol{\Sigma}}^2 \,, \tag{7}$$

with $\|\boldsymbol{A}\|_{\boldsymbol{W}}^2 = \boldsymbol{A}^{\mathrm{T}} \boldsymbol{W}^{-1} \boldsymbol{A}$.

It is worth noting that least squares estimation is often applied for parameter estimation irrespective of the statistical model (5). However, although the resulting parameter vector estimate then satisfies (7), it may not be the optimal solution for the model (5). Moreover, assignment and interpretation of measurement uncertainty becomes problematic if the statistical properties of the data are ignored.

Maximum likelihood estimation can be considered as a numerical optimization problem [9]. The optimization merit function is given by equation (6) and is typically non-linear. In contrast to linear optimization, the solution space of non-linear problems can be very complex and many (local) solutions may exist. In general, non-linear optimization has many pitfalls that have to be considered in order to obtain a reliable parameter estimate. For instance, stopping of the iterations is decided, based on user-defined tolerances, and numerical calculation of the model function's Jacobian requires appropriately small step sizes. Convergence of optimization routines is typically proven under the assumption of an appropriate choice of method parameters. Hence, reliable parameter estimation requires a careful usage of the applied non-linear optimization method.

An often applied optimization method in the case of non-linear least squares is the Levenberg-Marquardt method [9]. This is an iterative method where in each step the Jacobian of the model function $H(s; \boldsymbol{\theta})$ with respect to $\boldsymbol{\theta}$ is employed in order to progress to a solution of (7). In many software environments, such as LabView, Matlab and SciPy, the Levenberg-Marquardt method is the default method for non-linear least squares problems. However, like all iterative solution methods, the Levenberg-Marquardt method requires defining an initial starting point $\boldsymbol{\theta}^{(0)}$ and only provides local solutions to problem (7). That is, for a different starting point, the outcome of the optimization might differ. It is thus advisable to repeat the optimization process with different initial parameter estimates.

An alternative approach to the maximum likelihood method for parameter estimation is the application of Bayesian inference [10, 11]. Therefore, in addition to the likelihood function, a probability distribution function (PDF) modelling the *a priori* knowledge about the parameters is employed. Parameter estimation in this context is then applied in terms of a probability calculus using Bayes' Theorem, carried out numerically, e.g. by means of Markov Chain Monte Carlo (MCMC) sampling [11]. The result of such a Bayesian inference is a *posterior* PDF modelling the (probabilistic) knowledge about the parameter values after taking into account the measurement data. The benefit of the Bayesian approach here is that no numerical optimization has to be applied and that uncertainties associated with the parameter estimate can be directly obtained from the posterior PDF. However, care has to be taken when no actual prior knowledge about the model parameters is available, and a careful convergence analysis of the MCMC sampling has to be carried out in order to obtain reliable results [11]. In the following, we focus on the maximum likelihood estimation and refer

the reader interested in details about the Bayesian approach to parameter estimation to [10, 11] and references therein.

3 Frequency Domain Identification

The transfer function model (3) gives rise to a frequency domain representation of the dynamic system by replacing the variable s with $j\omega$ with $j = \sqrt{-1}$ and the radial frequency $\omega = 2\pi f$ giving

$$H(j\omega) = \frac{\sum_{k=0}^{K} b_k (j\omega)^k}{\sum_{l=0}^{L} a_l (j\omega)^l} \,. \tag{8}$$

Identification of the system parameters in the frequency domain requires measurements of the frequency response of the dynamic system over the whole range of relevant frequencies [12]. This can be achieved either frequency-by-frequency using sinusoidal excitations [13] or by application of the discrete-time Fourier transform (DFT) to a time domain calibration measurement of input and output signal [14].

In any case, parameter identification based on equation (8) requires measurement of the complex-valued frequency response values $\boldsymbol{H} = (H(f_1), \ldots, H(f_N))^{\mathrm{T}}$, represented either by means of the real and the imaginary part of $\boldsymbol{H}$ or of the corresponding amplitude and phase values. The uncertain knowledge about these values is modelled by a (multivariate) probability density function (PDF) or is given as an estimate of the values and an associated matrix $\boldsymbol{U}$ of (mutual) uncertainties.

When the frequency response measurements are carried out by means of a sinusoidal excitation experiment, amplitude and phase values $\tilde{\boldsymbol{H}} = (|H(f_1)|, \ldots, \measuredangle H(f_N))$ with associated uncertainties are typically available [13, 15]. In general, the values at different frequencies are correlated, for instance, due to being obtained with the same measurement set-up. However, in practice the correlation between the estimates at different frequencies is often considered to be negligible. The corresponding statistical model for the measurement errors in equation (5) is then given by $\boldsymbol{\varepsilon} \sim N(0, \boldsymbol{\Sigma})$ with known diagonal matrix $\boldsymbol{\Sigma}_{ii} = u_i^2$, where u_i denotes the uncertainty associated with the i-th component of the vector $\tilde{\boldsymbol{H}}$. Depending on the type of the transfer function model (3), a linear or non-linear least squares method can then be applied for the determination of transfer function parameter estimates [13, 16].

In the case of time domain measurement and subsequent application of the discrete Fourier transform (DFT) to obtain frequency response values, the model (5) depends on the statistical model of the time domain measurements [14]. Determination of the likelihood function for frequency domain maximum likelihood estimation is thus more complicated than for the case of sinusoidal excitation and the time domain estimation might be more appropriate then. In addition, systematic errors introduced by the non-ideal DFT itself have to be taken into account in the subsequent uncertainty analysis [17].

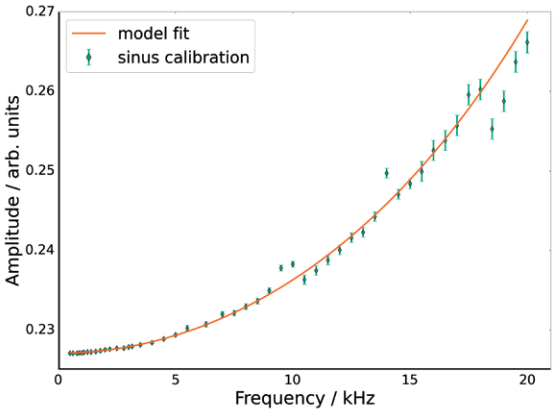

Figure 2:
Estimated transfer function for sinusoidal excitation data.

4 Time Domain Identification

The time domain description of a transfer function model is obtained by taking the inverse Laplace transform of equation (4)

$$x(t) = (h_{\boldsymbol{\theta}} * y)(t) \,, \tag{9}$$

where $h_{\boldsymbol{\theta}}(t) = h(t; \boldsymbol{\theta})$ denotes the system's impulse response function and '$*$' means convolution [1]. The statistical models

$$y(t) = y_0(t) + \varepsilon_y \,, \tag{10}$$

$$x(t) = x_0(t) + \varepsilon_x \tag{11}$$

have to be set up by taking into account measurement noise, systematic influences of the involved measurement devices and other sources of uncertainty [18]. When the uncertainty in y is negligible and the statistical model (11) for x is covered by a normal distribution with known covariance matrix $\boldsymbol{\Sigma}$, then the parameter estimation becomes the least squares problem

$$\hat{\boldsymbol{\theta}} = \arg\min_{\boldsymbol{\theta}} \| \boldsymbol{x} - (h_{\boldsymbol{\theta}} * \boldsymbol{y}) \|_{\boldsymbol{\Sigma}}^2 \tag{12}$$

with vector $\boldsymbol{x} = (x(t_1), \ldots, x(t_N))^{\mathrm{T}}$ of system output values and the corresponding input values $\boldsymbol{y} = (y(t_1), \ldots, y(t_N))^{\mathrm{T}}$.

Note that a non-parametric estimation of the impulse response $h(t)$ from measured system input $y(t)$ and output $x(t)$ requires a deconvolu-

tion, which is an ill-posed inverse problem [19]. The corresponding model for the estimation of the impulse response in the time domain is given by

$$h(t) = (x * y^{\dagger})(t) + \varepsilon, \tag{13}$$

where $y^{\dagger}$ denotes the regularized inverse of y [19, 20]. It is worth noting that (13) is typically applied in the frequency domain for ease of calculation.

For the more general dynamic system model (1)-(2) an ordinary differential equation (ODE) has to be solved. When the uncertainty in $y(t)$ can be neglected, the statistical model is then given by

$$x(t) = g(y(t), z(t; \boldsymbol{\theta}), t; \boldsymbol{\theta}) + \varepsilon_x, \tag{14}$$

which is derived from the measurement equation (2). Note that in order to calculate $z(t)$, the differential equation

$$\dot{z}(t; \boldsymbol{\theta}) = f(z(t; \boldsymbol{\theta}), y(t), t; \boldsymbol{\theta}) \tag{15}$$

has to be solved. To this end, typically numerical integration, such as the backward differentiation formula or a Runge-Kutta method can be applied [21]. Software tools for this task are available in almost all major scientific software packages. However, the numerical optimization in conjunction with numerical ODE integration requires careful selection of the step size tolerances of the ODE solver and of the numerical differentiation in the optimization routine. For instance, the application of the Levenberg-Marquardt method for the optimization problem

$$\hat{\boldsymbol{\theta}} = \arg\min_{\theta} \| \boldsymbol{x} - g(\boldsymbol{y}, \boldsymbol{z}, \boldsymbol{\theta}) \|_{\Sigma}^{2}, \tag{16}$$

in the case of normally distributed errors ε_x with known covariance $\boldsymbol{\Sigma}$ requires differentiation of g with respect to $\boldsymbol{\theta}$ which itself requires solving the ODE (15). Hence, at each iteration in the optimization process a numerical differentiation of the ODE integration method has to be carried out with precision being high enough for a reliable parameter estimation result. In some cases, this may require use of an optimization routine which does not require differentiation, such as the Powell method [4, 9].

Figure 3 shows the outcome of a time domain parameter estimation for a shock force calibration experiment. In this example, the system model equation (1) models the dynamics of the measurement system as a series of mass-spring-damper elements. Measured data (14) in this case is the sensor output signal and the acceleration of one of the involved masses, see [4] for details.

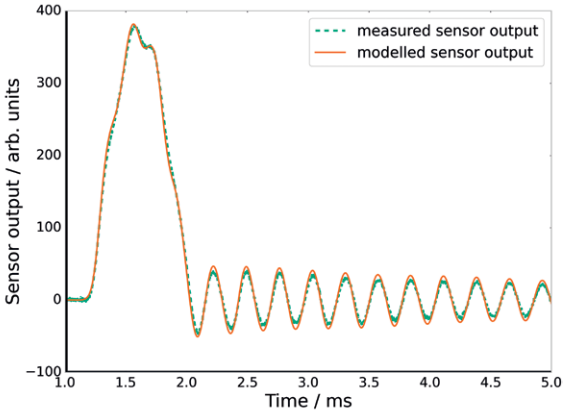

Figure 3:
Time domain parameter estimation for shock calibration of a force sensor.

5 Evaluation of Uncertainty

In order to provide the parameter estimates as part of a calibration result, reliable uncertainties have to be associated with the estimated parameters in line with GUM [6, 22]. Statistically speaking, the task of parameter estimation is a regression. Although this task is very common in metrological applications, so far there is no generally accepted approach to the corresponding GUM-compliant evaluation of uncertainties. The GUM itself provides an example for uncertainty evaluation for linear least squares, see H.3 in [6] or example 3 in 6.2.2 in [22]. There are a number of publications which assess the applicability of the GUM framework to regression models. For instance, in [23] a Bayesian inference approach is compared to an application of GUM-S1 Monte Carlo. The authors conclude that GUM-S1 does in general not provide a Bayesian solution, opposed to what is stated in the introduction of GUM-S1 [22]. Furthermore, the authors in [23] point out that the measurement model is ambiguous in contrast to the assumptions made by the GUM as it depends on the actual data and not the physical model alone.

Despite the pitfalls of the application of GUM to least squares and other regression problems, this task is routinely considered in many metrological applications. Therefore, the statistical model (5) has to be replaced by a GUM-compliant measurement model. For the linear least squares problem, i.e. a linear mathematical model and normally distributed data with known covariance $\boldsymbol{\Sigma}$, the measurement model is

$$\hat{\boldsymbol{\theta}} = \arg\min_{\theta} \| \boldsymbol{y} - \boldsymbol{H}\boldsymbol{\theta} \|_{\Sigma}^{2} \tag{17}$$

which can also be written as

$$\hat{\boldsymbol{\theta}} = (\boldsymbol{H}^{\mathrm{T}}\boldsymbol{\Sigma}^{-1}\boldsymbol{H})^{-1}\boldsymbol{H}^{\mathrm{T}}\boldsymbol{\Sigma}^{-1}\boldsymbol{y}\,. \tag{18}$$

The uncertainty associated with this estimate is then calculated as the variance of this expression and results in

$$\boldsymbol{U}_{\hat{\theta}} = (\boldsymbol{H}^{\mathrm{T}}\boldsymbol{\Sigma}^{-1}\boldsymbol{H})^{-1}\,. \tag{19}$$

For a non-linear optimization often an approach is chosen that mimics the linear least squares case. Therefore, the Jacobian of the optimization merit function at the final iteration is employed together with the covariance matrix associated with the data points [16, 24]. Another approach is the utilization of the Hessian matrix of the least squares cost functional [24]. However, the resulting uncertainties may be underestimated in the case of uncertainties in the independent variables (time or frequency in the here considered scenarios), see [24]. To this end, the authors in [16] propose the application of a Monte Carlo method instead of a linearized propagation with closed formulas. In a Monte Carlo propagation of uncertainties for a parameter estimation problem, the input quantities and their associated uncertainty are given by the calibration data. As a measurement model, equation (6) is considered and propagation of uncertainties is carried out according to GUM-S2 [22]. As discussed in section 3, non-linear optimization requires careful choice of the numerical method and its parameters. This is of particular importance for the application of Monte Carlo where the optimization has to be repeated many times in an automated way.

Irrespective of whether closed formulae are applied or a Monte Carlo propagation is carried out, the ambiguity of the measurement model and the difference to the result of a full Bayesian treatment remain. This makes a general GUM-compliant approach for uncertainty evaluation in parameter estimation based on statistical arguments very challenging. However, this has been recognized by the BIPM JCGM working groups and a supplement addressing this issue for the case of least squares regression is in preparation [25].

6 Conclusions

The characterization of a dynamic system in terms of a parametric model allows a versatile utilization of the calibration result. In its mathematical description, parameter estimation is a regression problem which itself can be interpreted as a numerical optimization problem. Both are well-established disciplines in mathematics and statistics and many scientific software packages contain efficient tools for their application. However, care has to be taken in the determination of the statistical model of the measured data and in the application of the estimation method in order to obtain a reliable calibration result.

Unfortunately, there is no general commonly accepted GUM-compliant approach yet. To this end, some authors have proposed approaches for certain non-linear least squares scenarios. A more general approach would be to fully embrace the Bayesian framework, and to carry out Bayesian inference not only for the interpretation of uncertainty, but for parameter estimation, too.

Acknowledgements

This work was supported by the EMRP program of the European Union. The EMRP is jointly funded by the EMRP participating countries within EURAMET and the European Union.

References

[1] A. V. Oppenheim and R. W. Schafer, *Discrete-Time Signal Processing*, Prentice Hall, 1989.

[2] C. Elster and A. Link, *Uncertainty Evaluation for Dynamic Measurements Modelled by a Linear Time-invariant System*, Metrologia, 45, pp. 464–473, 2008.

[3] P. Hessling, *Linear Calibration of Axial Load Fatigue Testing Machines*, Technical report, Nordtest NT-TR 579, 2006.

[4] M. Kobusch, S. Eichstädt, L. Klaus, T. Bruns, *Investigations for the Model-based Dynamic Calibration of Force Transducers by Using Shock Excitation*, ACTA IMEKO, 4 (2), pp. 45–51, 2015.

[5] L. Klaus, T. Bruns and M. Kobusch, *Modelling of a Dynamic Torque Calibration Device and Determination of Model Parameters*, ACTA IMEKO, 3 (2), pp. 14–18, 2014.

[6] BIPM, IEC, IFCC, ISO, IUPAC, IUPAP & OIMl: *Guide to the Expression of Uncertainty in Measurement*, International Organization for Standardization, Geneva Switzerland, 1995.

[7] B. Arendacká, A. Täubner, S. Eichstädt, T. Bruns and C. Elster, *Linear Mixed Models: GUM and Beyond*, Measurement Science Review, 14, pp. 52–61, 2014.

[8] A. Björck, *Numerical Methods for Least Squares Problems*, SIAM, 1996.

[9] J. Nocedal and S. J. Wright, *Numerical Optimization*, Springer, 1999.

[10] J. O. Berger, *Statistical Decision Theory and Bayesian Analysis*, Springer, 2006.

[11] A. Gelman, J. B. Carlin, H. S. Stern, D. B. Dunson, A. Vehtari and D. B. Rubin, *Bayesian Data Analysis*, Chapman & Hall/CRC Texts in Statistical Science, 2013.

[12] R. Pintelon and J. Schoukens, *System Identification: A Frequency Domain Approach*, John Wiley & Sons, 2001.

[13] A. Link, A. Täubner, W. Wabinski, T. Bruns and C. Elster, *Modelling Accelerometers for Transient Signals Using Calibration Measurements upon Sinusoidal Excitation*, Measurement, 40, pp. 928–935, 2007.

[14] C. Matthews, F. Pennecchi, S. Eichstädt, A. Malengo, T. Esward, I. Smith, C. Elster, A. Knott, F. Arrhén and A. Lakka, *Mathematical Modelling to Support Traceable Dynamic Calibration of Pressure Sensors*, Metrologia, 51, pp. 326, 2014.

[15] N. Medina and J. de Vicente, *Force Sensor Characterization under Sinusoidal Excitations*, Sensor, 14, pp. 18454–18473, 2014.

[16] A. Malengo and F. Pennecchi, *A Weighted Total Least Squares Algorithm for any Fitting Model with Correlated Variables*, Metrologia, 50, pp. 654–662, 2013.
[17] W. L. Briggs and V. E. Henson, *The DFT: An Owner's Manual for the Discrete Fourier Transform*, Society for Industrial and Applied Mathematics, 1995.
[18] S. Eichstädt and C. Elster, *Towards a Harmonized Treatment of Dynamic Metrology*, 20th IMEKO TC4 International Symposium, Benevento, Italy, 2014.
[19] S. M. Riad, *The Deconvolution Problem: An Overview*, IEEE, 74, pp. 82–85, 1986.
[20] S. Eichstädt, *Analysis of Dynamic Measurements – Evaluation of Dynamic Measurement Uncertainty*, PhD thesis, TU Berlin, Germany, PTB-Bericht IT-16, 2012, ISBN 978-3-86918-249-0S.
[21] J. C. Butcher, *Numerical Methods for Ordinary Differential Equations*, Wiley, 2008.
[22] BIPM, IEC, IFCC, ISO, IUPAC, IUPAP and OIML, *Evaluation of Measurement Data – Supplement 2 to the "Guide to the Expression of Uncertainty in Measurement" – Extension to any Number of Output Quantities*, Joint Commitee for Guides in Metrology, Bureau International des Poids et Mesures, JCGM 102, 2011.
[23] C. Elster and B. Toman, *Bayesian Uncertainty Analysis for a Regression Model Versus Application of GUM Supplement 1 to the Least Squares Estimate*, Metrologia, 48, pp. 233–240, 2011.
[24] A. Balsamo, G. Mana and F. Pennecchi, *The Expression of Uncertainty in Non-Linear Parameter Estimation*, Metrologia, 43, pp. 396–402, 2006.
[25] BIPM JCGM-WG1, *Evaluation of Measurement Data – Applications of the Least Squares Method*, http://www.bipm.org/en/publications/guides/#gum, (Retrieved: 2015-08-11).

Towards a Shock Tube Method for the Dynamic Calibration of Pressure Sensors

Stephen Downes, Andy Knott*, Ian Robinson

National Physical Laboratory, Hampton Road, Teddington, United Kingdom TW11 0LW

* Andy Knott, "Force Metrology", National Physical Laboratory, UK, e-mail: andy.knott@npl.co.uk

Updated version of the original article in **Philosophical Transactions A of the Royal Society**, DOI: 10.1098/rsta.2013.0299

Abstract

In theory shock tubes provide a pressure change with a very fast rise time and calculable amplitude. This pressure step could provide the basis for the calibration of pressure transducers used in highly dynamic applications. However, conventional metal shock tubes can be expensive, unwieldy, and difficult to modify. We describe the development of a 1.4 MPa (maximum pressure) shock tube made from PVC-U pressure tubing which provides a low-cost, light, and easily modifiable basis for establishing a method for determining the dynamic characteristics of pressure sensors.

1 Introduction

Many pressure measurements are made dynamically, as there is the need to measure pressures which are rapidly changing. It is necessary to show that the sensor's output provides an accurate representation of the pressure throughout the measurements [1–3]. At present, many sensors used in such applications are only calibrated using static methods due to the difficulty of generating known pressure changes of the required rate and amplitude. An example can be found in combustion engines where the in-cylinder pressure varies periodically from 0.1 MPa to 10 MPa, at frequencies of up to 30 kHz [4–6]. The pressures are measured using electro-mechanical sensors, which are calibrated statically, and it is not known if their dynamic characteristics cause their statically-determined sensitivity to change as the frequency increases. This can lead to errors in the measured pressures and may also cause problems if a sensor has to be replaced. If sensors are calibrated both statically and dynamically, the reliability and uncertainty of the measurements will be improved.

Dynamic calibration requires a source with known characteristics in both amplitude and frequency. A shock wave generated in a shock tube has a rise time of the order of 1 ns and the amplitude of the pressure step generated upon reflection of the wave from the end face of the tube can be calculated. This makes it an ideal candidate for a pressure calibration standard if it can be verified that the magnitude of the pressure step can be determined accurately from ideal gas theory using readily-measured parameters such as shock wave velocity and static temperatures and pressures. We have investigated the application of a novel shock tube, made from plastic tubing, to the determination of the frequency response of pressure sensors and have made significant progress towards extending SI pressure measurements to the dynamic regime.

As the aim of this investigation is to provide a means of calibrating the dynamic response of pressure sensors, the theory cannot be validated simply by comparing the measured and the calculated pressures. It is assumed that the pressure indicated by the sensors is independent of the gas species and, at present, it is also assumed that the sensors are linear and that the uncertainties associated with non-ideal behaviour of the gases are significantly lower than those associated with the experimental measurements. By comparing the theoretical and measured values of the pressure steps for different pressures and gas species it should be possible both to assess the quality of the measurement system and determine the dynamic calibration of the sensor. However this task is complicated by the non-ideal behaviour of both the shock tube and the sensor, both of which are investigated here.

2 Shock Tube Theory

A simple shock tube consists of two straight tubes of the same circular cross-section that are separated by a diaphragm. One tube contains a low pressure "driven" gas and the other is filled with a "driver" gas. Gas is added to the driver side until the diaphragm ruptures allowing the driver gas to generate a series of compression waves within the driven gas which coalesce to form a shock wave that propagates into the remaining undisturbed driven gas. The release of pressure at the diaphragm causes an expansion wave to propa-

gate back into the driver section. Simultaneously, a contact surface between the driver and driven gases, which moves more slowly than the shock wave, propagates along the tube behind the shock front. The length of the driven tube section and the relative velocity between the shock wave and contact surface ultimately determine the time over which useful measurements can be made.

The pressures, temperatures, and densities generated within a uniform diameter, low-pressure shock tube can be derived from ideal gas theory. The shock front has a thickness of a few hundred nanometres [7]; thus, to an observer at rest, the pressure across a shock wave moving at 500 $m \cdot s^{-1}$ rises from its initial value to its relatively constant post-shock value in a time period of the order of a nanosecond. The pressure remains constant for a few milliseconds after the shock wave has passed depending on the tube dimensions, sensor location, gas species used in the driver and driven sections, and the starting pressures and temperatures. The pressure change can therefore be considered as a step generating all frequencies above a low frequency limit, which is proportional to the reciprocal of the time that the pressure remains constant.

Figure 1 shows the stages of operation of a shock tube. Figure 1a shows the condition of the tube at the point that the diaphragm bursts. The driver section is at a uniform pressure p_4 and temperature T_4 and the driven section is at a uniform pressure p_1 and temperature T_1. In figure 1b the diaphragm has burst and the shock front is propagating into the driven gas with a constant pressure p_2 behind the shock. The contact surface between the driven and driver gases is propagating in the same direction as the shock front but at a lower speed. In figure 1c the rarefaction wave has reflected from the end of the driver section and the reflected rarefaction wave is propagating towards the other end of the tube. In figure 1d the shock wave has reflected from the end of the tube and the pressure in the end section has risen to p_5 with an associated temperature T_5. The reflected shock wave propagates back into the part of the tube at pressure p_2 until it meets the contact surface where it is partially reflected and partially transmitted. At the time of arrival of the shock wave a sensor in the centre of the end wall of the tube would see a pressure step of amplitude $(p_5 - p_1)$ and the measured pressure would remain stable at p_5 until the arrival of the shock wave reflected from the contact surface.

The magnitude of this step can be determined from ideal gas theory; the analysis can be found in [8–10], and is reproduced below. The pressure p_2 is calculated from a knowledge of p_1, γ_1 (the ratio of the specific heat at constant pressure to that at constant volume for the driven gas), and the Mach number M_S of the advancing shock wave:

$$p_2 = p_1\left(1+\frac{2\gamma_1}{\gamma_1+1}(M_S^2-1)\right) .$$

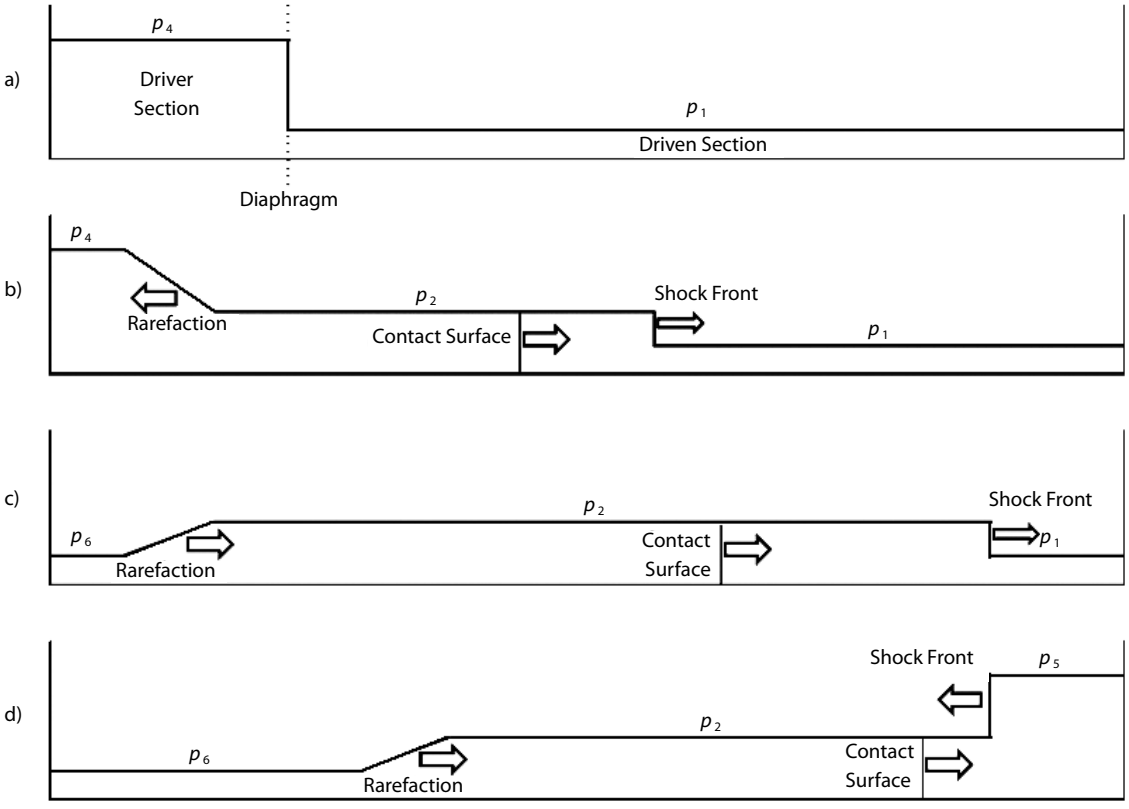

Figure 1:
Shock tube operation.

The Mach number of the shock is the ratio of the speed of the shock wave to the speed of sound a_1 in the undisturbed driven gas. The speed of the shock wave is calculated from measurements of the times that the shock wave passes two pressure sensors mounted a known distance apart in the wall of the tube. The speed of sound

$$a_1 = \sqrt{\frac{\gamma_1 R T_1}{m_1}},$$

where T_1 is the measured initial temperature (in K) of the driven gas, m_1 is its molecular weight and R is the gas constant.

The pressure p_5 existing after reflection of the shock from the end wall can be calculated from p_1, p_2, and $\alpha_1 = (\gamma_1 + 1)/(\gamma_1 - 1)$:

$$p_5 = p_2 \left(\frac{(\alpha_1 + 2)\frac{p_2}{p_1} - 1}{\frac{p_2}{p_1} + \alpha_1} \right).$$

For a specific driven gas at a known starting pressure, the magnitude of the pressure step $(p_5 - p_1)$ is simply a function of the shock wave Mach number; for air ($\gamma_1 \approx 1.4$) starting at atmospheric pressure ($p_1 \approx 0.1$ MPa) and room temperature, this function is shown in figure 2.

M_S increases with the pressure ratio across the diaphragm; it can be increased further by increasing the speed of sound in the driver gas, either by heating it or by using a lighter gas, such as helium or hydrogen.

The relationship between the driver pressure p_4, the driven pressure p_1 and the Mach number M_S is given by:

$$\frac{p_4}{p_1} = \frac{1}{\alpha_1}\left(\frac{2\gamma_1 M_S^2}{\gamma_1 - 1} - 1 \right) \left(1 - \frac{\left(\frac{1}{\alpha_4}\right)\left(\frac{a_1}{a_4}\right)\left(M_S^2 - 1\right)}{M_S} \right)^{\frac{-2\gamma_4}{\gamma_4 - 1}},$$

where γ_4 is the ratio of specific heats for the driver gas, $\alpha_4 = (\gamma_4 + 1)/(\gamma_4 - 1)$ and a_4 is the speed of sound in the undisturbed driver gas. Figure 3 shows the pressure step $(p_5 - p_1)$ for air, helium, and argon as a function of the pressure p_1 in the driven section for a constant pressure $p_4 = 1.4$ MPa of nitrogen in the driver section.

The temperature T_5 of the gas after the reflection of the shock wave can be calculated from the following equations:

$$\frac{T_2}{T_1} = \frac{p_2}{p_1}\left(\frac{\alpha_1 + \frac{p_2}{p_1}}{1 + \alpha_1 \frac{p_2}{p_1}} \right)$$

and

$$\frac{T_5}{T_2} = \frac{p_5}{p_2}\left(\frac{\alpha_1 + \frac{p_5}{p_2}}{1 + \alpha_1 \frac{p_5}{p_2}} \right).$$

The assumption that the gases behave ideally will not hold if the molecular energies produced by the generation and reflection of the shock wave are not significantly lower than the dissociation and ionization energies of the gases used (typically greater than 5 eV). Figure 4 shows the temperature of the driven gas after the reflection of the shock wave from the end of the tube. The results are calculated for a pressure of 1.4 MPa in the driver section. The thermal energy associated with this

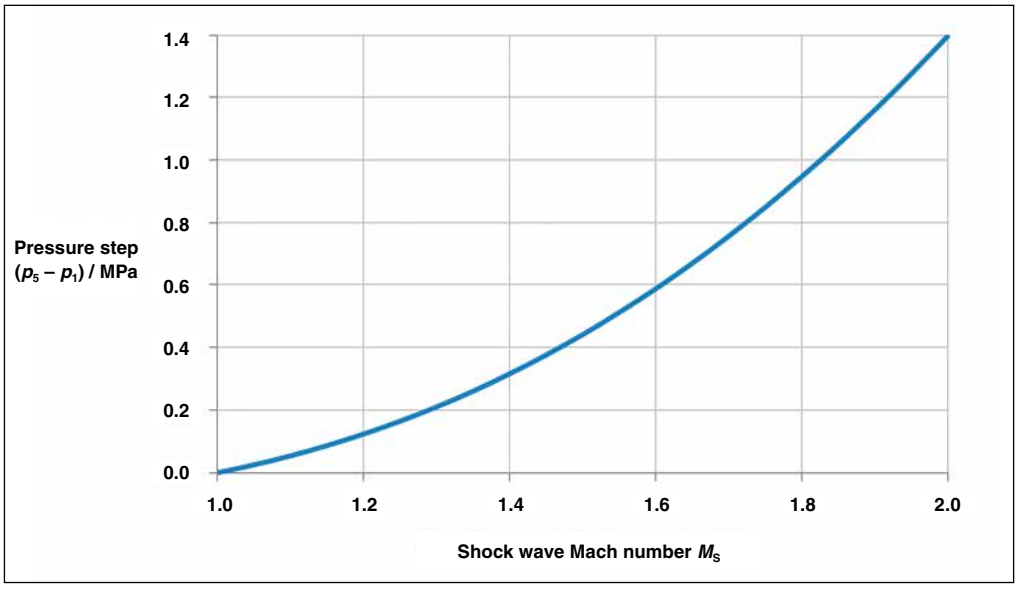

Figure 2:
Pressure step versus shock wave Mach number.

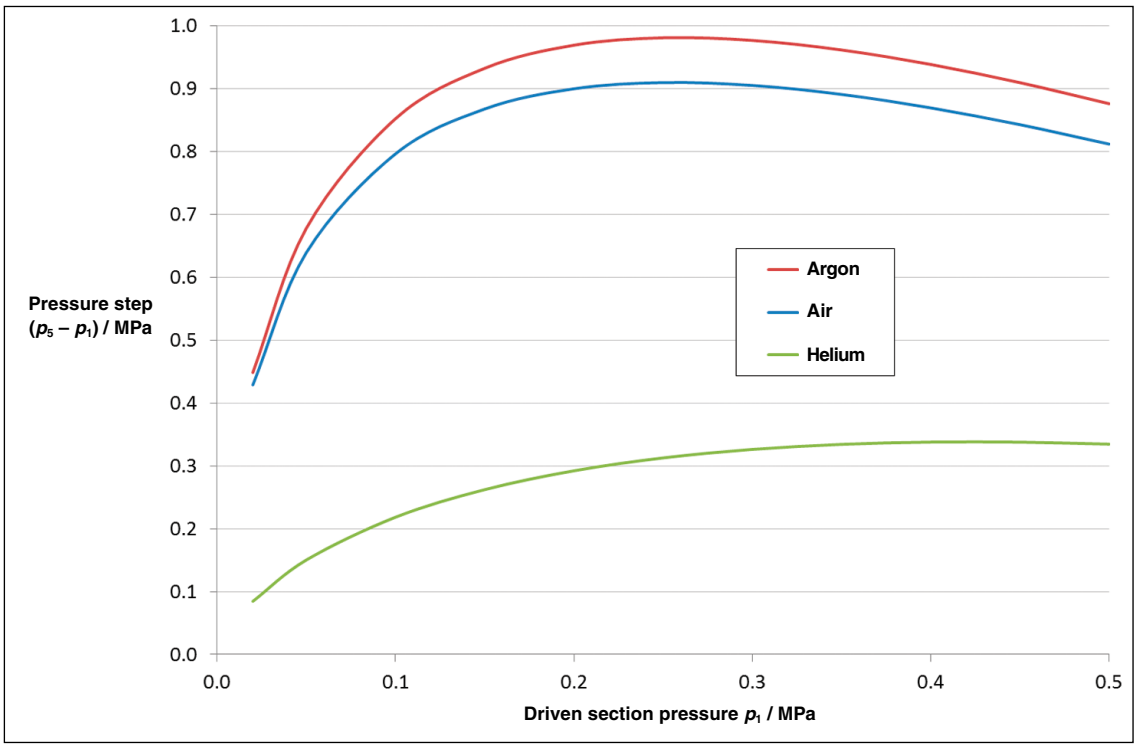

Figure 3: Generated pressure step versus initial driven pressure.

temperature is kT/e eV where k is the Boltzmann constant and e is the elementary charge. Argon at 0.02 MPa reaches a temperature of 1300 K with an equivalent energy of 0.11 eV. Typical operation of the tube with air at 0.1 MPa reaches a temperature of 600 K with an equivalent energy of 0.05 eV. These energies are orders of magnitude below the dissociation and ionization energies of the gases used, and the temperatures reached in this shock tube are therefore insufficient to cause significant deviations from ideal gas behaviour.

3 Construction of the Shock Tube

Conventional shock tubes are made from metal tubing and are costly, heavy and relatively difficult to modify. The shock tube described below (and shown in figure 5) differs from conventional designs in that it is made from plastic tubing. This makes it cheap to manufacture, it is light enough so that the longest (6 m) section can be readily manoeuvred by one person, and it can be constructed and modified using readily available tools.

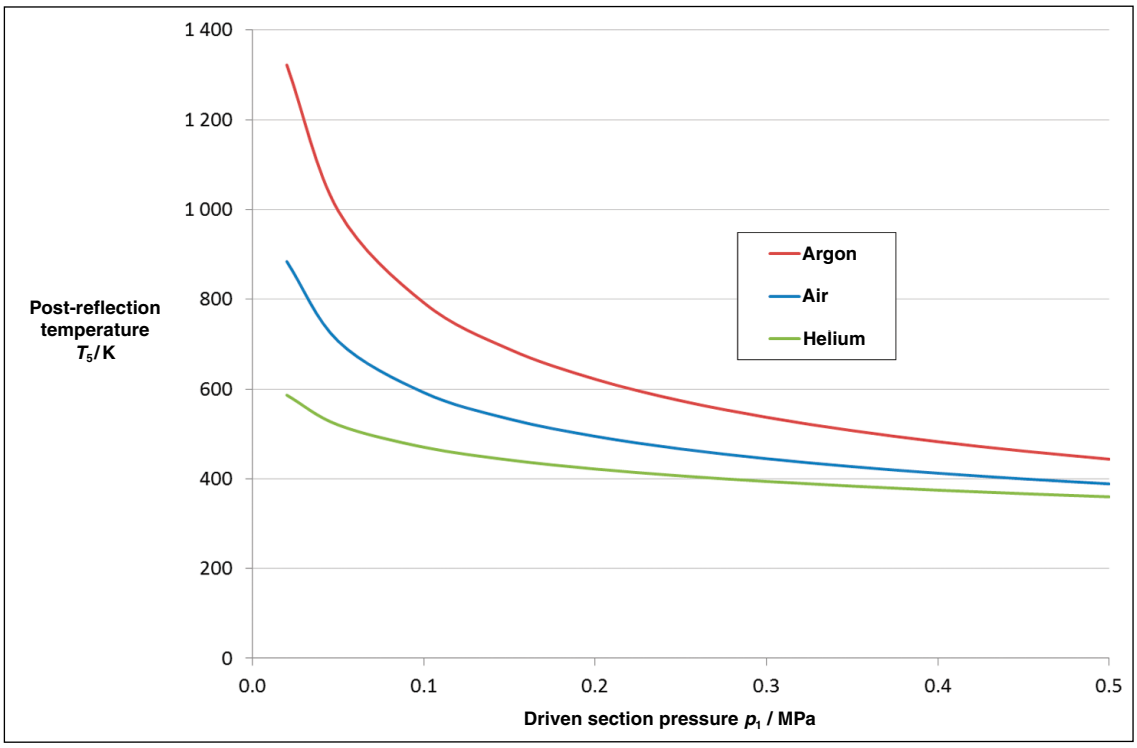

Figure 4: Post-reflection temperature versus initial driven section pressure.

The shock tube is manufactured from 76 mm i/d PVC-U tube with a 6.5 mm thickness wall which the manufacturers claim is suitable for use with gases with a maximum static working pressure of 1.5 MPa. The completed tube sections were limited to a working pressure of 1.4 MPa and were tested at a pressure approximately 50 % higher than this for a few minutes to ensure that they were safe for routine use at the working pressure. The pipe is cut to the required length and commercial plastic pipe flange adaptors, turned down to an outer diameter of just less than 123 mm, are glued to each end of the pipe and equipped with steel flanges. The flanges allow the pipe sections to be connected using four M16 steel bolts. Steel rings 6 mm thick with o-ring slots on both faces (shown in figure 6) are used to provide reliable seals between the faces of the flange adaptors and other parts of the shock tube. Driven sections of 2 m, 4 m, and 6 m in length have been constructed along with a 0.7 m driver section. The length of the driver section was chosen to limit the pressure-volume (PV) product to 4.5 kJ for a gas pressure of 1.4 MPa which is less than the 5 kJ statutory limit for this type of equipment. Most of the remaining parts – the pressurization flanges, the buffer section, and the sensor holder – were turned from an acetal rod.

4 Generating the Shock Wave

The rupture of a metal diaphragm caused by gas pressure provides a simple method for producing a shock wave. However, for a given thickness of diaphragm, the burst pressure will be fairly consistent and, unless a large range of thicknesses of material is available, this will limit the shock pressures that can be investigated. To provide a selectable pressure in the driver gas, an alternative technique uses two diaphragms separated by a small distance (25 mm–30 mm). This creates a third chamber in the shock tube: the "buffer". If, during pressurization, the pressure in the buffer is maintained at half the pressure in the driver section, it is possible to raise the pressure in the driver section to any pressure between one and two times the bursting pressure of the diaphragms. If the gas in the buffer is then vented, both diaphragms will burst in a rapid sequence producing the required shock wave driven by the chosen pressure in the driver section.

Figure 5:
NPL 1.4 MPa shock tube.

Figure 6:
A steel ring with o-rings mounted in each face.

The tube described can be used in either single or double diaphragm mode. In single diaphragm mode, the diaphragm is clamped between the plastic flanges terminating the tubes of the driver and driven sections. Intermediate steel ring and o-ring components (figure 6) ensure a good seal and prevent distortions of the diaphragm material which can produce leaks. The most effective diaphragm material for the generated driver pressures has been brass shim of either 0.1 mm or 0.05 mm thickness. The shim is supplied in rolls and is cut to fit the steel rings. The 0.1 mm sheet repeatedly bursts at a gauge pressure (i.e. a pressure above atmospheric) of approximately 1.35 MPa while the 0.05 mm sheet bursts at about 0.84 MPa.

In the double diaphragm arrangement, the two diaphragms are situated either side of a small buffer section which consists of a 29 mm thick acetal ring which can be pressurized independently of the driver and is pressurized as described above. To initiate diaphragm rupture, a local solenoid valve is operated to vent the buffer to atmosphere. Whilst this method provides the advantage of a selectable burst pressure it has the disadvantage of using twice as much diaphragm material for each operation of the tube and is more complex to set up as both diaphragms and the buffer ring have to be carefully positioned before the tube sections are clamped together.

The single diaphragm method has been used for most of the investigations in this study as it is simple and reliable, and the two burst pressures, which can be obtained with commercially available shim thicknesses, are usually sufficient.

5 Control System

The driver section is pressurized using bottled gas, initially nitrogen but helium and argon can also be used. The control system for the tube is fully automated using computer-controlled solenoid valves, temperature and pressure sensors.

The system is controlled by a program written in Python on a laptop computer running Linux. An Agilent 34970A data acquisition/switch unit, connected to the computer via a serial link, is used to interface to the shock tube. A digital interface

on the switch unit connects to a custom-built driver for the eight mains-operated solenoid valves needed to control the tube; the multiplexed voltmeter in the switch unit is used to measure both the voltages from the pressure transducers and the resistance of the platinum resistance thermometers.

Two gas manifolds are used: a high pressure manifold supplying the driver and buffer sections of the tube and a low pressure manifold supplying the driven section. A pressure transducer on the high pressure manifold enables the computer to determine if there is sufficient pressure in the manifold to operate the tube.

Three gas handling channels are provided which control the driver section, the buffer section, and the driven section. Each channel has a solenoid valve which vents the associated section to atmosphere and a pressure relief valve to ensure that the parts of the tube cannot be pressurized beyond their maximum working pressure. Each channel also has a solenoid valve and flow control valve which allow each section to be filled from its associated manifold at a controllable rate. The rate is set to allow time for pressure measurements to be made and acted upon by the computer to ensure accurate control of the pressure in each section of the tube. The pressure transducer for the driver section is mounted close to the pressurization port on the end flange of the driver to minimize measurement errors caused by flow-induced pressure drops in the supply tubing. In addition, to increase the speed of venting of the buffer section, the solenoid valve which vents it is mounted directly next to it. The driven section is provided with two extra solenoid valves. One isolates the driven section from the gas handling system to avoid the chance of damage to the pressure transducer caused by the rapid, possibly over-range, pressure changes which accompany the firing of the tube. The other connects a vacuum pump to the driven section to allow gas to be removed so that the section can be either used at different pressures or filled with pure gas for measurements involving gases other than air.

The temperature of the gas in the driven section is inferred from measurements of the resistance of general purpose Pt100 platinum resistance thermometers which are placed in good contact with the walls of the tube. The gas is left for a few minutes to come to thermal equilibrium with the walls before a firing and the temperatures near the two ends of the tube are measured; the thermometers are then removed from their wells to avoid their being destroyed by the accelerations of the tube which accompany a firing.

6 Shock Pressure Measurements

Two pressure sensors in the side wall of the driven section are used to derive the velocity, and thereby the Mach number, of the shock wave by measuring the time delay between shock detections, as demonstrated by figure 7 (derived from a different shock tube set-up). The sensors are at right angles to the shock front and so, although the shock wave has a rise time of the order of 1 ns, the rise time of the pressure recorded by the sensor is proportional to the diameter of the sensor diaphragm divided by the shock velocity. For the conditions in this shock tube, this time is of the order of 10 µs. The velocity can then be calculated from the known 400 mm separation between the sensors and the measured time interval between the two detections, with an uncertainty of approximately 1 %. This uncertainty is largely derived from our

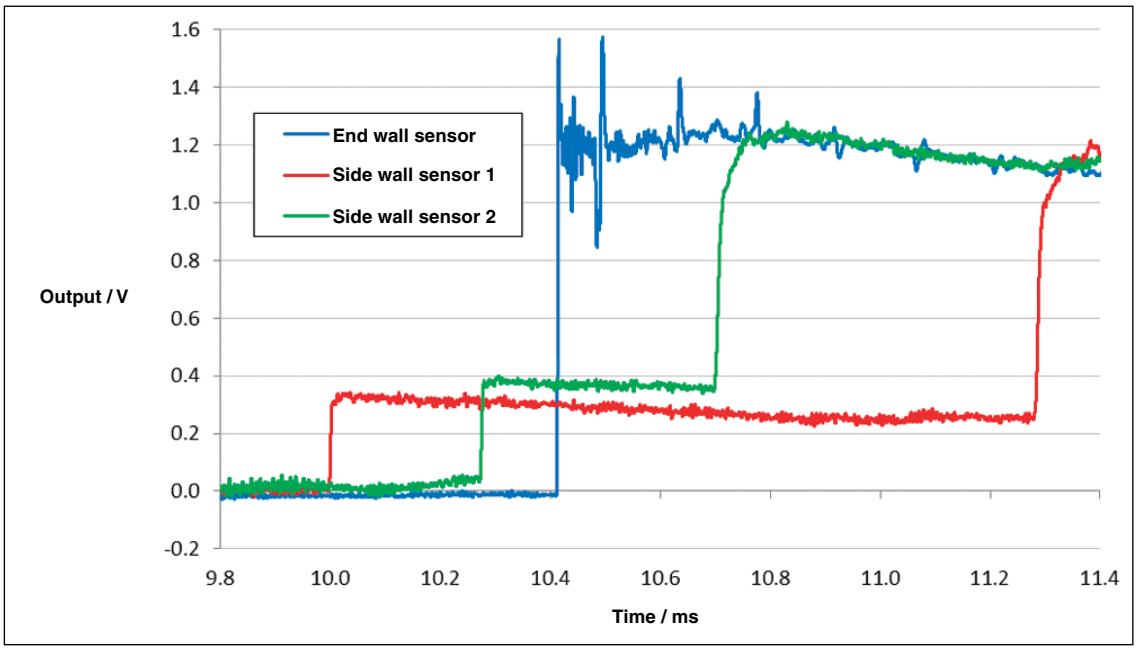

Figure 7: Estimation of the shock wave velocity. As the shock wave propagates down the driven section it first passes sensor 1 and then sensor 2 before reflecting from the end wall and travelling back past these two sensors.

present knowledge of the equality of the rise time of the sensors and charge amplifiers in response to the shock wave passing over the sensor diaphragm. In future, with further investigations, this uncertainty can be reduced considerably. The sensor having its dynamic response characterized is mounted centrally on the end wall of the driven section with its surface flush with the wall. Four identical piezoelectric sensors (Kistler model 603B) were used in this study; they have a 20 MPa input range with a natural frequency specified to be approximately 300 kHz. The output of each piezoelectric sensor was connected to a charge amplifier (Kistler 5015A) having a 200 kHz low pass filter on its voltage output. The outputs of the charge amplifiers are sampled synchronously using a flexible resolution digitizer (National Instruments PXI5922) having a resolution greater than 20 bits and a sampling rate of 2 MHz. Data is taken for a time of 200 ms with 10 ms of data acquired before the trigger event. The sampler is triggered on the rising edge of the output of the pressure transducer in the end wall of the shock tube.

7 Validating the Applicability of the Theory to the Operation of the Shock Tube

Ideal gas theory predicts that a perfect step, lasting several milliseconds, should be recorded by the data acquisition system when the shock wave is reflected from the end wall of the tube. However, in practice, many effects will prevent such an ideal event being recorded. For example, it has long been established that the pressure and temperature do not remain perfectly stable behind the reflected shock front [11–12]; but these and other effects must be investigated both directly and indirectly to eliminate/reduce their impact and to provide an estimate of the accuracy with which the pressure transducer can be calibrated by application of the ideal gas theory. The effects investigated include the following.

The effects of the diaphragm and tube length: the diaphragm does not open instantaneously and this could have an effect on the shock wave shape. The opening times of diaphragms vary considerably even within a single batch of diaphragm material, and the effect is likely to diminish with distance from the diaphragm. It is necessary to investigate the effect of differing diaphragms and the length of the tube on the shape of the pressure step.

The effects of secondary shock waves: these can be generated by the interaction of the main shock wave with imperfections in the tube; either on the inner surface of the tube or in the junction between the tube and the end wall. These secondary shock waves pass over the sensor following the reflection of the main shock and generate transient signals in the sensor output. The effect of these must be eliminated from the measurement.

The effects of accelerations: the firing of the tube and the reflection of shock and rarefaction waves cause accelerations of the tube wall and the sensor mount. Modern pressure sensors used in dynamic applications can be designed to be relatively insensitive to accelerations but investigations need to be made to characterize the effects of acceleration on the pressure measurements.

The effects of varying the gas species and initial pressure: changing the species and pressure of the driven gas constitutes a powerful test for the agreement between theory and practice. The theory used to derive figure 2 predicts the pressure step given a measurement of the velocity of the shock wave and the initial static pressure and temperature in the driven section. The results for differing gases/pressures can be compared by assuming that a stable, linear pressure sensor is used to measure the pressure step. The quality of the agreement between results for monatomic and diatomic gases of differing molecular weights provides a good test of both the theory and the practice in the particular environment of this shock tube and leads to a way of calibrating the pressure sensor.

8 Test Results

8.1 Diaphragm material

The theory of the shock tube assumes that the diaphragm is removed instantaneously at the time the tube is fired. This does not happen in practice and the diaphragm opens over a period of a few hundred microseconds. However as the shock wave moves ahead of the contact surface, created by the opening of the diaphragm, it will encounter undisturbed gas and after a short time its shape should be largely independent of how it was formed as long as the diaphragm does open fully in a relatively short time. Tests were carried out to assess the influence of different diaphragm materials and, by implication, differing opening characteristics, on the shape of the generated dynamic pressure signal. Diaphragms of aluminium, brass, and copper, of various thicknesses, were burst and the resulting pressure transducer waveforms are shown in figure 8 (to aid comparison, these have been normalized to a value of 1.0 corresponding to the initial peak output after arrival of the shock front).

These results are some of the first to be taken with the plastic shock tube and the sensor was mounted at the end of the tube close to the plane of the flange adaptor. In this position there are many features in the wall of the shock tube which can produce reflected shock waves moving across the tube and this is likely to be the cause of the

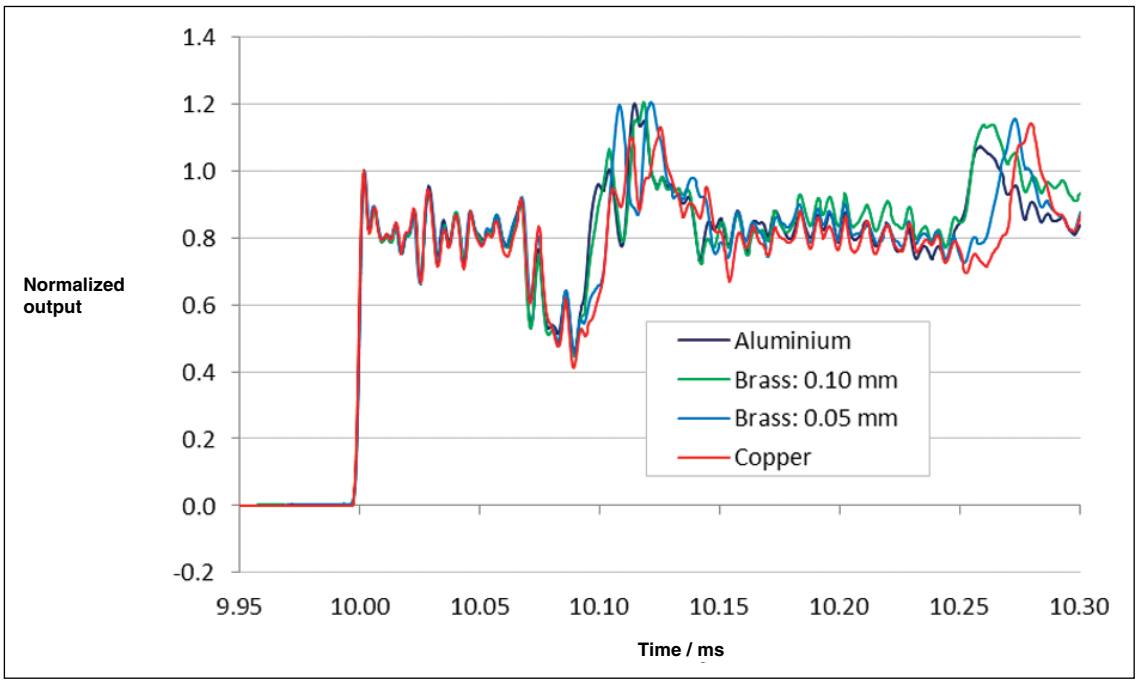

Figure 8: Comparison of diaphragm materials used in a single diaphragm arrangement. Burst pressures of approximately 1.3 MPa were obtained with the aluminium and brass (0.1 mm) diaphragms and approximately 0.8 MPa for copper and brass (0.05 mm).

feature seen in the period from 10.07 ms to 10.14 ms. The response of the transducer to the shock front in the first 0.06 ms is almost identical in all four cases suggesting that possible variations in the shock front due to differing diaphragm materials are insignificant when compared with other features seen in the output (possibly due to ringing in the dynamic response of the transducer).

8.2 Modifications to the sensor mount

In an attempt to reduce the magnitude of the pressure signal feature seen after 10.07 ms, the 70 mm diameter, 25 mm deep steel sensor holder was incorporated within a machined 80 mm long acetal rod which was bolted to an acetal flange. Figure 9 shows the rod and flange with a brass sensor holder. The rod diameter was adjusted to be a close fit within the tube. This moved the point at which the shock wave was reflected into the uniform section of the tube, providing fewer features to generate strong secondary shocks. The acetal rod was machined to leave an approximately 0.5 mm high annular lip around the steel sensor holder which could be removed later to determine the importance of such small features in generating secondary shock waves.

8.3 Driven section length / Burst pressure / Diaphragm configuration

With the location of the sensor mount altered, further tests were carried out with the two different thickness brass diaphragms, with different driven lengths, and with both single and double diaphragm

Figure 9: Acetal sensor mount showing annular lip that was machined flush with the insert (a brass insert is shown here).

arrangements. The results are shown in figure 10.

It is apparent that the periodic content of the output trace seems relatively unaffected by the various different experimental variations, particularly in the initial 0.06 ms period after arrival of the shock front, suggesting that these variations are of secondary importance. It can also be seen that the feature from 10.07 ms has changed significantly, and repeatably for the four different loading cases, from the previous experimental conditions, and that the pressure continues to vary significantly within the succeeding 0.05 ms period.

8.4 Further modifications to the transducer mount

The annular lip, left on the acetal rod (figure 9), was machined and then polished flush with the steel sensor holder. Figure 11 compares the results obtained in the two subsequent tests with those from the previous runs using the 0.1 mm brass diaphragm material and a 4 m driven section.

It is clear that this modification has significantly

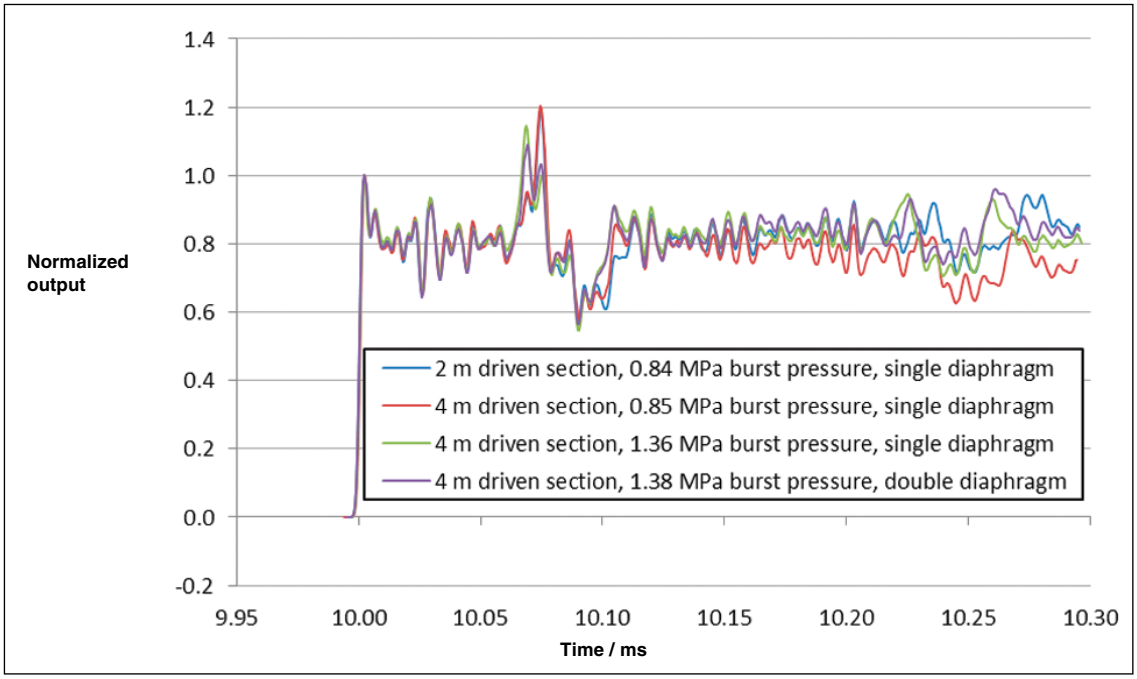

Figure 10:
Effects of driven section length, driver section pressure, and diaphragm configuration.

reduced the magnitude of the previously identified characteristic, lending support to the hypothesis that this was the result of pressure variations initiated at the sensor mount/tube interface when the shock front arrived. Any disturbances originating from the area around the tube wall, travelling at the speed of sound in the heated gas behind the reflected shock front (approximately 490 $m \cdot s^{-1}$) will reach the centre of the transducer diaphragm after an interval of approximately 0.08 ms which is consistent with the results obtained.

The pre-modification traces also show disturbances to an underlying flat response at about 0.24 ms after arrival of the shock front – this could be explained by the pressure waves generated at the tube edge 'bouncing' across the face of the sensor mount, travelling a distance of three radii before impinging on the transducer's face for a second time. These effects, although much smaller in magnitude, are still apparent when using the modified mount.

8.5 Driven pressure values

The driven section of the tube is able to have its initial pressure varied, to either above or below atmospheric pressure, to vary the amplitude and speed of the pressure step. A set of three tests was performed with the initial driven section absolute air pressure being set to 0.008 MPa, 0.034 MPa,

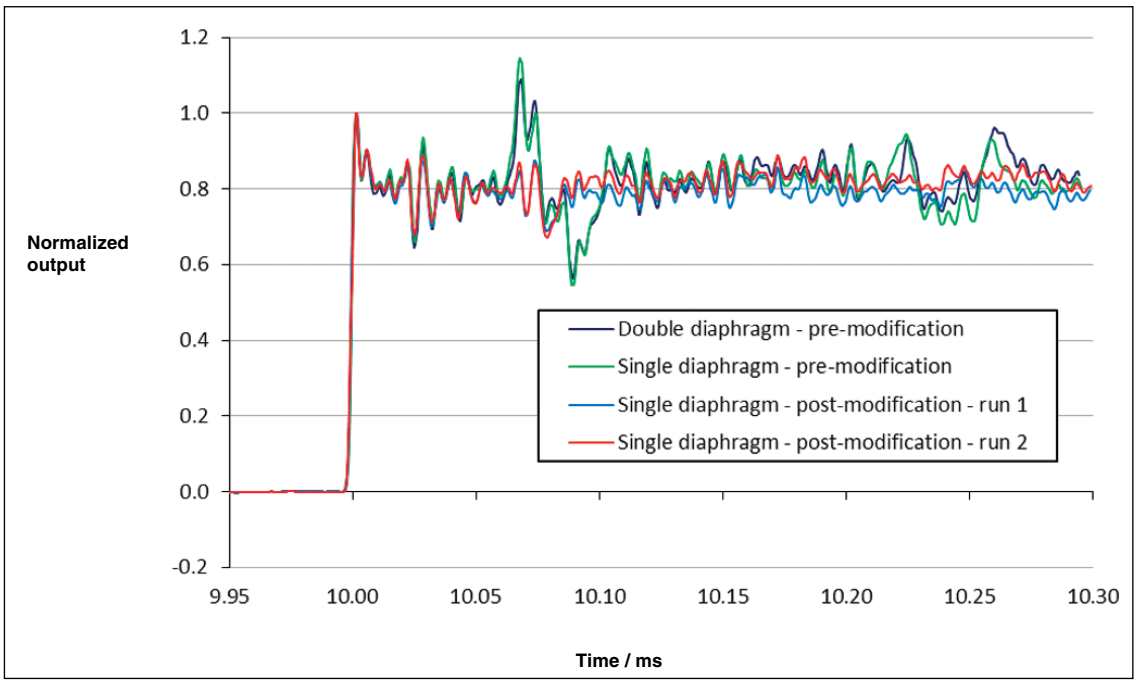

Figure 11:
Effect of transducer mount modification.

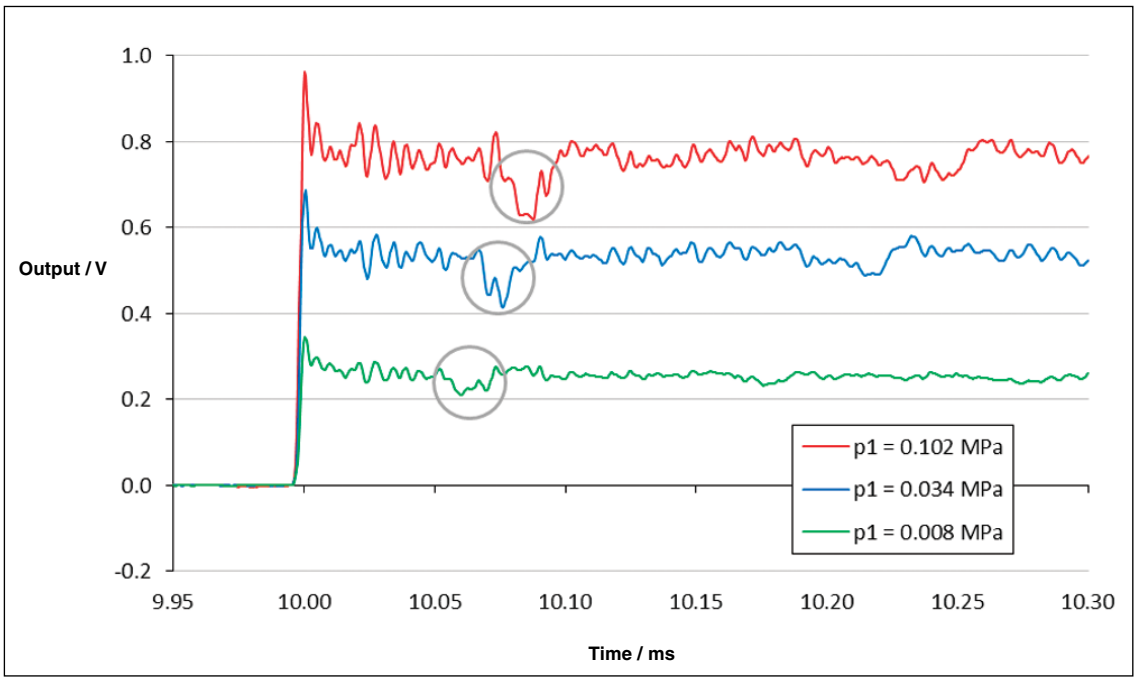

Figure 12:
Effect of varying initial driven section pressure.

and 0.102 MPa, using the 0.05 mm brass diaphragm material (figure 12).

The results demonstrate an increase in pressure step magnitude with an increase in initial pressure in the driven section; shock front velocity measurements also agree with theory, showing an increase in velocity with a decrease in driven section pressure (from 554 $m \cdot s^{-1}$ at 0.102 MPa, through 680 $m \cdot s^{-1}$ at 0.034 MPa, to 864 $m \cdot s^{-1}$ at 0.008 MPa). When the normalized output traces are plotted against time (figure 13), the first anomalous portion can be seen to occur at different times (these events are also indicated by the grey circles in figure 12) – this is explained by the increase in speed of sound in the gas caused by the higher temperatures resulting from the tests with lower pressure in the driven section (figure 4). The second anomalous section also arrives correspondingly earlier in the lower pressure tests (at around 10.17 ms when p_1 = 0.008 MPa and 10.21 ms when p_1 = 0.034 MPa, as opposed to 10.24 ms when p_1 = 0.102 MPa).

8.6 Driven gas

As shown in the theory section, the two gas species used within the driver and driven sections affect the magnitude of the generated pressure step. Two pairs of tests were carried out with the 0.1 mm brass diaphragm material using first helium and then argon

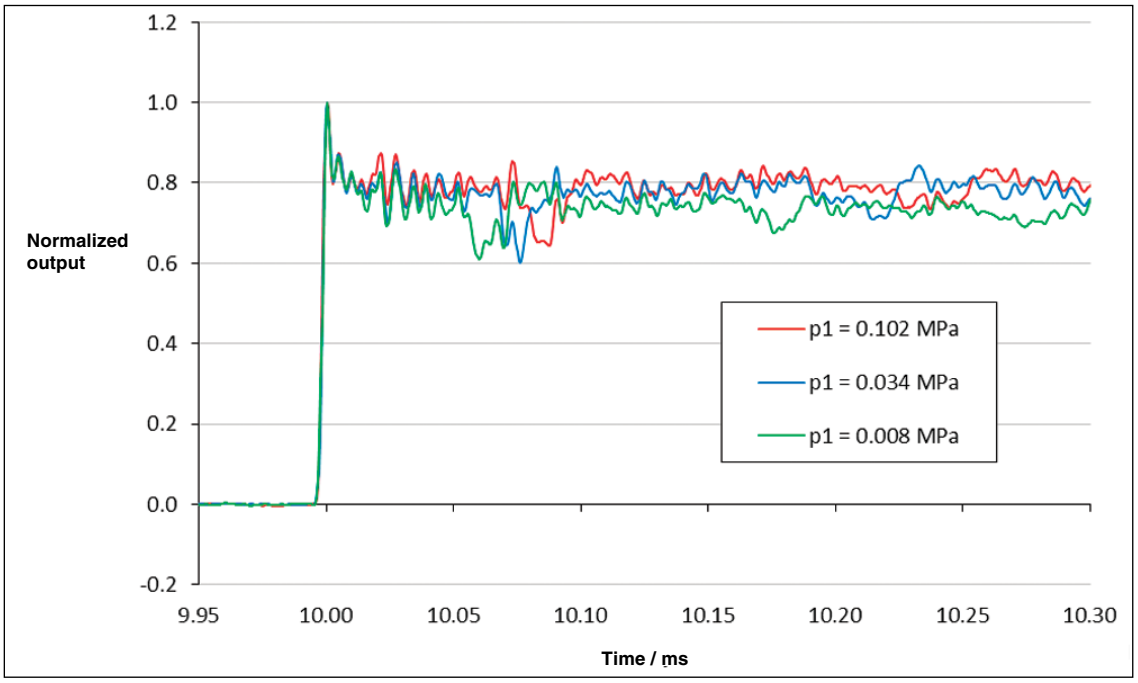

Figure 13:
Normalized results showing effect of varying initial driven section pressure.

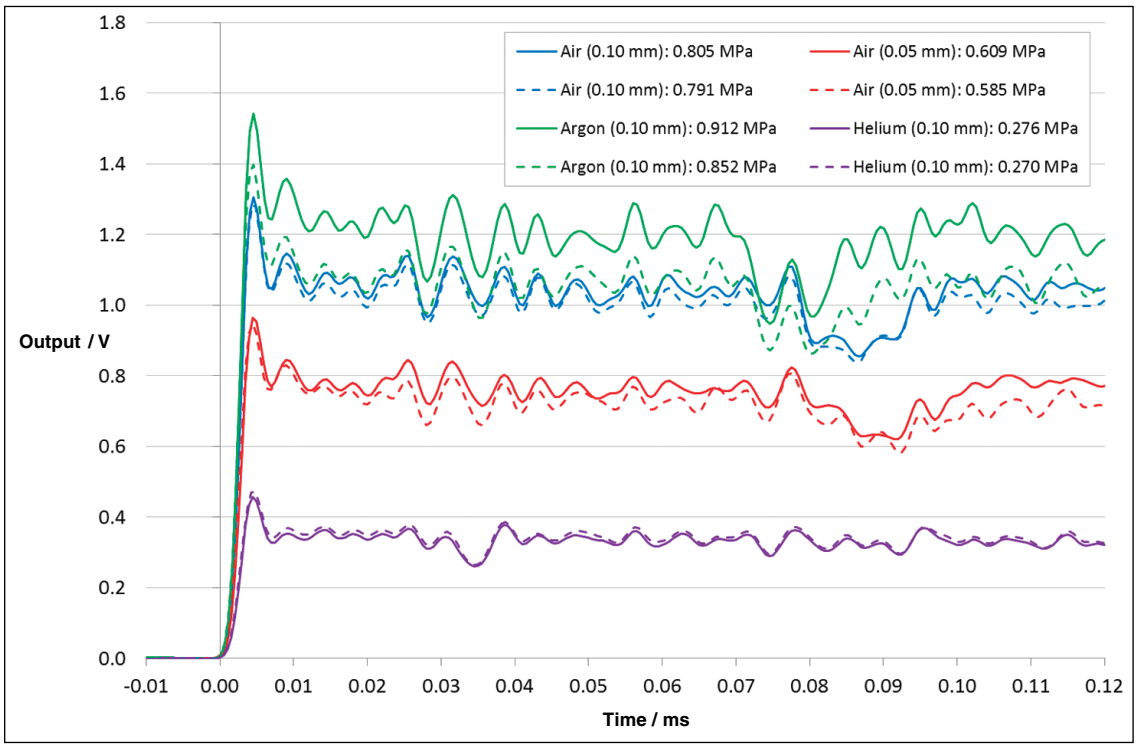

Figure 14:
Variation of driven section gas species.

(both nominally at atmospheric pressure) within the driven section, and the resulting measurements compared with the traces obtained with air in the driven section, for both thickness diaphragms. For each trace, given in figure 14, the magnitude of the generated pressure step at the tube end, calculated from the ideal gas theory, is given within the key. The waveforms are plotted in terms of voltage rather than pressure to emphasize that voltage is the quantity recorded and that the static sensitivity of the gauge is not necessarily correct on this timescale.

If we assume that the value of the pressure step calculated from theory is correct and remains constant throughout the period of the measurement, it is possible to calculate the instantaneous sensitivity of the sensor. Figure 15 shows the results replotted as the sensitivity of the sensor in units of pC·bar^{-1}. This simplifies comparison with the sensor's static sensitivity of –4.759 pC·bar^{-1}, as determined by its manufacturer.

The agreement between the four dynamic traces (which are derived from the means of each pair of

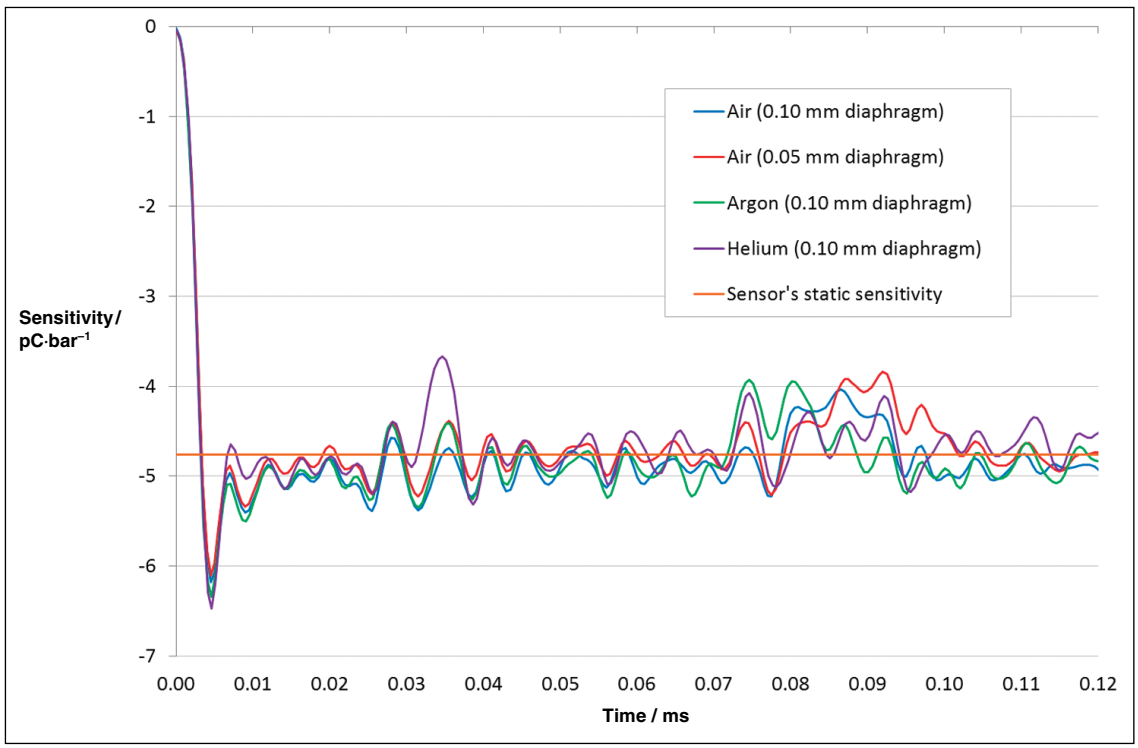

Figure 15:
Pressure sensor sensitivity in response to pressure step.

traces given in figure 14), both in terms of absolute magnitude and in terms of amplitude and frequency content around the underlying trend, gives confidence that the theory is correctly predicting the behaviour of the gas within the tube. Discrepancies between the traces, such as the early arrival of the anomalous portion within the helium trace, can be explained by factors such as the much faster speed of sound in the lighter gas. The agreement with the sensor's static sensitivity gives further confidence that the pressure step is being calculated correctly.

Comparison of the results in figure 15 assumes that the sensor has a linear response; in subsequent work the linearity condition can be relaxed by generating pressure steps which are calculated to be identical in different gas species. As long as the sensor response is not affected by gas species, the linearity of the sensor does not affect the result and allows uncertainties due to the operation of the shock tube to be assessed at a number of pressures. The results can then be used to assess the linearity of the sensor.

The possibility that a significant proportion of the dynamic content of the waveforms might be due to the mechanical vibration of parts of the shock tube apparatus, rather than the transducer itself, still needed to be investigated.

8.7 Sensor mount block material

Although the sensor is designed to be insensitive to acceleration, the magnitudes of the accelerations generated by the shock wave in the sensor mounting block are very high. In order to determine how much of the frequency content of the transducer output might be due to acceleration, as opposed to its inherent dynamic response to a pressure step, sensor mounting blocks of different material, but identical geometry, were manufactured to enable accelerations of different amplitude and frequency to be applied to the sensor. Figure 16 gives typical responses from steel, aluminium, and brass mounts.

Although the underlying characteristics obtained from the three mounts are broadly similar, there are significant differences in the amplitudes of the variation about this underlying trend. The increased amplitudes of the dynamic components recorded during the aluminium and brass sensor mount tests, when compared with the steel mount, suggest that vibration of these components may be a significant factor in the sensor output. The elastic modulus of aluminium is approximately three times lower than that of steel, and that of brass a factor of approximately two times lower, suggesting that the resulting dynamic elastic strains within sensor mounts of these materials may be significantly higher than those in a steel sensor mount when subjected to the same step force input.

In order to compare the frequency content of the outputs obtained using the three different block materials, a basic Fourier transform of the time series data was performed, and the results are shown in figure 17.

These plots further demonstrate that the output of the pressure transducer, in response to a step change in input, is strongly influenced by the material of the mount in which it is supported, with frequency peaks (shown circled in grey)

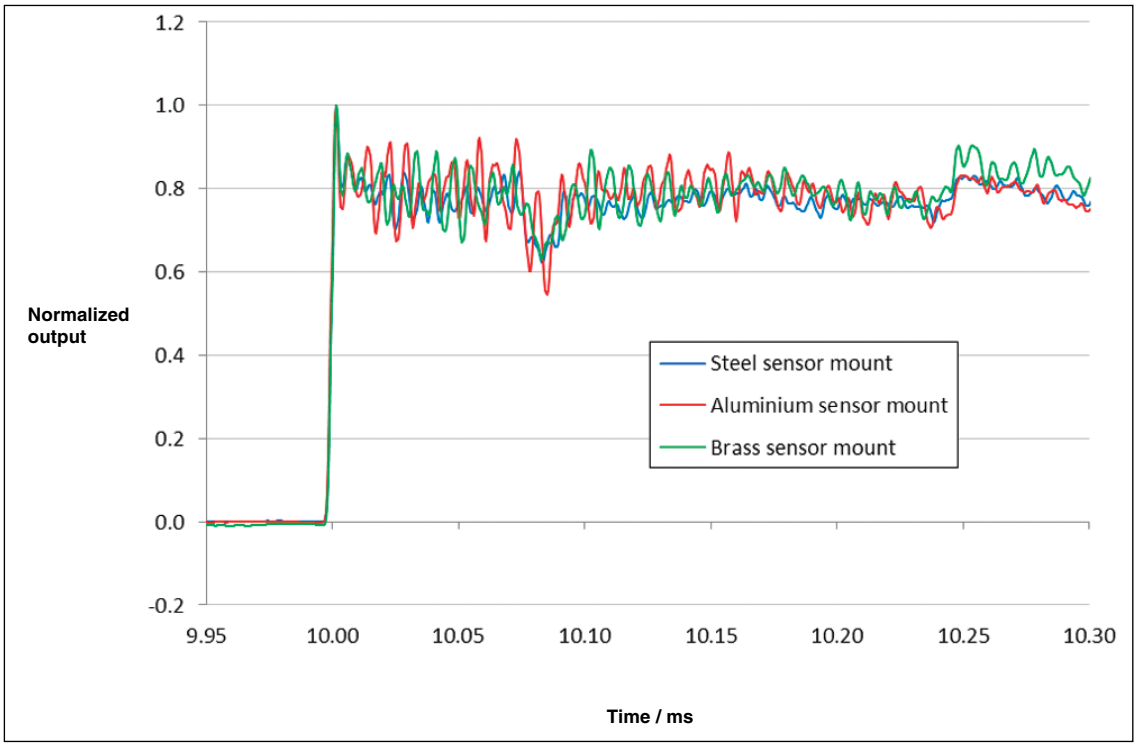

Figure 16: Results obtained with different sensor mount materials.

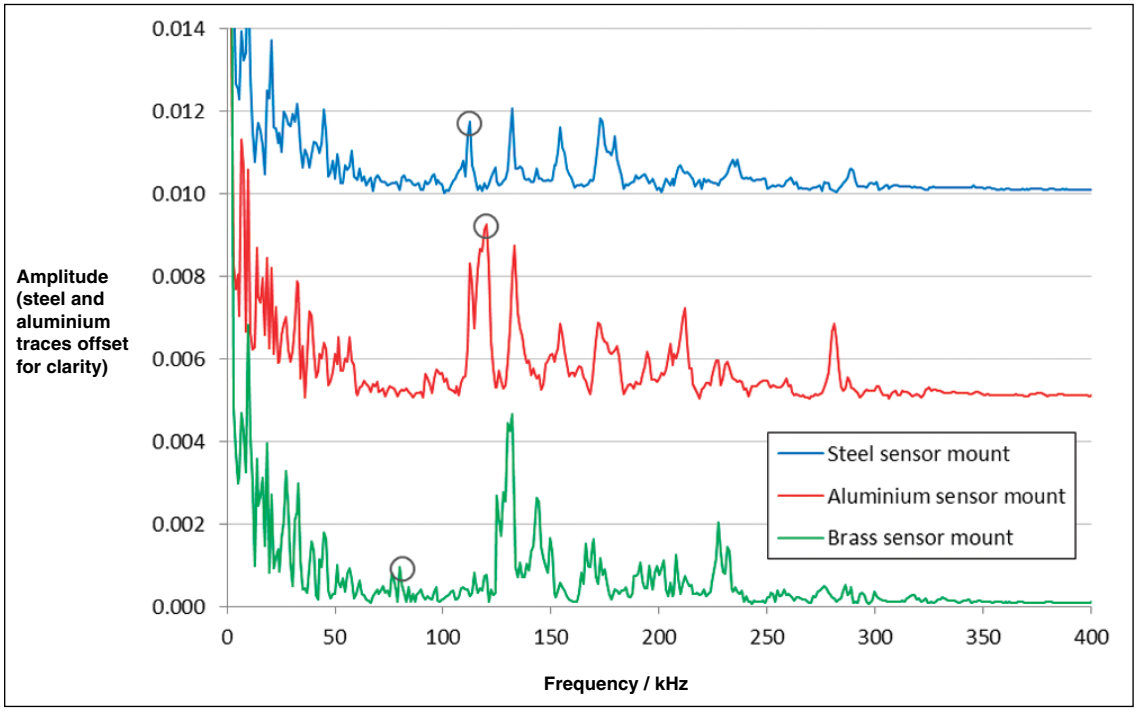

Figure 17: Fourier transform of results obtained with different sensor mount materials.

coinciding with the primary mode of longitudinal vibration for each mount [13] – the lower amplitude of the peak for the brass mount is likely to be due to the sensor's inbuilt acceleration compensation being more effective at lower frequencies. Vibration of the mount will produce acceleration-induced charges within the sensor, generating spurious signals. Methods to reduce or separate these signals from the underlying pressure response need to be investigated and developed.

9 Conclusions

We have developed a novel plastic shock tube and have investigated the effect of diaphragm material, thickness, and configuration, and driven section length, on its operation, and none were found to affect the measured pressure trace significantly. Driven section pressure and gas species were varied and the effects of these variations were found to be consistent with ideal gas theory as applied to a shock tube. The results of the tests performed within the 1.4 MPa shock tube therefore demonstrate that it has the capability to act as a primary dynamic pressure standard, generating extremely rapid pressure steps of calculable magnitude, to characterize the dynamic performance of pressure sensors. As pressure sensors may also be sensitive to acceleration, further work is required to eliminate any effect of acceleration of the sensor mounting block on the calibration result. It should be noted that the method of mounting the sensor in practical applications will be critical to its dynamic performance.

Acknowledgements

This work is supported by the National Measurement Office, an executive agency of the Department for Business, Innovation & Skills, under its Engineering and Flow Metrology Programme, and has also received support from the European Metrology Research Programme (EMRP). The EMRP is jointly funded by the EMRP participating countries within EURAMET (the European Association of National Metrology Institutes) and the European Union.

References

[1] T. J. Esward, *Analysis of Dynamic Measurements: New Challenges Require New Solutions*, XIX IMEKO World Congress, Lisbon, Portugal, 2009.

[2] S. Eichstädt, *Deconvolution Filters for the Analysis of Dynamic Measurement Process: A Tutorial,* Metrologia, 47, pp. 522–533, 2010.

[3] C. Bartoli, M. F. Beug, T. Bruns, C. Elster, T. Esward, L. Klaus, A. Knott, M. Kobusch, S. Saxholm and C. Schlegel, *Traceable Dynamic Measurement of Mechanical Quantities: Objectives and First Results of this European Project*, International Journal of Metrology and Quality Engineering, 3, pp. 127–135, 2012.

[4] M. Syrimis and D. N. Assanis, *Knocking Cylinder Pressure Data Characteristics in a Spark-Ignition Engine*, Journal of Engineering for Gas Turbines and Power, 125 (2), pp. 494–499, 2003.

[5] C. Hudsona, X. Gaoa and R. Stoneb, *Knock Measurement for Fuel Evaluation in Spark Ignition Engines*, Fuel, 80 (3), pp. 395–407, 2001.
[6] M. Brunt, C. Pond and J. Biundo, *Gasoline Engine Knock Analysis using Cylinder Pressure Data*, International Congress and Exposition, Detroit, USA, 1998.
[7] H. J. Pain and E. W. E. Rogers, *Shock Waves in Gases*, Reports on Progress in Physics, 25 (1), pp. 287–336, 1962.
[8] D. W. Holder and D. L. Schultz, *On the Flow in a Reflected-Shock Tunnel*, HMSO, London, 1962.
[9] J. Teichter, *Design of a Shock Tube*, SP Measurement Technology, Borås, Sweden, 2005.
[10] R. J. McMillan, *Shock Tube Investigation of Pressure and Ion Sensors Used in Pulse Detonation Engine Research*, Air Force Institute of Technology, Dayton, USA, 2004.
[11] E. L. Petersen and R. K. Hanson, *Nonideal Effects Behind Reflected Shock Waves in a High-Pressure Shock Tube*, Shock Waves, 10 (6), pp. 405–420, 2001.
[12] S. Li, W. Ren, D. F. Davidson and R. K. Hanson, *Boundary Layer Effects Behind Incident and Reflected Shock Waves in a Shock Tube*, 28th International Symposium on Shock Waves, Manchester, United Kingdom, 2012.
[13] S. Downes, A. Knott and I. Robinson, *Determination of Pressure Transducer Sensitivity to High Frequency Vibration*, IMEKO 22nd TC3, 12th TC5 and 3rd TC22 International Conferences, Cape Town, South Africa, 2014.

Measuring Dynamic Pressure by Laser Doppler Vibrometry

Thomas Bruns*, Oliver Slanina

* Dr. Thomas Bruns, Department "Velocity", PTB, e-mail: thomas.bruns@ptb.de

Abstract

The primary calibration of pressure transducers is at present realized by static procedures only. Subsequent dynamic calibrations in this field are realized by comparison measurements with a statically calibrated reference sensor. This paper describes a route to gain traceability for dynamic calibration by means of laser interferometry. As an instantaneous inertia-free measurement, the described procedure has the potential to measure the so far unknown dynamic response of pressure transducers directly with far higher bandwidth than available by the use of a classical reference transducer. This article describes the general principle employed to gain traceability, the experimental set-ups which are used for the realization, some thermophysical and interferometric background of the measurements, and the first measurement results acquired with the new set-up.

1 Introduction

Traceability of pressure measurements for static as well as dynamic applications is nowadays exclusively provided in terms of a chain of static comparison calibrations to reference standard transducers with typically a deadweight pressure balance at the top end as primary realization of pressure in terms of force per cross-sectional area.

While this is an effective procedure for static measurements, in the case of dynamic measurements this process leaves the user blind to inertia effects compromising his measurement data. That means, the transducer itself may react to a dynamic input signal with a specific response that originates from the mechanical design as much as from the original pressure input. Parts of the mechanical components of the transducer, like the sensitive membrane, are accelerated under pressure load. Since those parts have a certain mass and are coupled to the housing with a certain stiffness, they form a mechanical oscillator that may respond with its eigenmodes.

An additional influence arises from the coupled electronics in terms of a conditioning amplifier, which may even be embedded into the transducer and therefore inaccessible. These components of the measuring chain have a limited bandwidth and often high-pass characteristics, which may lead to distortions of the output in comparison to the input.

As a consequence, the metrology of dynamic pressure signals is currently affected by several imponderabilities which lead to a certain uneasiness concerning the reliability of such measurements in many industrial areas.

Therefore it is desirable to establish a calibration method that provides a proper representation of the dynamic pressure input signal devoid of inertia effects and independent of a classical reference transducer.

If inertia is an issue, usually optical methods using light as a means of measuring are the answer. Accordingly, PTB followed an approach to measure the dynamic pressure in a calibration device by using laser interferometric means.

2 The Interferometric Principle

The laser Doppler vibrometer (LDV), which is used in the proposed device, is by principle a modified Mach-Zehnder interferometer (cf. figure 1), where the reference beam is shifted in its optical frequency due to Bragg refraction in an acousto-optical modulator (AOM or Bragg cell). In the case of the device used in our application, the frequency shift is 40 MHz. This has the consequence that the photodiode detects an interferogram intensity-modulated with 40 MHz if the object beam is reflected from a non-moving target, or more precisely, when the object beam passes a constant optical path length before it is superposed to the reference beam. Any dynamic change of the optical path length results in an additional frequency shift to frequencies higher or lower than 40 MHz depending on the direction.

A measurement of a dynamically changing optical path length results in a frequency-modulated (FM) signal output of the photodetector (PD) that can be analysed by any FM demodulation technique.

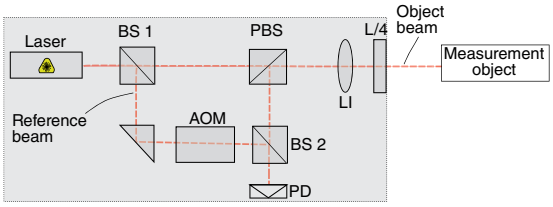

Figure 1:
Internal set-up of the heterodyne laser Doppler interferometer (BS = beam splitter, PBS = polarizing BS, L/4 = quarter wave plate, LI = lens, AOM = acousto-optical modulator (Bragg cell), PD = photodetector).

This principle makes these devices very sensitive even to small changes in the optical path length. Since no mechanical parts are included in the measurement, these systems provide a high bandwidth of measurement, in our case in the megahertz range, which is roughly an order of magnitude more than the classical electro-mechanical transducer systems are able to provide.
In addition, the frequency response is rather flat if proper care is taken into account and a so-called digital demodulation is applied. A flat frequency response means that the dynamic output from the device can be considered (simply) proportional to the input measurand over a wide range of frequencies.

3 The Device Set-Up

In the calibration system described here, a hydraulic medium is used to generate and transmit the pressure. The medium is compressed by means of a cylindrical piston that is forced into the medium and therefore reduces the available volume. Accordingly, the pressure and density of the medium increase while the volume decreases. The dynamic force that drives the piston into the medium is generated by an impacting steel ball which hits the top end of the piston (cf. figure 2)

The object beam of the LDV described in the previous section is transmitted through the volume of the transparent hydraulic medium and, after passing it, is reflected by a mirror or retroreflector.

The device under test (DUT) or pressure sensor to be calibrated is mounted in a drilled hole on the side of the pressure vessel. Its sensitive front has direct contact with the pressurized medium. A catcher mechanism (not drawn in figure 2) prevents the steel ball from bouncing on the piston. With drop heights of up to 1500 mm, pressure intensities up to 800 MPa (8000 bar) are achievable.

4 Physics of Compression

When the medium is compressed, the mass density increases and, in conjunction, the optical index of

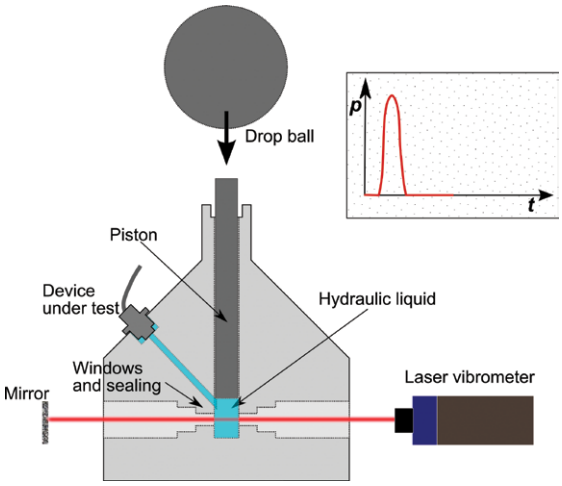

Figure 2:
Drawing of the interferometric measurement set-up used with PTB's drop weight pressure calibration device.

diffraction changes. This change of index of diffraction is the fundamental effect facilitated in the device. It is generally described by the Clausius-Mossotti relation

$$\frac{n^2-1}{n^2+2} = pk \quad \text{or} \quad n^2 = \frac{1+2pk}{1-pk} \,, \tag{1}$$

where n is the index of diffraction, ρ is the mass density, and k is a material-dependent constant factor.

For the measuring laser beam, the change in refractive index is an effective change in the optical path length between the exit aperture of the LDV and the retroreflector. The optical path length is given as the product of the index of diffraction n and the geometric path length s_{geo} *as*

$$s_{opt}(t) = n(t) \cdot s_{geo} \,. \tag{2}$$

As the index of diffraction changes with time, the optical path length becomes a time-dependent quantity, too.

The dynamic change accordingly generates a dynamic frequency shift of the FM signal of the LDV's photodiode. The frequency shift is a measure of the pressure change over time. However, due to the non-linearity of the governing equation (1), the relation between the two is not simply proportional.

5 The Link to Static Pressure

With the equations above, material properties (k) as well as geometric design properties of the device (s_{geo}) enter into the evaluation of pressure. While the first are largely unknown, especially for high pressure, the latter are not easy to determine. This holds specifically for the geometric path length of the laser beam within the pressure vessel. There is, however, a solution to this problem which works without explicit measurement of those quantities. This solution involves a static calibration of

the system consisting of LDV, pressure vessel and retroreflector in relation to static pressure. If the pressure-input-to-voltage-output characteristics of the system are determined statically, these can be applied to dynamic measurements subsequently due to the fact that the LDV employs a principle unaffected by inertia, and provides a by far higher bandwidth than the electro-mechanical system under test.

For the purpose of the static calibration, the mounting hole for the DUT is sealed and a pressure balance is connected to the tube where otherwise the piston is guided. The pressure balance provides a highly precise reference pressure to the vessel that is increased stepwise by the sequence of applied deadweights. During the whole sequence the displacement output of the LDV is acquired by the data acquisition system. The step-like sequence of pressure steps is converted into a step-like sequence of LDV output voltages (cf. figure 3).

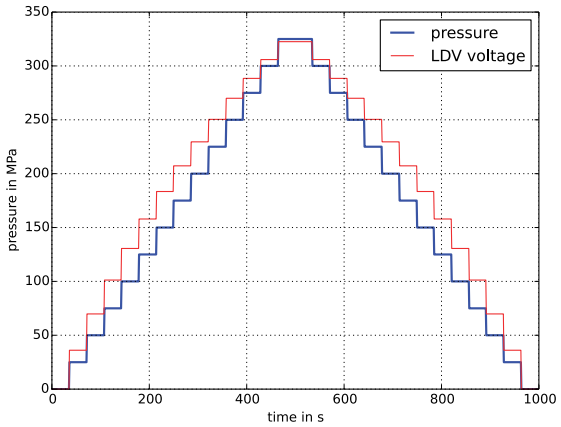

Figure 3: Example of a step-like sequence of applied pressure levels in the process of static calibration of the laser interferometric measurement set-up (so far hypothetical).

For this static calibration the transitions from pressure level to pressure level are ignored and only the stationary signals of each level are evaluated. Unfortunately, due to the form of the Clausius-Mossotti relation, the shape of the resulting calibration curve is non-linear but can be approximated with low deviations by a polynomial of third order (cf. figure 4). It is currently not completely clear what implications arise from the non-linearity for the dynamic calibration in terms of, e.g., harmonic distortion.

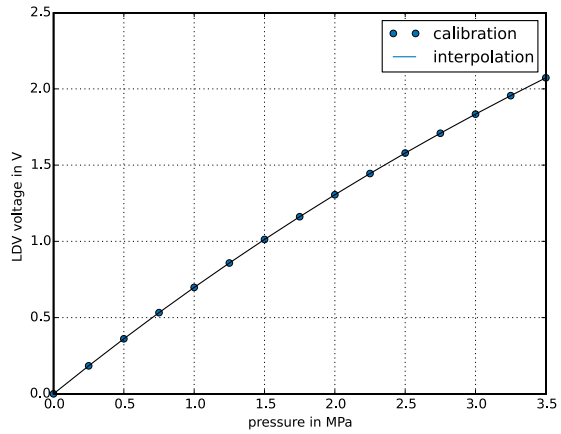

Figure 4: Characteristic curve of the dependence of the LDV output voltage on the applied pressure derived by fitting from the stepwise calibration points at discrete pressure levels.

6 Challenges

On closer inspection one has to realize that there are further systematic differences between the pressurization during an impulse load by an impacting ball and the static calibration.

When a medium is compressed, energy is introduced into the medium. As a consequence, the medium heats up if a finite compression takes place in a finite time. Therefore, the medium encounters an increase in density due to loss of volume and an increase in temperature due to the energy deposited during the compression work. Since pressure, on the microscopic scale, is related to the momentum transferred by the molecules of the medium to the walls of the vessel while moving in Brownian motion, it is dependent on the effective frequency of momentum transfer and thus the density, but also on the effective speed of those molecules and thus the temperature.

According to the previously described mechanism, the hydraulic medium in the pressure vessel heats up shortly during compression, when the steel ball hits the piston, and cools down again during the subsequent expansion or relaxation, when the ball bounces back and the piston returns to its original position. The time scale of this process is a few milliseconds. In this short time the energy deposited in the hydraulic medium has no time to become dissipated by heat conduction. Accordingly, this process can be considered adiabatic.

The compression process during the static calibration, however, performs on a time scale of hundreds of seconds. There is plenty of time for heat dissipation towards thermal equilibrium at all pressure levels. Accordingly, this process can be considered isothermal.

The relationship between pressure and density for a hydraulic medium is different for isothermal and adiabatic processes. Since the LDV method is in fact sensitive to density changes, and ignorant of the temperature of the medium, the consequence is a systematic deviation of the static calibration characteristics from the dynamic measurement situation.

Based on the available material data, the amount of this systematic effect can be estimated and either be considered as a measurement uncertainty or (possibly) corrected for [1].

Another effect that has to be considered in terms of a disturbance or measurement uncertainty component is the inevitable geometric expansion of the pressure vessel during loading. This effect generates a superposed change of the geometric path length, where fractions of the geometric path initially propagating through air in the unloaded case will then propagate through the compressed medium in the loaded case (the sealing glass windows are

considered as incompressible). This is in fact a superposition of two disturbing effects, the first is the geometric expansion and the second is the media change for parts of the path length. The first effect can only be minimized by the choice of the material and technical design of the sealing, which has to be as stiff as possible. The latter effect can be avoided by a modification of the pressure vessel, which adds some volume of the hydraulic media at ambient pressure to the pressurized chamber. Thus, the parts of the ambient pressure volume will be replaced by the high pressure volume without a change of the media [2]. However, this modification is future work and has not yet been implemented in the current test set-up.

7 First Measurements

Despite the further optimizations already described, first measurements were performed with a test set-up depicted in the photograph of figure 5. These were supposed to answer several questions, among which the general feasibility of the method was not the least important. Other practical questions are related to leakage effects of the piston guide way, signal quality and intensity of the LDV, achievable pressure intensities in relation to drop height, and the possible optical disturbances generated by the inevitable mechanical vibration due to the impact of the drop ball.

The hydraulic medium of choice was bis(2-ethylhexyl) sebacate. The pressure reference for these tests was a calibrated piezoelectric pressure transducer, since the linking of the LDV to static pressure was not yet available.

Figure 6 presents the measurement signals for two drops from different heights. The pressure is according to the reference sensor's indication, the LDV voltage is sampled from the analogue displacement output of the LDV controller. The effect of the previously described non-linearity is clearly detectable in the different pulse shapes of the sensor signal compared to the corresponding LDV voltage signal. Apparently the relationship is beyond simple scaling of the signals.

A plot of the LDV output voltage versus the reference pressure, like in figure 7, shows, however, that both measurements follow the same characteristic sensitivity curve.

8 Summary and Outlook

Within the joint research project *Traceable Dynamic Measurement of Mechanical Quantities*, a JRP of the European Metrology Research Program, PTB has set up a new kind of dynamic pressure calibration device for high hydraulic pressures up to several 100 MPa. In order to prevent inertia effects from influencing the measurements, an

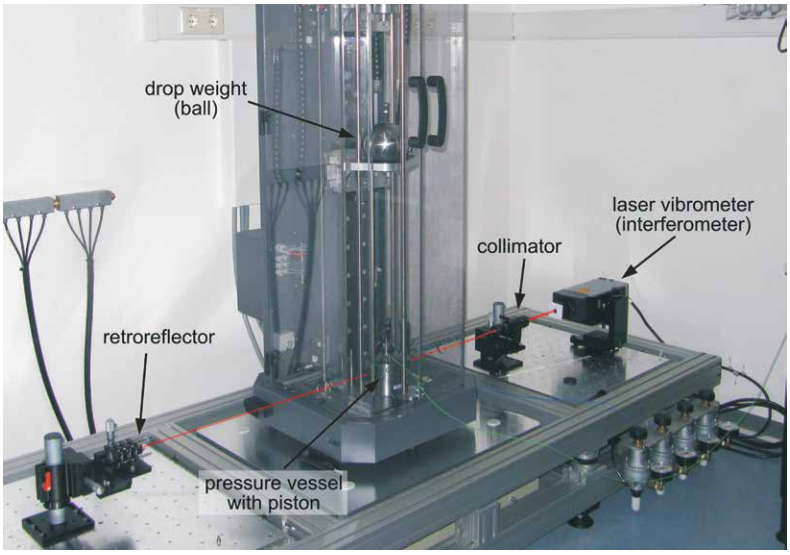

Figure 5:
Photography of the current interferometric drop weight pressure calibration set-up with the main components labeled.

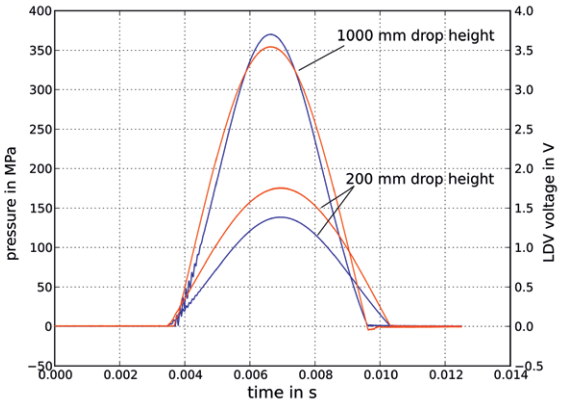

Figure 6:
Pressure pulse measurements from two different drop heights. Red curves are the reference pressure sensor signals, blue curves are LDV displacement signals.

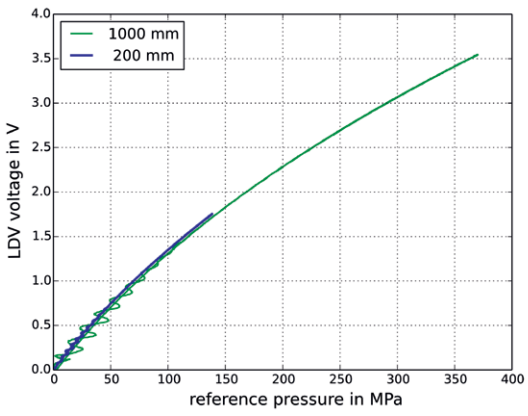

Figure 7:
LDV voltage in dependence on reference pressure for the time series data of figure 6.

interferometric principle is implemented. A heterodyne Mach-Zehnder Interferometer is used to measure the change of the index of diffraction in the pressurized hydraulic medium while a dynamic pressure signal is generated by a drop weight hitting a piston.

While first measurements provided promising signals with good general quality, there are still further investigations necessary to make this new method a national standard. Among other aspects, the non-linearity of the underlying physics has to be investigated and the major sources of measurement uncertainty need to be identified.

Acknowledgements

This work was supported by the European Metrology Research Programme (EMRP). The EMRP is jointly funded by the EMRP participating countries within EURAMET and the European Union.

References

[1] T. Bruns, E. Franke and M. Kobusch, *Linking Dynamic to Static Pessure*, Metrologia, 50, pp. 580–585, 2013, doi: 10.1088/0026–1394/50/6/580.

[2] H. Schramm, *Grundlagenuntersuchungen für die interferometrische Druckmessung unter Nutzung der Druckabhängigkeit des Brechungsindex*, diploma thesis, section 3.7, Hochschule Anhalt, Köthen, Germany, 2013.

Characterization of Force Transducers for Dynamic Measurements

Michael Kobusch*

1 Introduction

The measurement of time-dependent forces has gained particular importance over the past years. In this context, increasing demands on measurement accuracy have brought new challenges to be solved for the metrological community.

Dynamic force measurements are widely used and play an important role in many industrial areas, for example in the field of material testing, automation and handling engineering, production engineering, vibration tests of mechanical and electronical components for the aerospace industry, and crash tests for safety standards in the automotive industry.

Depending on the specific dynamic application, the nature of the dynamic force differs considerably from case to case. For example, sinusoidal (or periodic) forces are usually applied in fatigue tests, step-like and continuous forces in machining processes, and shock forces in crash tests. A requisite for reliable dynamic measurements is the establishment of an infrastructure for traceable dynamic measurements that is capable of covering such very different load conditions.

1.1 Measurement standards and practice

Whereas the static calibration of force transducers is described by international standards (DIN EN ISO 376, [1]), documentary standards or commonly accepted guidelines and procedures for dynamic measurements are still lacking. Therefore, it is common practice to perform dynamic measurements with force transducers which are only statically calibrated.

However, there is wide agreement that dynamic calibrations are actually needed. To give an example, standards on instrumentation for crash tests in the automotive industry (ISO 6487 [2], SAE J211/1 [3]) already specify error limits for the amplitude response of measurement transducers, pointing out that satisfying methods for dynamic force calibrations currently do not exist.

Only for the special application of the dynamic force calibration for uniaxial fatigue testing, an international standard (ISO 4965 [4]) has been defined which is based on comparison methods using sinusoidal excitation.

Because of the unsatisfying normative situation, some information about the dynamic performance of a force transducer is often obtained by performing additional measurements using suitable dynamic testing devices. Such measurements are especially well suited to investigate about whether the dynamic measuring behaviour of a force transducer has changed in the course of time and if a replacement is needed. Therefore, some dynamic testing for comparison purposes is already widely used in industry.

1.2 Metrological challenge

If a force transducer is subjected to dynamic loads, the mechanical structure reacts with frequency-dependent inertia forces that compromise the input force to be measured [5]. Further influences may result from the coupled mechanical environment, e.g. the force introduction, the adaptation at the base, or other components of the measurement set-up.

Moreover, the dynamic behaviour of the electrical signal chain must also be considered to fully understand the dynamic measurement data. In general, dynamic measurements are concerned with a frequency-dependent measurement behaviour that may arise to some extent.

Given the diversity of dynamic applications and their specific signals, it is important to know under which conditions dynamic effects should be taken into account and whether dynamic measurements can still be performed with statically calibrated transducers. In this context, the disturbing inertia forces must not exceed the required measurement uncertainty. To be able to give a satisfying estimation, knowledge of the dynamic behaviour of the transducer as well as of the measuring set-up is needed.

1.3 Dynamic suitability

As a first step, the selection and assessment of a force transducer to be used for dynamic mea-

* Dr. Michael Kobusch, Working Group "Impact Dynamics" e-mail: michael.kobusch@ptb.de

surements is frequently based on its **fundamental resonance frequency**, which denotes the lowest mechanical resonance along the measuring axis for a transducer rigidly mounted at its base. A respective frequency value is often specified in the data sheets. A normative document that includes this characteristic parameter relevant to dynamics is the German Directive VDI/VDE 2638 [6] on the characteristics of force transducers.

Knowledge of the fundamental resonance gives a first indication of the usable frequency range. However, one has to keep in mind that the resonance of a mechanical structure depends on its elastically coupled mass elements. For instance, a combination of high stiffness and small vibrating mass will give high frequencies. In a given application, force transducers are always coupled to a mechanical environment resulting in a dynamic behaviour that may differ substantially from that of the bare transducer.

It becomes clear that the fundamental resonance does not suffice to understand the dynamic measurement behaviour of a force transducer in its application. Instead, it is very important to have information about the structural distribution of the transducer's **stiffness** and **mass**, which actually is the key data for a profound understanding of its dynamic performance.

Within the scope of the European research project EMRP IND09 *Traceable Dynamic Measurement of Mechanical Quantities*, the general approach of a **model-based calibration** has been followed. The dynamic behaviour of the force transducer, as well as of its measurement set-up, is described by an appropriate physical model, which for example consists of a series arrangement of spring-coupled lumped masses. In this model, the transducer's dynamic properties are characterized by its model parameters which denote the transducer`s structural distribution of mass, stiffness and damping.

2 Force Transducers

Modern force transducers are electromechanical devices that use a force sensing element introduced into the force flow. By principle, a force transducer is always coupled to its mechanical environment on both sides of the transducer's body. An acting input force causes a small elastic deformation of the mechanical structure which is generally assumed to be proportional to the electrical output signal of the force measuring element.

Strain gauge transducers and piezoelectric transducers represent two types of force transducers that nowadays have the greatest importance for industrial applications. Figure 1 exemplarily shows three different models, two strain gauge transducers and one piezoelectric transducer, which were investigated in the aforementioned European research project. The transducers have greatly differing designs, dimensions and masses, and are all suited for compressive and tensile forces, as their mechanical couplings are realized by central threaded connectors.

For a given nominal capacity, a piezoelectric transducer is usually more compact, smaller and of higher stiffness than a strain gauge transducer. Therefore, piezoelectric force transducers have comparably high resonant frequencies, which makes them better suited for dynamic measurements at first glance.

2.1 Strain gauge force transducers

This type of force transducer uses strain gauges as the measuring principle to sense the elastic deformations resulting from an applied input force. A strain gauge picks up the surface strain of the underlying structure, and the mechanically elongated sensing element proportionally changes its electrical resistance. Typically four strain gauges

Figure 1:
Three force transducers investigated in the scope of the project EMRP IND09 (from left to right): HBM U9B / 1 kN, Interface 1610/2.2 kN, Kistler 9175B (–8 kN…30 kN).

are connected to a Wheatstone bridge circuit to compensate influences from parasitic loads and temperature effects, and to obtain a larger signal with a good signal-to-noise ratio. A connected bridge amplifier feeds the supply voltage and amplifies the small force-proportional bridge signal.

A great variety of mechanical designs of strain gauge force transducers has been developed in the past in order to optimally meet the individual measurement requirements. However, strain gauges are always bonded at defined locations of preferably strong and uniform strain. For this reason, a strain gauge transducer usually features a structural part of comparably high compliance, which can be termed *measuring spring*.

For dynamic measurements, the dynamic behaviour of the bridge amplifier has to be taken into account. For detailed information on the traceable dynamic calibration of bridge amplifiers please refer to the respective contribution given in this issue.

2.2 Piezoelectric force transducers

A piezoelectric force transducer uses a piezoelectric element to generate a force-proportional electrical charge signal. The transducer typically consists of two ring-shaped quartz disks that are contacted by an electrode foil, and a lower and upper force introduction part. A central screw connection usually pre-loads the sensor element to enable measurements of tensile forces as well.

The piezoelectric measurement principle only allows quasi-static measurements with long time constants of the amplifier's high-pass filter; however, true static measurements are not possible. As the principle is not based on mechanical deformation, the transducers have high structural stiffness which makes them well suited for dynamic measurements.

Piezoelectric force transducers are either available with electrical charge output (charge type), or with voltage output (IEPE type) featuring integrated electronics.

Again, the dynamic behaviour of the electrical signal chain has to be considered for dynamic measurements. Information on the traceable dynamic calibration of charge and voltage amplifiers is found in a respective article in this issue.

2.3 Application notes

It is difficult to make general recommendations regarding the selection of suitable force transducers for dynamic measurements, as the transducer's mechanical environment as well as superposed parasitic loads may have great influence on the dynamic measurement performance.

First of all, the user has to realize the fact that the high precision of static force measurements might be substantially compromised for dynamic measurements. Good static performance does not automatically mean good dynamic performance, and vice versa. For dynamic loads, the transducer output signal is affected by the inertia forces of the transducer's internal mechanical structure, which means that the structural design is of great importance. Some criteria for dynamic force measurements are given in the following.

Depending on the transducer's structural design and the coupling to its mechanical environment, the measurement set-up might react with low-frequency bending modes that could limit the usable frequency range. Therefore, low sensitivity against parasitic forces and moments is an important criterion for suitable force transducers if bending modes might be excited.

In order to get an estimate of the dynamic behaviour of the force transducer and/or its mechanical environment, it would be of great benefit to perform a modal analysis by means of finite element modelling. This analysis would give valuable information about the system's resonant modes that could be expected.

The stiffness of the mechanical couplings at both ends of the force transducer, i.e. the stiffness of the adaptation parts and of their respective contact surfaces, plays an important role for the dynamic performance. To shift possible coupling resonances to high frequencies and thus to obtain a broad dynamic bandwidth, the coupling stiffness should be as high as possible. The stiffness of screw connections is a complex topic with many influencing factors, e.g. material pairing, surface size, flatness, roughness, lubrication, and setting.

High stiffness requires large pretension forces, and the contacting surfaces should be large, flat and slightly lubricated, and the setting should be kept small. However, to achieve reproducible conditions for the elasticity of screw connections, it is recommended to fasten screw connections with defined torque.

One aspect sometimes not properly taken into account in dynamic applications is the asymmetric design of many force transducers, in particular of strain gauge transducers. With greatly different values of the structural mass above and below the transducer's measuring spring, the performance of the dynamic measurement application may greatly depend on the orientation of the mounted force transducer. To minimize the influences from the internal inertia forces, the larger mass component (transducer base mass) should be fixed at the more rigid part of the application where the vibrations are small, whereas the smaller mass component (transducer head mass) should be orientated towards the measuring side.

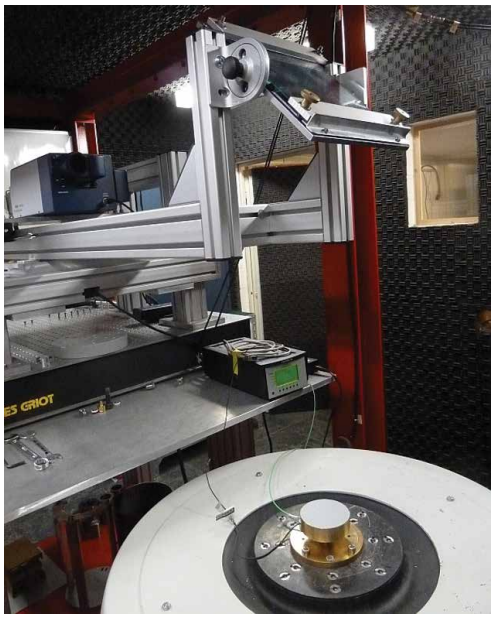

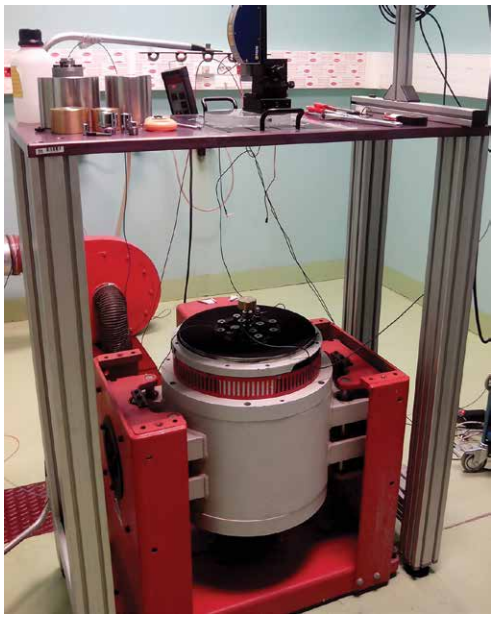

Figure 2:
Dynamic calibration devices with sinusoidal force excitation at PTB (top), CEM (centre), LNE (bottom).

Regarding the electrical measuring chain, signal conditioners and measuring amplifiers have to be suitable for the required dynamic bandwidth and their frequency responses have to be known and taken into account. In addition, special care might be taken to minimize influences from electromagnetic noise as such parasitic signal components could be in phase with the dynamic force input signal. The electromagnetic susceptibility of the force transducer with its cabling might be experimentally tested by probing the environment with an unmounted transducer.

3 Traceability Techniques

Sinusoidal forces and pulse-shaped forces have the greatest practical importance for the dynamic calibration of force transducers. With these two types of dynamic excitation, which are rather different in the time and frequency domain, the great variety of dynamic force measuring tasks can be covered with considerable good practical orientation.

Within the scope of the project EMRP IND09, the research was focused on dynamic calibration devices and measurement methods applying traceability with primary methods. Calibration devices for dynamic forces have been developed at three participating national metrology institutes providing both sinusoidal force calibrations (see figure 2, PTB in Germany, CEM in Spain, LNE in France) as well as shock force calibrations (PTB).

In each case, traceability of the dynamic force is based on the measurement of inertia forces using laser interferometers. According to Newton's law, the acting dynamic force $F(t)$ of an accelerated mass is given by the product of the mass m and the time-dependent linear acceleration $a(t)$ as $F = m{\cdot}a(t)$.

3.1 Sinusoidal force calibration

Whereas PTB had already started its research on dynamic force calibrations with sinusoidal excitation years ago [5, 7], the creation of a respective infrastructure at other NMIs was one of the important goals of the European joint research project.

Within the scope of the project, sine force calibration devices providing traceability with primary methods were developed and tested at PTB, LNE and CEM (cf. figure 2). The commissioned set-ups cover a frequency range from DC to 1 kHz and beyond, and provide force amplitudes up to 10 kN.

Each device uses an electrodynamic shaker system to excite the base of the force transducer under test mounted at the vibrating shaker platform and loaded at its top with a comparably large load mass. This vibrating mass body generates a sinusoidal inertia force which defines the reference signal.

A schematic drawing of such a primary sine force calibration device is shown in figure 3. The vertical

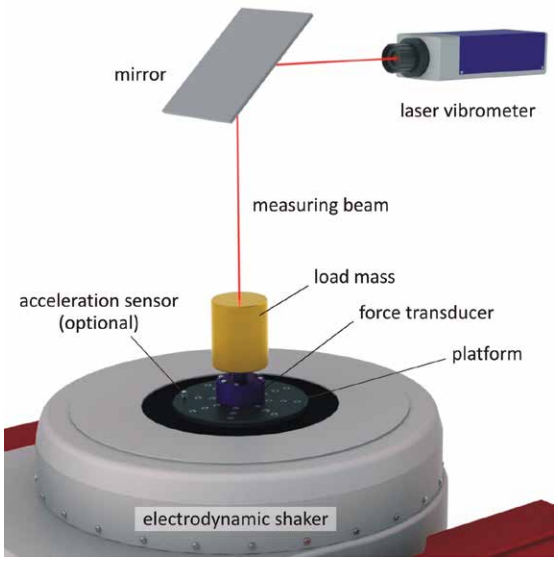

Figure 3:
Schematic drawing of the measurement set-up for sinusoidal force calibration.

dynamic motion of the load mass is measured by means of a laser vibrometer. An optional acceleration sensor is used to acquire the motion of the shaker. The excitation is controlled by the dynamic signal supplied by a function generator, fed to a power amplifier providing the current signal that drives the coil of the shaker platform. The force transducer under test is subjected to sinusoidal forces of varying frequency, and its amplitude and phase responses related to a reference force signal, i.e. the dynamic sensitivity, are evaluated as the dynamic calibration result.

The French national metrology institute LNE recently installed a shaker system providing forces up to 330 N; and the Spanish institute CEM commissioned a shaker system for sinusoidal forces up to 3 kN. Three electrodynamic shaker systems are available at PTB, a small one for force amplitudes up to 100 N and frequencies ranging from 10 Hz to 2 kHz, a medium-sized shaker (up to 800 N, frequencies 10 Hz to 3 kHz), and a large shaker providing forces up to 10 kN and sine excitations from 10 Hz to 2 kHz. At the moment, only PTB offers a calibration service for sinusoidal forces up to 2 kN force amplitude and 2 kHz excitation frequency which is anchored in its quality management system. More information about the state of the art of sinusoidal force calibrations at PTB and CEM is given in [8] and [9], respectively.

With the provision of a basic infrastructure for sine force calibrations at three European national metrology institutes, first international comparison measurements could be performed with the selected force transducers. The dynamic forces were generated with load masses of approximately 1 kg, 2 kg, 4 kg, 6 kg and 12 kg. Whereas the smallest mass bodies could be directly screwed onto the transducer under test, the larger masses required employing an adapter.

As an example, figure 4 presents the comparison of the dynamic sensitivity of the strain gauge force transducer Interface 1610 / 2.2 kN. The measurements were performed at the institutes CEM and PTB applying the small load masses of 1 kg and 2 kg. It is seen that the dynamic sensitivity generally decreases with frequency. The measurement results of both laboratories are in good agreement, as the relative deviation is in the order of about 1 %.

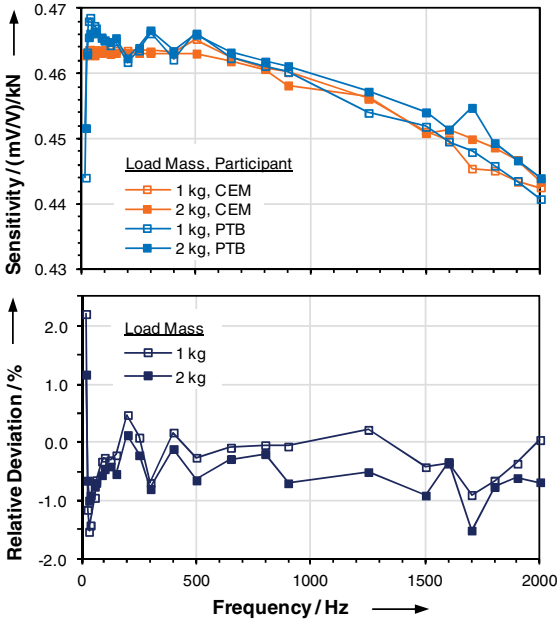

Figure 4:
Comparison of the dynamic sensitivity of the force transducer Interface 1610 / 2.2 kN measured at CEM and PTB using load masses of 1 kg and 2 kg: dynamic sensitivity (top), deviation between CEM and PTB (bottom).

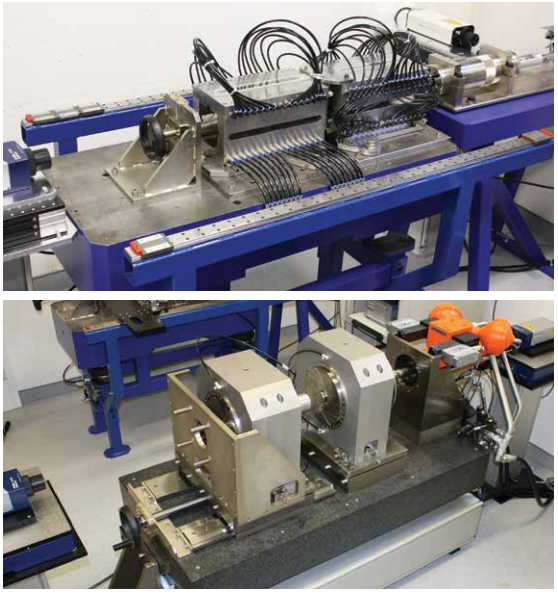

Figure 5:
Shock force calibration devices at PTB: 20 kN device (top), 250 kN device (bottom).

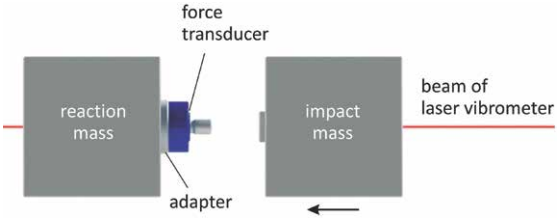

Figure 6:
Schematic drawing of the measurement set-up for shock force calibration.

3.2 Shock force calibration

Within the scope of the EMRP project, the method of shock force calibration was investigated at PTB using the two primary shock force calibration devices shown in figure 5.

Shock calibrations are performed with force pulses of defined amplitude, shape and duration. Here, the ratio between the pulse height of the transducer's output signal and the reference input force – the shock sensitivity – is often considered as the typical measurement result. However, former investigations with acceleration sensors showed that the pulse height ratio can be insufficient for calibration purposes as the associated signal shape and spectral content are of great influence. In this case, consistency between the different results from sinusoidal and shock calibration requires knowledge of the transducer's characteristic mechanical parameters that define its dynamic behaviour [10, 11].

The working principle of the primary shock force calibration devices is sketched in figure 6. Two airborne mass bodies are brought to collision with the force transducer under test mounted in between. The dynamic inertia forces of both the impacting mass body and the reacting mass body

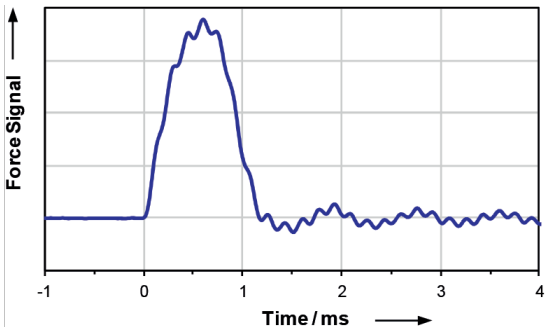

Figure 7:
Shock force signal with excited modal oscillations measured with a 225 kN strain gauge force transducer.

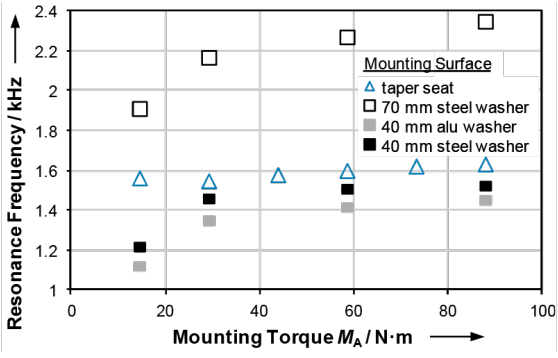

Figure 8:
Influence of the adapter's mounting conditions on the lowest resonance: variation of the mounting torque, different mounting surfaces.

are measured using two laser vibrometers. The smaller 20 kN shock calibration device employs mass bodies of 10 kg each, and the larger 250 kN device of 100 kg. More information about the calibration devices is given in [12, 13].

Experiments at the larger 250 kN shock force calibration device proved that the shock response of a force transducer may not only depend on its internal elastic properties, but also on its mounting conditions [14]. The example in figure 7 presents a shock force pulse with strong signal ringing which exhibits two oscillation frequencies, where its lowest resonance considerably depends on the achieved stiffness of the adapter mounting, which was proved by testing different mounting surfaces and mounting torque (figure 8). In case of strong ringing, the pulse shape of the inertia forces may substantially differ from that of the transducer output. The calculation of the transducer's true dynamic input forces will consequently require the above-mentioned model-based calibration approach.

First trials on the parameter identification (see section 3.3) indicated that such signal ringing presumably carries the information to unambiguously identify the transducer's dynamic properties from

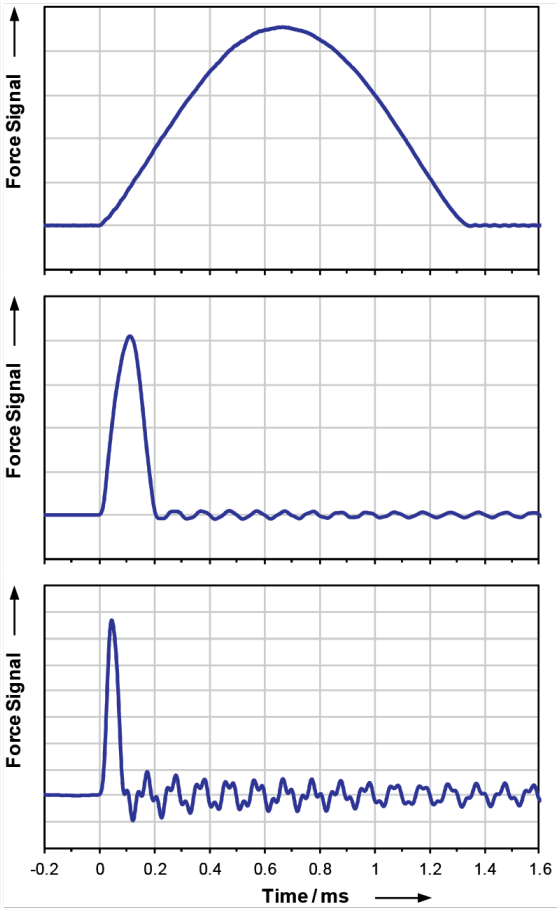

Figure 9:
Shock force pulses obtained with different impact masses: force transducer HBM U9B / 1kN, impact mass body of 10 kg (top), pendulum mass of 89 g (centre) and 7 g (bottom).

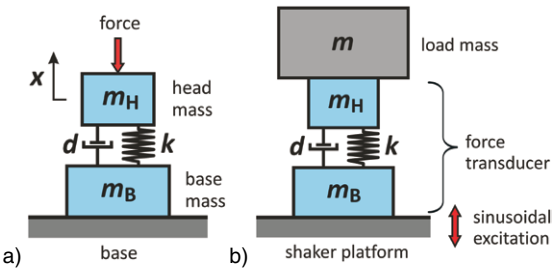

Figure 10:
Basic mass-spring-damper model of a force transducer (a), model of the sine force calibration device (b).

shock force measurements. The measurements at the 20 kN device have shown that the shock pulses achieved with an impact mass of 10 kg are way too broad to considerably excite the resonances of the small UBM U9B / 1 kN. To excite the resonances to a greater extent, new shock experiments were performed in which the airborne impact mass body of 10 kg was replaced by a much smaller pendulum mass [15]. The force pulses obtained with the three different impact masses are shown in figure 9. Whereas the impact mass of 10 kg generates a smooth pulse of 1.3 ms without ringing, the pendulum mass of 7 g yields a pulse of 0.1 ms followed by a pronounced ringing that reveals the mechanical resonances of the transducer under test.

3.3 Model-based calibration

To understand the dynamic behaviour of a force transducer in a given measurement set-up and with force signals of different types in the time and frequency domain, the characteristic parameters of the force transducer under test are determined using a model-based description of the force transducer and the used calibration device. This approach principally allows a linking between the different calibration results from different calibration methods and calibration devices [16].

To be more specific, the sine force calibration method measures the frequency response of the transducer's dynamic sensitivity determined by applying different load masses, adapters and couplings. And in the case of shock force calibrations, different mechanical set-ups can give shock sensitivity results that depend on the particular pulse shape.

Figure 10a presents the basic model of a force transducer, in which the dynamic behaviour is modelled by a mass-spring-damper system of one degree of freedom (linear displacement x). The transducer is characterized by four model parameters: head mass m_H, base mass m_B, stiffness k, damping d. The transducer output signal is assumed to be proportional to the elongation of the spring element. To describe the transducer's dynamic response in a considered mechanical

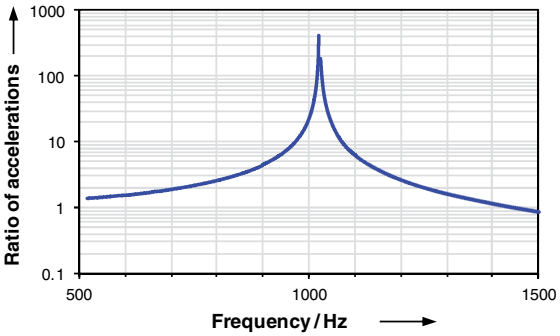

Figure 11:
Mechanical resonance of the transducer HBM U9B / 1 kN applied with a load mass of 1 kg measured at CEM.

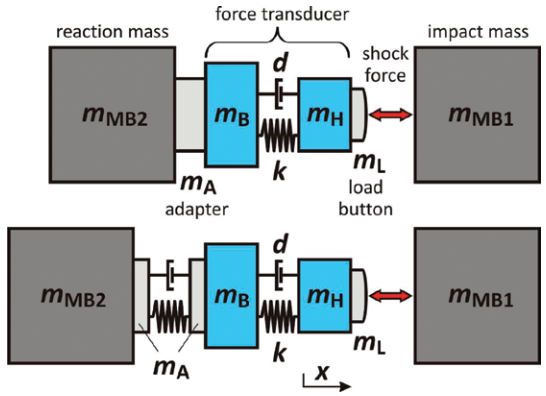

Figure 12:
Models of the shock calibration device with three and four model masses.

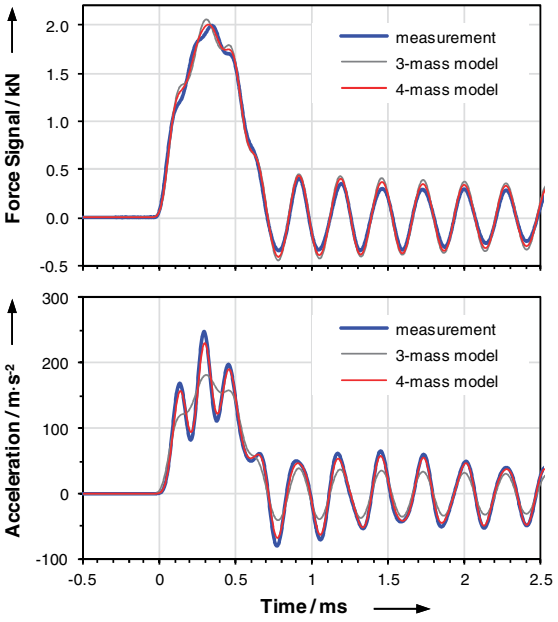

Figure 13:
Comparison of measured and modelled shock responses of the Interface 1610 / 2.2 kN, force signal and acceleration of the reaction mass.

measurement set-up, an appropriately extended model has to be applied that accounts for the two elastic couplings that connect force transducer and mechanical environment.

The corresponding model of the sine force calibration device is shown in figure 10b. The upper end of the force transducer (model mass m_H) is rigidly connected to the load mass m that generates the desired sine force when a sinusoidal acceleration is applied at the transducer's base. This mechanical system exhibits a characteristic resonance of the spring-coupled mass. For neglected damping, the resonance frequency is given by

$$f_{Res} = \sqrt{k/(m + m_H)}/(2\pi) \; .$$

The example in figure 11 visualizes the measured resonance of the HBM U9B / 1 kN which was loaded with a load mass of 1 kg. The diagram shows the ratio of the two accelerations which were picked up at the top of the load mass and the shaker platform, respectively. At the resonance frequency near 1 kHz, the acceleration ratio exceeds the value of 400, which demonstrates that the damping is very small. With an estimate of m_H, the unknown model parameter k can be identified from the shown frequency response.

Whereas the previous consideration assumes a rigid coupling of the load mass, the more generalized case of an elastic coupling requires a model that introduces a second spring element between load mass m and head mass m_H.

In the area of shock force calibration, the parameter identification process was investigated with the models sketched in figure 12 [19]. In the upper model, the shock force calibration device is described by three model masses (impact mass, head mass with load button, reaction mass with adapter and base mass), whereas the lower model uses four model masses, in which the force transducer is elastically coupled to the reaction mass.

As an example, figure 13 compares the measured and modelled signals of a shock calibration of the force transducer Interface 1610 / 2.2 kN. The transducer output signal is shown in the upper diagram, the acceleration of the reaction mass in the lower one. The best agreement between experimental and theoretical signals is achieved with the 4-mass model that considers the elastic coupling at the base of the transducer.

The identification of the transducer's characteristic model parameters from measured sine and shock force calibration data is a topic of current research. The investigated methods and procedures for the parameter identification are based on a fitting of modelled and measured data in the time or frequency domain. The experiences with the different force transducers under test have shown that the consistency of the parameter results obtained from sine and shock force calibration data still need to be improved in order to fully understand the dynamic measurement behaviour under different conditions. For this purpose, it is helpful to analyse the modal vibrations of the mounted force transducer and its measurement set-up by means of finite element calculations [17]. Consequently, the model descriptions and fitting procedures may then be modified to better agree with the dynamic measurement signals.

4 Conclusions and Outlook

This article gives an overview of the recent research activities conducted in the work package *Dynamic Force* of the joint research project EMRP IND09 *Traceable Dynamic Measurement of Mechanical Quantities*.

The approach of a model-based calibration is proposed in which the dynamic behaviour of the force transducer is described by characteristic model parameters. Dynamic calibration measurements with sinusoidal or shock excitation are used to identify these parameters. Having identified the model parameters of the force transducer, its dynamic measurement behaviour in a given mechanical set-up can be calculated by applying an appropriately expanded model which describes the transducer connected to its mechanical environment. In this context, the corresponding model parameters of the coupled environment have to be known sufficiently well, e.g. determined by dedicated measurements. In the end, the interesting dynamic measurand, i.e. the force input signal or the signal at a specific location within the force train, can be derived by means of a signal deconvolution process.

As an important achievement for the metrological community, first international dynamic comparison measurements could be performed thanks to new dynamic force calibration devices which were put into service. In addition, the joint work on mathematical modelling and parameter identification gave great impulses and the chosen path of the model-based dynamic calibration will be continued.

Future work will focus on the application of the proposed dynamic calibration methods to the various types of force transducers. The results from sine and shock force calibration measurements will be compared, and the corresponding models will be refined until consistent results are obtained at the end. This research will further include the investigation of the numerous influences on the parameter identification process and the evaluation of the measurement uncertainties for the parameter identification.

Acknowledgements

The author would like to thank his colleagues Sascha Eichstädt, Christian Schlegel and Oliver Slanina from PTB, as well as Nieves Medina from CEM, for their valuable contributions to this paper. This work was supported by the EMRP program of the European Union. The EMRP is jointly funded by the EMRP participating countries within EURAMET and the European Union.

References

[1] DIN EN ISO 376, *Metallische Werkstoffe – Kalibrierung der Kraftmessgeräte für die Prüfung von Prüfmaschinen mit einachsiger Beanspruchung*, Beuth, Berlin, Germany, 2005.

[2] International Standard ISO 6487, *Road Vehicles – Measurement Techniques in Impact Tests – Instrumentation*, International Organization for Standardization, Geneva, Switzerland, 2002.

[3] American Standard SAE J211-1, *Instrumentation for Impact Test – Part 1 – Electronic Instrumentation*, SAE International, Warrendale, USA, 2007.

[4] International Standard ISO 4965, *Metallic Materials – Dynamic Force Calibration for Uniaxial Fatigue Testing*, International Organization for Standardization, Geneva, Switzerland, 2012.

[5] R. Kumme, *The Main Influences on the Dynamic Properties of Force Measuring Devices*, XIV IMEKO World Congress, pp. 102–107, Tampere, Finland, 1997.

[6] VDI-Richtlinie VDI/VDE/DKD 2638, *Kenngrößen für Kraftaufnehmer - Begriffe und Definitionen*, Beuth, Berlin, Germany, 2006.

[7] R. Kumme, *A New Calibration Facility for Dynamic Forces up to 10 kN*, XVII IMEKO World Congress, pp. 305–308, Dubrovnik, Croatia, 2003.

[8] C. Schlegel, G. Kieckenap, B. Glöckner, A. Buß and R. Kumme, *Traceable Periodic Force Measurement*, Metrologia, 49, pp. 224–235, 2012.

[9] N. Medina, J. L. Robles and J. de Vicente, *Realization of Sinusoidal Forces at CEM*, IMEKO International TC3, TC5 and TC22 Conference, Cape Town, South Africa, 2014.

[10] A. Link, A. Täubner, W. Wabinski, T. Bruns and C. Elster, *Calibration of Accelerometers: Determination of Amplitude and Phase Response Upon Shock Excitation*, Measurement Science and Technology, 17, pp. 1888–1894, 2006.

[11] T. Bruns, A. Link and C. Elster, *Current Developments in the Field of Shock Calibration*, XVIII IMEKO World Congress, Rio de Janeiro, Brazil, 2006.

[12] M. Kobusch, S. Eichstädt, L. Klaus and T. Bruns, *Investigations for the Model-based Dynamic Calibration of Force Transducers by Using Shock Excitation*, ACTA IMEKO, 4 (2), pp. 45–51, 2015.

[13] M. Kobusch, T. Bruns, L. Klaus and M. Müller, *The 250 kN Primary Shock Force Calibration Device at PTB*, Measurement, 46 (5), pp. 1757–1761, 2012.

[14] M. Kobusch, *Influence of Mounting Torque on the Stiffness and Damping Parameters of the Dynamic Model of a 250 kN Shock Force Calibration Device*, 7th Workshop on Analysis of Dynamic Measurements, Paris, France, 2012.

[15] M. Kobusch, S. Eichstädt, L. Klaus and T. Bruns, *Analysis of Shock Force Measurements for the Model-based Dynamic Calibration*, 8th Workshop on Analysis of Dynamic Measurements, Turin, Italy, 2014.

[16] M. Kobusch, A. Link, A. Buss and T. Bruns, *Comparison of Shock and Sine Force Calibration Methods*, IMEKO TC3, TC16 and TC22 International Conference, Merida, Mexico, 2007.

[17] M. Kobusch, L. Klaus and T. Bruns, *Model-based Analysis of the Dynamic Behaviour of a 250 kN Shock Force Calibration Device*, XX IMEKO World Congress, Busan, Republic of Korea, 2012.

Calibration of Bridge-, Charge- and Voltage Amplifiers for Dynamic Measurement Applications

Leonard Klaus*, Thomas Bruns and Henrik Volkers

* Leonard Klaus, Working Group "Impact Dynamics", PTB, e-mail: leonard.klaus@ptb.de

Reprint of the original Article in **Metrologia 52** (2015) 72–8, DOI:10.1088/0026-1394/52/1/72

1 Introduction

For the dynamic measurement of mechanical quantities, the European research project *Traceable Dynamic Measurement of Mechanical Quantities* within the framework of the European Metrology Research Programme (EMRP) focused on the development of procedures for traceable measurements of the quantities force, pressure and torque [1–3]. This Joint Research Project (JRP) conjoined experimentalists and mathematicians from nine European National Metrology Institutes (NMIs) for research on the measurands force, pressure and torque. For dynamic measurements of any of these quantities, the respective sensor typically needs to be complemented by a conditioning amplifier. Therefore, these amplifiers were included in the research work as a major component of the traceability chain.

The majority of measurements are carried out with transducers having a bridge-, charge- or voltage output. These different types of output signals need to be conditioned in order to be digitized by an analogue-to-digital converter for further processing. For the conditioning of the signals, which may include the amplification, the decoupling and the conversion of quantities, signal conditioning amplifiers – also called measuring amplifiers – are used. Both terms will be used synonymously in the subsequent text. A typical measuring chain that consists of a transducer, an amplifier and a data acquisition system (DAQ) is depicted in figure 1.

To obtain traceable measurements, all components of the measuring chain have to be calibrated and analysed regarding their influence on the measurement result and an associated measurement uncertainty has to be assigned to each component.

While such procedures are well established for static measurements, there are no standardized procedures yet in the field of dynamic measurements. The requirements for the dynamic calibration of bridge amplifiers are already included in international standards [4], although there are no commercially available calibration devices yet. Currently, standards describing the procedures of a dynamic calibration of conditioning amplifiers are under development in national and international standardization working groups, namely the German DKD Fachausschuss "Kraft und Beschleunigung" (technical committee on "Force and Acceleration") and the Working Group 6 of ISO TC 108/SC 3 "Use and calibration of vibration and shock measuring instruments". This will remedy the current lack of validated procedures within the foreseeable future.

The subsequent section will provide an overview of the current state of knowledge and will further give an outline of what is to be expected from the future documentary standards.

2 Requirements for Conditioning Amplifiers

In theory, conditioning amplifiers should have no influence on the content of the measured signal in the frequency range of interest and should only convert the signal in the desired manner. However, in reality influences of conditioning amplifiers exist and need to be determined through proper calibration. In the field of acceleration measure-

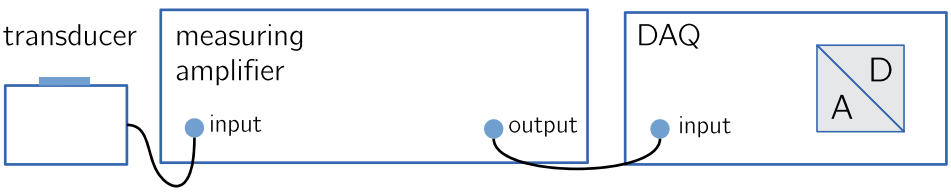

Figure 1:
Measuring chain consisting of a transducer, a measuring amplifier and a data acquisition system.

ment some experience in the dynamic calibration of charge amplifiers exists. This knowledge has now been extended to the development of calibration procedures for various types of conditioning amplifiers. Above all, the following types of amplifiers were considered in the JRP and hence, in this paper:

- Voltage amplifiers
- Charge amplifiers
- IEPE amplifiers, and
- Bridge amplifiers.

In the following paragraphs, the peculiarities of the different devices are briefly introduced.

2.1 Properties of conditioning amplifiers

Real amplifiers exhibit a frequency-dependent behaviour described by their frequency response function. This response may in turn depend to some extent on the properties of the connected source (transducer). These dependencies need to be characterized by means of calibration. To be able to calibrate a measuring amplifier, the device should be linear and time-invariant (LTI).

Linearity:
the output scaling factor should not depend on the level of the input signal of the amplifier.

Time invariance:
the frequency response function should not change over time.

The assumption of an LTI behaviour of conditioning amplifiers is a prerequisite for the applicability of the calibration procedures described in this paper.

2.2 Different types of amplifiers used for dynamic measurements

2.2.1 Voltage amplifier

Voltage amplifiers are used to condition input voltages to proportional output voltages. Two main applications exist:

- For small input voltages, voltage amplifiers are used for signal amplification.
- They are also used as unity-gain followers for a decoupling of input and output in case of load-sensitive transducer outputs or to adapt the source impedance to the connected data acquisition channel.

2.2.2 Charge amplifier

These devices are used in conjunction with piezoelectric transducers to convert the charge generated by the transducer to a proportional low impedance voltage output. The internal circuitry of the input stage of these devices typically exhibits either high-pass characteristics, or drift behaviour, if the high pass is compensated for [5].

2.2.3 IEPE amplifier

Piezoelectric transducers may be supplied with embedded integrated electronics (integrated electronic piezoelectric, IEPE), which may be named ICP®, Deltatron®, Piezotron®, or similar, depending on the manufacturer. The specifications of IEPE transducers and their power supply are not defined in a standard specification and may differ in detail from manufacturer to manufacturer. However, the known types follow a common principle. The power supply of such a transducer is realized using a two-wire connection with a constant current feed. The voltage between the rails used for the power supply changes, depending on the measured quantity. It has a bias voltage level of typically 8 V to 12 V, which corresponds to the zero point of the measured quantity. The voltage will change proportionally to the measured quantity in a range of typically 0.5 V (minimum voltage, minimum value of the measurand) to 24 V (supply voltage, maximum value of the measurand). Besides the current supply and the bias voltage level, the working principle of an IEPE conditioning amplifier is related to that of a voltage amplifier used for decoupling of input and output.

2.2.4 Bridge amplifier

Bridge amplifiers are used for the signal conditioning of the Wheatstone bridge outputs of strain gauge or of piezoresistive transducers. The amplifier feeds the transducer's bridge circuit with a supply voltage. The voltage output of the bridge is dependent on the detuning of the bridge's resistors and additionally proportional to the supply voltage. Therefore, the output of a transducer is a ratiometric quantity and is usually given as the ratio of the bridge output voltage and supply voltage in mV/V. For correct signal conditioning, bridge amplifiers should implement this ratiometric principle by not only taking the output signal of the transducer into account, but by including the supply voltage level as well. It should be noted that for the scope of the work described here, only amplifiers providing a DC supply voltage are considered. So-called carrier frequency bridge amplifiers are typically dedicated to static measurement exercises and therefore are not discussed here.

Carrier frequency bridge amplifiers can be used in a frequency range of only about 20 % of the carrier frequency, which is usually below 5 kHz. Even then, deviations of more than 10 % in the magnitude response have to be taken into account [6]. Furthermore, it should be noted that according to the common units of the input in mV/V and the output in V, the unit of the frequency response function of these devices is, in fact,

$$\frac{\mathrm{V}}{(\mathrm{mV/V})}\,.$$

3 Procedures for Dynamic Calibration

The goal of a calibration is the determination of the properties of interest of the device under test (DUT) with a known measurement uncertainty. For the conditioning amplifier, which can presumably be described as an LTI system, the property of interest is the frequency response function.

3.1 Frequency response function

The complex-valued frequency response function $\underline{H}\,(\mathrm{i}\omega)$ describes the time-dependent input–output behaviour of an LTI system in the frequency domain for an angular frequency $\omega = 2\pi f$, where f is the frequency in Hz. For continuous systems, the frequency response function is defined as the ratio of the output $\underline{Y}\,(\mathrm{i}\omega)$ over the input $\underline{X}\,(\mathrm{i}\omega)$ as

$$\underline{H}(\mathrm{i}\omega) = \frac{\underline{Y}(\mathrm{i}\omega)}{\underline{X}(\mathrm{i}\omega)}\,. \tag{1}$$

Its magnitude $A(\omega)$ is given by

$$A(\omega) = |\underline{H}(\mathrm{i}\omega)| = \sqrt{\mathrm{Re}^2\left(\underline{H}(\mathrm{i}\omega)\right) + \mathrm{Im}^2\left(\underline{H}(\mathrm{i}\omega)\right)} \tag{2}$$

and describes the conversion and scale- or gain factor of the device. The phase response function $\varphi(\omega)$ is given by

$$\varphi(\omega) = \tan^{-1}\left(\frac{\mathrm{Im}(\underline{H}(\mathrm{i}\omega))}{\mathrm{Re}(\underline{H}(\mathrm{i}\omega))}\right) \tag{3}$$

and characterizes the signal delay between input and output.

To derive the phase angle from the complex frequency response function, a four-quadrant inverse tangent calculation should be applied. If the two-quadrant inverse tangent calculation is used, a correction of φ for $\pm\,\pi$ may be necessary as this function is only defined in the range $-\pi/2 < \varphi < \pi/2$.

3.2 Excitation signal

The dynamic excitation of the measuring amplifier's input quantity used for calibration can be carried out in different ways, e.g. by transient, random noise or periodic excitation signals. The most commonly used excitation signal is the monofrequent sinusoidal excitation. Its advantages are the selectable excitation frequency, duration and magnitude, but the comparably long measurement time to obtain the complete frequency response function is disadvantageous. Since non-sinusoidal excitations can usually be related to sinusoidal excitations by Fourier methods, all subsequent considerations will be focused on the latter.

For an excitation signal $x(t)$ of a sinusoidal excitation with the magnitude A_x, the angular frequency ω and the phase φ_x is described by

$$x(t) = A_x \cdot \sin(\omega t + \varphi_x) = a_x \sin(\omega t) + b_x \cos(\omega t)\,, \tag{4}$$

with $A_x = \sqrt{a_x^2 + b_x^2}$ and $\varphi_x = \tan^{-1}(a_x/b_x)$. The output signal can be described accordingly as

$$y(t) = A_y \cdot \sin(\omega t + \varphi_y) = a_y \sin(\omega t) + b_y \cos(\omega t)\,. \tag{5}$$

With this definition the frequency response function can be written in the form

$$\underline{H}\left(\mathrm{i}\omega\right) = \frac{A_y(\omega)}{A_x(\omega)} \cdot \mathrm{e}^{\mathrm{i}\left(\varphi_y(\omega) - \varphi_x(\omega)\right)}\,. \tag{6}$$

The excitation frequency f should be chosen appropriately for the later application. The recommended frequency values often used in acoustics and vibration calibrations are given in ISO 266 [7]. These *recommended frequencies* are equally spaced in the frequency domain on the logarithmic scale. The width between the frequency steps can be chosen based on the desired number of frequency steps for a fixed interval.

3.3 Amplifier settings

A calibration result can only be valid for one certain set of settings of the amplifier under test, which include gain, corner frequencies of high-pass and low-pass filters, transducer sensitivity and possibly other parameters. It is essential to document the settings at which the amplifier was calibrated. These settings should be chosen according to the later application.

3.4 Linearity

For the above-mentioned frequency response function used to describe the dynamic behaviour, the

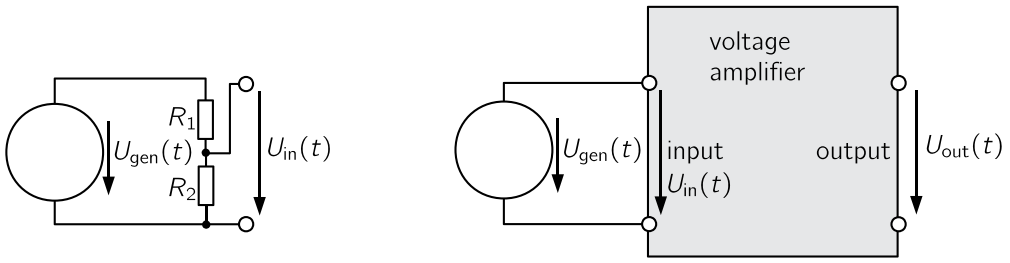

Figure 2: Schematic representation of a calibration set-up for voltage amplifiers using a signal generator and a voltage divider (left), or a signal generator only (right).

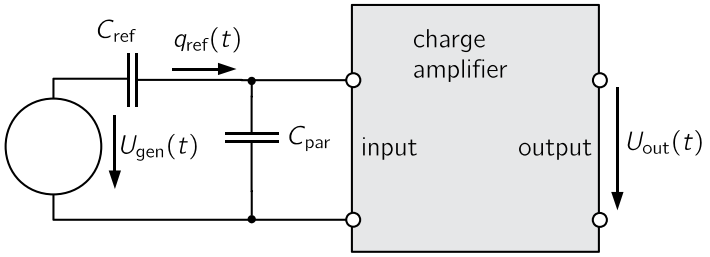

Figure 3: Schematic diagram of a calibration set-up for charge amplifiers.

linearity of the DUT is mandatory and should be ensured during calibration. Nonlinearities cause distortions of the sinusoidal shape of the output signal and can be estimated by analysing the harmonic signal components.

3.5 Stability

The requirement of the time-invariant behaviour can be proved by repeated calibrations over a prolonged period of time.

4 Calibration Set-Ups

4.1 Voltage amplifier calibration set-up

For the calibration of voltage amplifiers, a calibration set-up as depicted in figure 2 can be used. The time-dependent voltage output U_{gen} of the signal generator is coupled directly to the input of the voltage amplifier under test (in the case of small gain factors) or can be down-converted by means of a calibrated voltage divider (in the case of large gain factors).

The measurands of this set-up are the input voltage of the amplifier $U_{in}(t)$, which may be calculated from a calibrated generator voltage and the output voltage $U_{out}(t)$ of the amplifier. In terms of equations (4) and (5), this means

$$x(t)=U_{in} \cdot \sin(\omega t+\varphi_{in}) \text{ and} \quad (7)$$

$$y(t)=U_{out} \cdot \sin(\omega t+\varphi_{out}) . \quad (8)$$

4.2 Charge amplifier calibration set-up

In order to calibrate a charge amplifier it is necessary to convert the generator voltage from the previously described set-up to an input charge q_{ref} [8]. For this purpose, a high precision capacitance C_{ref} is employed as shown in figure 3.

Assuming that the input impedance of the charge amplifier is negligible, the reference charge q_{ref} for the charge amplifier under test can be derived as

$$q_{ref}(t) = U_{gen}(t) \cdot C_{ref} . \quad (9)$$

In terms of equation (4) the input measurand is given as

$$x(t) = U_{gen} \cdot C_{ref} \cdot \sin(\omega t + \varphi_{in}) . \quad (10)$$

Under this assumption, parallel capacities C_{par} (e.g. from the transducer cable) will not influence the amount of charge at the amplifier input. However, it was found that the total capacitance at the input ($C_{ref} + C_{par}$) may influence the charge amplifier's frequency response function [9]. This effect is typically small, but may not be negligible in applications with a demand for low measurement uncertainties.

4.3 IEPE amplifier calibration set-up

IEPE conditioning amplifiers can be calibrated using a measuring set-up similar to a set-up for low gain voltage amplifiers. Instead of a direct connection of the signal generator and the amplifier under test, an IEPE simulator is connected between the signal generator and the IEPE conditioner [10], converting the generated voltage into an IEPE transducer-like output signal. This set-up is depicted in figure 4.

For the determination of the frequency response function of an IEPE signal conditioner, two connection schemes are possible with such a set-up:

- Calibration with a calibrated IEPE simulator. If the IEPE simulator's frequency response

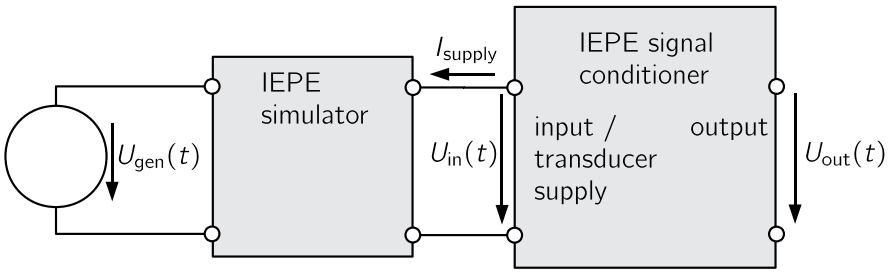

Figure 4:
Calibration set-up for IEPE conditioning amplifiers including an IEPE simulator.

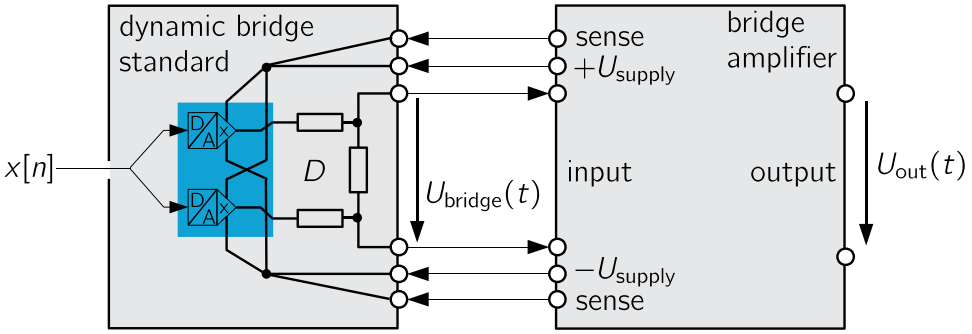

Figure 5:
Schematic representation of a bridge amplifier calibration set-up with an MDAC dynamic bridge standard.

function was determined prior to the calibration of the IEPE conditioning amplifier, a known input voltage can be used for the excitation following

$$x(t)=U_{gen} \cdot \sin(\omega t+\varphi_{in}) \quad (11)$$

and applying a correction according to the procedures described in section 9.

- Calibration by measuring U_{in} instead of U_{gen}. If the output signal of the IEPE simulator is acquired instead of the input signal, the influences of the IEPE simulator are excluded from the measurement.

$$x(t)=U_{in} \cdot \sin(\omega t+\varphi_{in}) + U_{offset} \quad (12)$$

However, it has to be kept in mind that there will be a voltage offset U_{offset} due to the IEPE feeding, which can lead to reduced voltage measurement precision due to the disadvantageously large input voltage ranges of the data acquisition device. Additional influences due to the voltage measurement in the measuring chain must be analysed as well.

4.4 Dynamic bridge standard calibration set-up

For the dynamic calibration of bridge amplifiers, different calibration set-ups have been developed at the NMI level. They all feature a ratiometric measurement principle. An older approach generates the small excitation voltages by means of an inductive coupling, which is limited at low frequencies [11]. Therefore, no DC measurement ($f = 0$ Hz) is possible.

A new approach generates the bridge signals by using two multiplying digital-analogue converters (MDACs) and a resistive voltage divider [12–13]. The principle is depicted in figure 5. With this principle, bridge excitation frequencies down to DC are possible; in fact, arbitrary signals could be generated as well. As part of work package 4 of the aforementioned EMRP project, the dynamic bridge standards were further developed to enable phase measurements and a traceable calibration was carried out. An international bilateral comparison of the different dynamic bridge standards is currently under way to ensure comparability in the range of the estimated measurement uncertainties.

The dynamic bridge standard simulates the output signal of a strain gauge transducer. The device is connected to the bridge amplifier under test and provides a similar input resistance to a strain gauge transducer. The output voltage of the simulated bridge depends directly on the bridge supply voltage, because the supply voltage is the reference voltage for the multiplying DACs. In the case of bridge amplifiers equipped with a control of the bridge excitation voltage by means of a 6-wire connection using sense wires, these wires are connected to the MDACs in the bridge standard so as to behave similarly to a real transducer.

As the dynamic bridge standard generates the predefined traceable voltage ratio, the measurand for a magnitude calibration of a bridge amplifier is solely the output voltage of the amplifier. In order to determine the phase response, the dynamic bridge standard supplies a complementary normalized signal output, which provides a signal synchronous to the voltage ratio. With reference to this 'synchronization signal', the time delay and therefore the phase response of the amplifier can be calibrated.

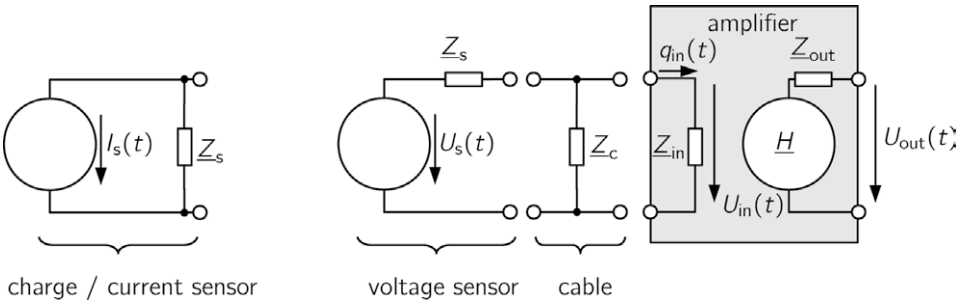

Figure 6. Schematic diagram including impedances for current or charge measurements (left) and for voltage measurements (right).

5 Data Acquisition and Analysis

The methodology presented here is implemented in the respective laboratories of PTB and to our knowledge in many other NMI laboratories, namely in the field of vibration metrology. Nevertheless, other valid set-ups and methods are conceivable.

To calculate the frequency response function (see equation (1)), the input and output quantities have to be acquired with two measurement channels. For proper signal acquisition, several criteria should be complied with:

- Common sample clock for the two channels (or sample clocks of an integer ratio).
- Synchronous start of sampling.
- Common sampling interval (window width) of an integer multiple of the mains period.
- Sample frequency that covers the bandwidth of the nominal frequency f and existing harmonics (Nyquist criterion).

Considering this in all of the previously described set-ups, two sampled time series of sinusoidal voltage signals $\{x_i\}$ and $\{y_i\}$ are acquired[1], which is – irrespective of a constant factor (e.g. C_{ref}) – a discretized realization of the continuous signals $x(t)$ and $y(t)$ (see equations (4) and (5)).

Through the application of a linear least squares fit of the named equations to the sampled time series, the parameters a_x, b_x and a_y, b_y can be determined easily. With the transformations given in section 3.2, the frequency response function is thus derived according to equation (6) by subsequent measurements at all desired angular frequencies ω.

6 Influence of the Impedance

Every signal input, signal output and connecting cable has its inherent complex impedance which, if not taken into account, can add systematic deviations to the measurements. Figure 6 shows the two set-ups for the voltage and for the charge measurements. If the typically used coaxial cables are significantly shorter than the wavelength of the signal, they can be modelled by a parallel capacitance $\underline{Z}_c$.

The output voltage $\underline{U}_{out}$ of a measuring amplifier is dependent on the output scaling factor described by the frequency response function $\underline{H}$ as

$$\underline{U}_{out} = \underline{H} \cdot \underline{U}_{in} \tag{13}$$

for voltage amplification, and

$$\underline{U}_{out} = \underline{H} \cdot \underline{q}_{in} \tag{14}$$

for charge conditioning, respectively.

The voltage at the input of the amplifier $\underline{U}_{in}$ can deviate from the sensor output voltage $\underline{U}_s$ because of the influences of the impedances

$$\underline{U}_{in} = \underline{U}_s \cdot \left(1 + \underline{Z}_s \left(\frac{1}{\underline{Z}_{in}} + \frac{1}{\underline{Z}_c}\right)\right)^{-1}. \tag{15}$$

Accordingly, the input $\underline{q}_{in}$ of a charge measurement can deviate from the output charge $\underline{q}_s$ according to

$$\underline{\theta}_{in} = \underline{\theta}_s \cdot \left(1 + \underline{Z}_s \left(\frac{1}{\underline{Z}_{in}} + \frac{1}{\underline{Z}_c}\right)\right)^{-1}. \tag{16}$$

7 Measurement Uncertainty Contributions of Realized Calibration Facilities

The measurement uncertainties for dynamic calibrations are based on the quality of the device under test as well as on the calibration set-up. The major components for the measurement uncertainty of the set-up can be (see [8–12]):

- Non-linearities of the A/D conversion for single frequency ratio measurement.
- Calibration uncertainties of the used reference capacitance (for charge amplifier calibration).
- Calibration uncertainties of the IEPE simulator (for IEPE amplifier calibration).
- Calibration uncertainties of the dynamic bridge standard (for bridge amplifier calibration).
- Noise of the input voltage (generator) and of the output voltage (conditioning amplifier).

[1] In the case of the dynamic bridge standard, the input is not acquired but defined by the programmed signal. However, the analysis procedure is easily adaptable.

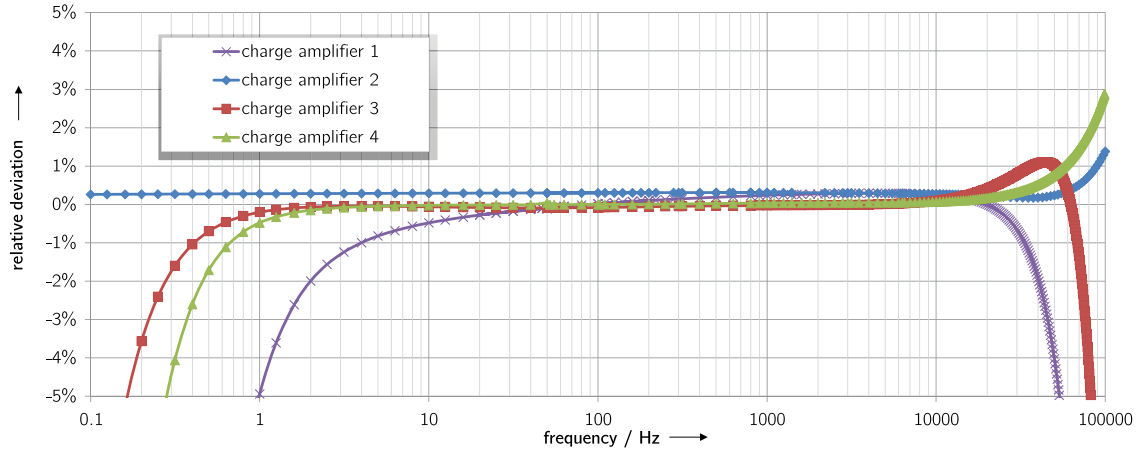

Figure 7: Magnitude responses of four different commercially available charge amplifiers in the frequency range of 0.1 Hz to 100 kHz.

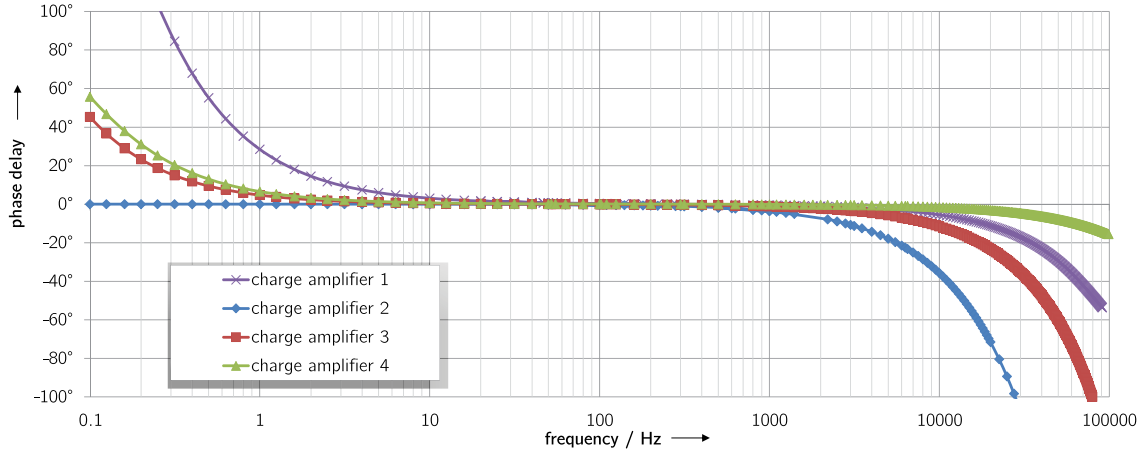

Figure 8: Phase responses of four charge amplifiers in the frequency range of 0.1 Hz to 100 kHz.

Hence, a rough estimate shows that the claims of some 10^{-3} to 10^{-4} of relative combined expanded uncertainty for magnitude are feasible for charge amplifier calibration [8–9] with the proper equipment and under good conditions, depending, of course, on the details of the implementation. The relative expanded measurement uncertainties of IEPE and the bridge amplifiers, again for magnitude calibration, will be in the ranges of tenths of per cent [10–12].

Not only do NMIs carry out traceable calibrations of charge amplifiers, but accredited laboratories also compare their calibration results in a national comparison programme [14]. The measurement uncertainties of accredited calibration laboratories for the available calibrations (charge amplifiers, voltage amplifiers, but not yet bridge amplifiers) are typically in the range of $0.3\,\% < U(k = 2) < 1\,\%$ and typically available for magnitude calibration only.

8 Measurement Results of the Calibration of Amplifiers

To show the importance of a suitable calibration for amplifiers used for dynamic measurements, different calibration results for bridge-, charge-, voltage- and IEPE conditioning amplifiers are presented. All analysed amplifiers are commercially available. They were produced by different manufacturers.

The charge-, voltage- and IEPE conditioning amplifier calibrations were carried out in a frequency range from 0.1 Hz to 100 kHz. All high- and low-pass filters were disabled or set to their lowest (high-pass filter) or highest (low-pass filter) value, respectively. The deviations in the magnitude responses are given with respect to the nominal value, set at the amplifier.

Three of the four charge amplifiers show a typical high-pass behaviour in their amplitude response (figure 7). Charge amplifier 2 has the option to disable its high-pass filter, which resulted in a much better low-frequency behaviour but also in a drifting DC bias voltage (which does not become obvious from the frequency response data). It was found that even with high-pass filters set at the lowest value, the filter settings can still influence the measuring results in the frequency range up to 10 Hz. The low-pass filters of three amplifiers (amplifiers 2, 3, 4) show a significant overshooting behaviour, which should be considered with caution. The corresponding phase response of the same four charge amplifiers is shown in figure 8. The phase and the magnitude responses can differ substantially from amplifier to amplifier.

The calibration results for the magnitude (figure 9) and phase response (figure 10) of four different voltage amplifiers show the smallest fre-

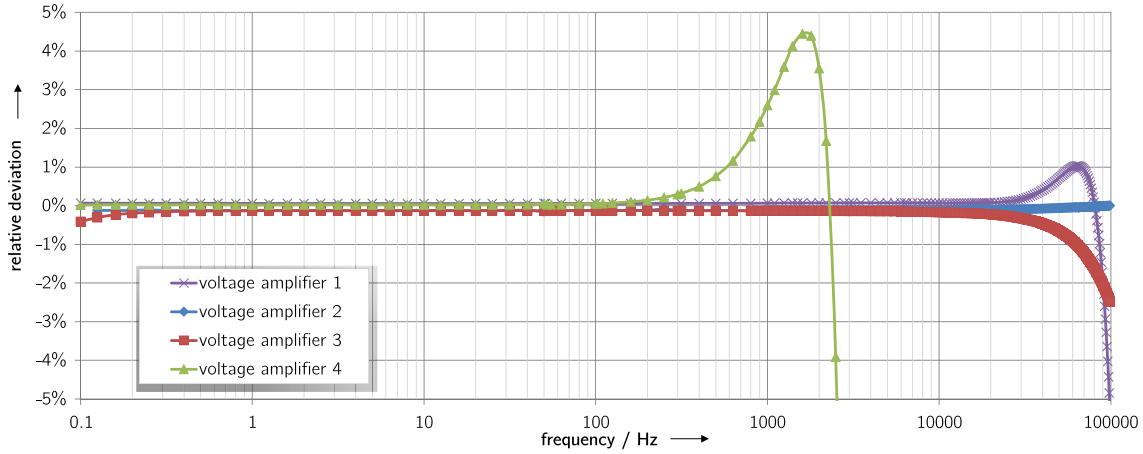

Figure 9: Magnitude responses of four different commercially available voltage amplifiers in the frequency range of 0.1 Hz to 100 kHz.

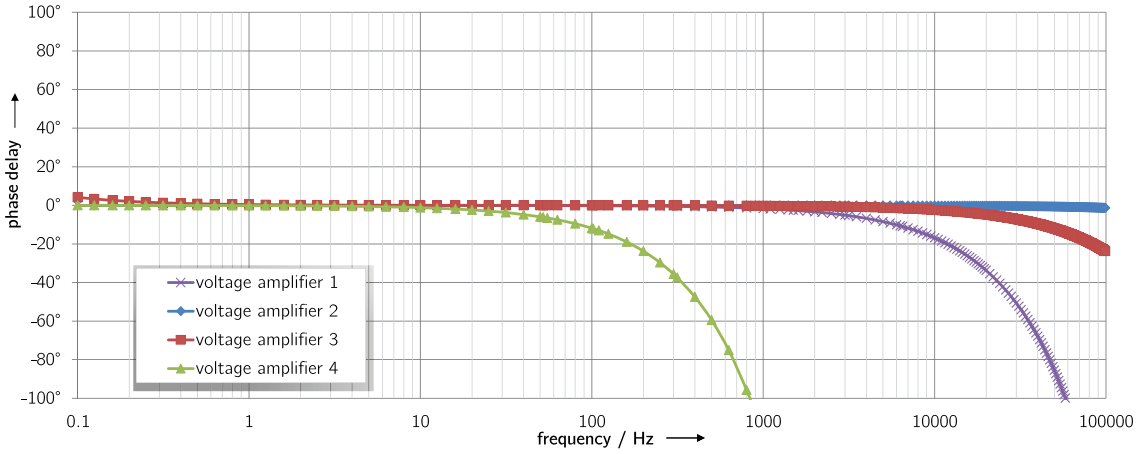

Figure 10: Phase responses of four voltage amplifiers in the frequency range of 0.1 Hz to 100 kHz.

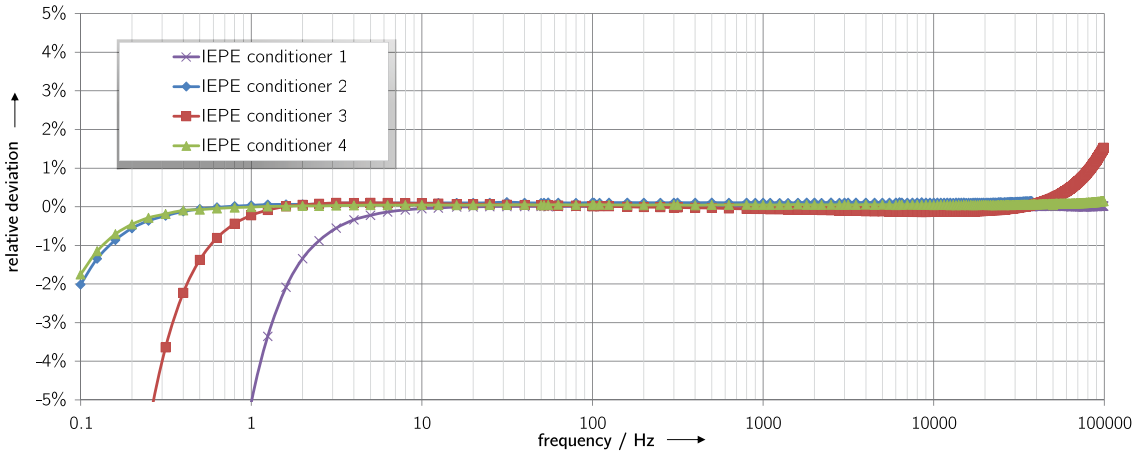

Figure 11: Magnitude responses of four different commercially available IEPE conditioning amplifiers in the frequency range of 0.1 Hz to 100 kHz.

quency-dependent deviations at low frequencies. Again, the low-pass filter can produce significant overshooting even in a frequency range of a few hundred hertz (voltage amplifier 4), which affects the phase response accordingly.

All investigated IEPE conditioning amplifiers have a significant high-pass behaviour as depicted in figures 11 and 12, which can affect low frequency measurements.

In figures 13 and 14, the magnitude and phase response of four bridge amplifiers are shown. The calibration measurements were carried out using the dynamic bridge standard of PTB in a frequency range of 10 Hz to 10 kHz. The excitation level was 2 mV/V; all filters were switched off or set to their highest value available.

It becomes obvious from the calibration results that bridge amplifiers can have a significant varying magnitude response even in low frequency regions, which shows the importance of dynamic calibrations. The phase responses of the four analysed amplifiers show significantly differing behaviour. The four bridge amplifiers under test had a phase delay of at least 15° to 20° at 10 kHz. But bridge amplifier 2 exhibited a much stronger phase delay.

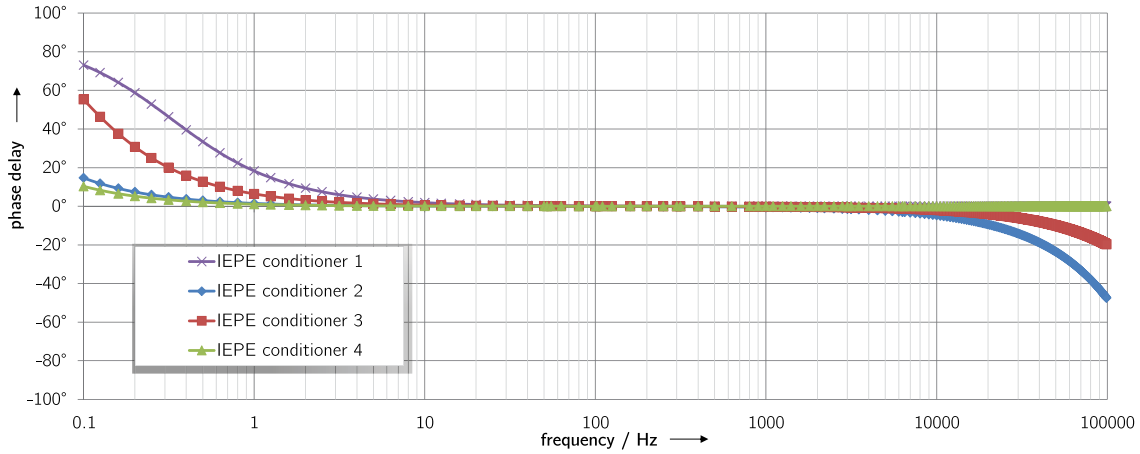

Figure 12:
Phase responses of four IEPE conditioning amplifiers in the frequency range of 0.1 Hz to 100 kHz.

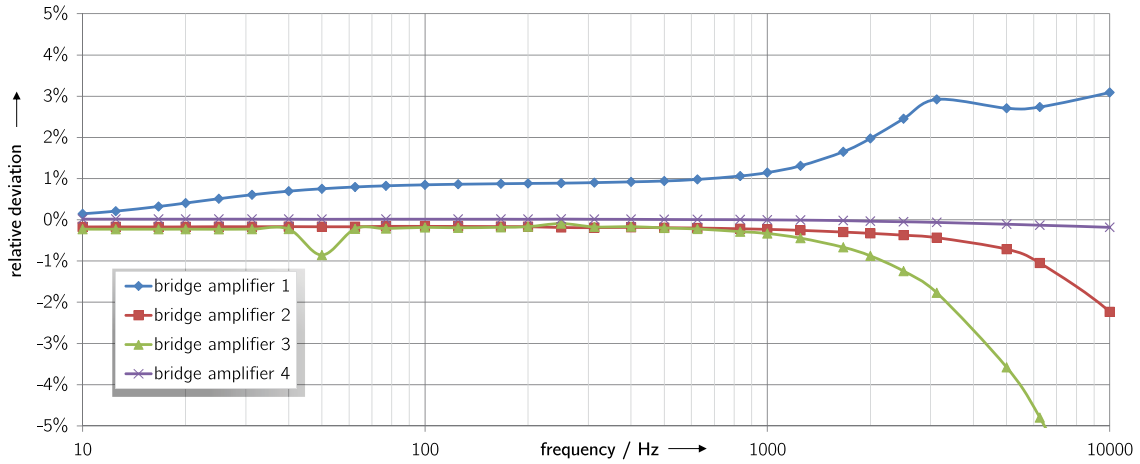

Figure 13:
Magnitude responses of four different commercially available bridge amplifiers in the frequency range of 10 Hz to 10 kHz.

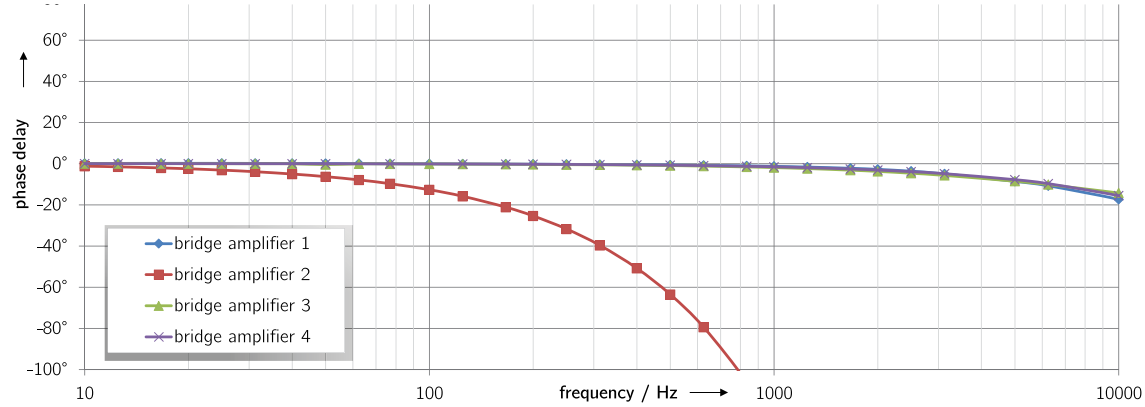

Figure 14:
Phase responses of four bridge amplifiers in the frequency range of 10 Hz to 10 kHz.

9 Correction of the Frequency-dependent Behaviour

The calibration results can be used to correct the dynamic influences of the amplifier in the measurement chain. In case the magnitude response function $A_{\mathrm{cal}}(\omega)$ and the phase response function $\varphi_{\mathrm{cal}}(\omega)$ of an amplifier are known from calibration, the magnitude $A_{\mathrm{meas}}(\omega)$ and phase $\varphi_{\mathrm{meas}}(\omega)$ of the measured data can be corrected in the frequency domain as

$$A_{\mathrm{corr}}(\omega) = A_{\mathrm{meas}}(\omega) \cdot A_{\mathrm{cal}}(\omega)^{-1} \qquad (17)$$

and

$$\varphi_{\mathrm{corr}}(\omega) = \varphi_{\mathrm{meas}}(\omega) - \varphi_{\mathrm{cal}}(\omega)\,. \qquad (18)$$

It should be kept in mind that the frequency response functions of the measuring amplifiers have to be assigned with their measurement uncertainty and will therefore influence the corrected data's uncertainty accordingly.

10 Summary

This paper shows that a dynamically calibrated measuring amplifier is a prerequisite for traceable calibration of transducers used for dynamic measurements of mechanical quantities. Guidance for the user on how different types of amplifiers could be calibrated is provided in the paper. Amplifiers of different types were exemplarily investigated. Calibration set-ups were presented for the different types of amplifiers applied with different types of sensors and the measurement uncertainties which can be realized with such set-ups were estimated. The calibration results of selected charge-, voltage- and bridge amplifiers, as well as IEPE conditioning amplifiers, have been exemplarily presented. These results demonstrate the importance of a dynamic calibration because of the deviating results obtained with different amplifiers. General assumptions regarding the suitability of a certain type of amplifier cannot be made, because all of the reviewed amplifiers showed some dependence in their frequency response function on dynamic excitation.

Acknowledgements

The authors would like to thank their colleague T. Beckmann for carrying out all of the charge-, voltage- and IEPE signal conditioning amplifier calibration measurements.

This work was part of the Joint Research Project IND09 *Traceable Dynamic Measurement of Mechanical Quantities* of the European Metrology Research Programme (EMRP). The EMRP is jointly funded by the EMRP participating countries within EURAMET and the European Union.

References

[1] EMRP JRP IND09 Traceable Dynamic Measurement of Mechanical Quantities, http://projects.ptb.de/emrp/ ind09.html (Retrieved: 2015-08-11).

[2] C. Bartoli , M. F. Beug, T. Bruns, C. Elster, T. Esward, L. Klaus, A. Knott, M. Kobusch, S. Saxholm, C. Schlegel, *Traceable Dynamic Measurement of Mechanical Quantities: Objectives and First Results of this European Project*, Int. J. Met. Qual. Eng., 3, pp. 127–135, (2013).

[3] C. Bartoli, M. F. Beug, T. Bruns, S. Eichstädt, T. Esward, L. Klaus, A. Knott, M. Kobusch and C. Schlegel, *Dynamic Calibration of Force, Torque and Pressure Sensors*, Joint IMEKO Int. TC3, TC5 and TC22 Conf., Cape Town, South Africa, 2014.

[4] ISO/TC 164/SC 5 2012 ISO 4965-1, *Metallic Materials – Dynamic Force Calibration for Uniaxial Fatigue Testing – Part 1: Testing Systems*, Geneva: International Organization for Standardization (ISO), 2012.

[5] H. Nozato, T. Bruns, H. Volkers and A. Oota, *Digital Filter Design with Zero Shift on Charge Amplifiers for Low Shock Calibration*, Meas. Sci. Technol., 25, 2014.

[6] K. Hoffmann, *An Introduction to Stress Analysis and Transducer Design Using Strain Gauges,* Hottinger Baldwin Messtechnik GmbH, pp. 133–134, Darmstadt, 1987.

[7] ISO/TC 43, 1997 ISO 266, *Acoustics: Preferred Frequencies for Measurements*, International Organization for Standardization (ISO), Geneva, 1997.

[8] T. Usuda, A. Oota, H. Nozato, T. Ishigami, Y. Nakamura and K. Kudo, *Development of Charge Amplifier Calibration System Employing Substitution Method*, IMEKO 20th TC3, 3rd TC16 and 1st TC22 Int. Conf., Merida, Mexico, 2007.

[9] H. Volkers and T. Bruns, *The Influence of Source Impedance on Charge Amplifier*, Acta IMEKO 2, pp. 56–60, 2013.

[10] G. P. Ripper, R. S. Dias, G. R. Micheli and C. D. Ferreira, *Calibration of IEPE Accelerometers at INMETRO*, Joint IMEKO Int. TC3, TC5 and TC22 Conf., Cape Town, South Africa, 2014.

[11] C. Schlegel, G. Kieckenap and R. Kumme, *Dynamic Calibration of Bridge Amplifiers Used for Periodical Force Measurement*, Conf. on Precision Electromagnetic Measurements, pp. 570–571, Washington, DC, USA, July 2012.

[12] M. F. Beug, H. Moser and G. Ramm, *Dynamic Bridge Standard for Strain Gauge Bridge Amplifier Calibration*, Conf. on Precision Electromagnetic Measurements, pp. 568–569, Washington, DC, USA, 2012.

[13] D. Georgakopoulos, J. M. Williams, A. Knott, T. J. Esward and P. S. Wright, *Dynamic Characterisation of the Electronic Instrumentation Used in the Calibration of Fatigue Testing Machines*, IEE Proc. Sci. Meas. Technol., 153, pp. 256–259, 2006.

[14] T. Bruns, P. Begoff and M. Mende, *Realization and Results of a DKD Interlaboratory Comparison Regarding the Measurand Acceleration*, Joint IMEKO Int. TC3, TC5 and TC22 Conf., Cape Town, South Africa, 2014.

Dynamic Measurements as an Emerging Field in Industrial Metrology

André Schäfer*

* Dr. Andre Schäfer, Hottinger Baldwin Messtechnik GmbH, Darmstadt, e-mail: andre.schaefer@hbm.com

1 Motivation

Since its foundation in the fifties of the last century, i.e. for more than six decades, our company has been serving mechanical engineering as a manufacturer of complete measuring chains from sensor through data processing to software. The first products were amplifiers and inductive transducers. In 1955, the company – as the first company in Europe at all – started the production of strain gauges. This turned out to be a huge success story. Today, strain gauge-based reference transducers and precision instruments are used in the static calibration of quantities such as force, torque and pressure, since this allows the lowest possible measurement uncertainty to be achieved for the measuring chain as a whole. So it is no wonder that in 1977, HBM was the first company ever in Germany to be accredited as an official DKD (German Calibration Service), now DAkkS, calibration laboratory.

HBM headquarters in Darmstadt, Germany.

Of course, given our wide range of industrial applications, we have also been among the first to see the emergence of new requirements in terms of measurement bandwidth and, in the last decade, also of dynamic measurement. Germany was among the leaders in addressing these new challenges. For example, Rohrbach in his *Handbook of Electrical Measurement of Mechanical Quantities* [1] issued in the sixties of the last century, having full understanding of the complexity of this new approach wrote: "… the frequency response of a force transducer heavily depends on the masses of the whole measurement set-up coupled to the transducer …" and "… in order to make statements on the transducer's behavior (in the application) the transducer has to be calibrated along with all coupled masses". This book not only talks force, but even covers torque already "… due to the analogue behaviour of translatory and rotatory movement the same basis has to be applied to the dynamic calibration of torque transducers …" .

2 Industry and Research Joining Together

The complexity of this approach may have been the reason why it has not been followed up in the following decades. Anyway, with the beginning of the new century, it suddenly gained a new urgency [2]. This was due to the fact that processes became faster and, e.g., power and efficiency measurement required that these aspects be looked into as well. In the beginning, dynamic calibration still meant that mechanical quantities were measured only in a state when they were constant over time; however, industrial users needed "a dynamic state" (varying over time-> which is what really happens in the application). For torque, a second phenomenon has to be considered, i.e. the fact that today torque transducers are mounted in calibration machines in non-rotating set-ups, while industrial users are interested in "rotating conditions". Therefore, the actual application is "dynamic". Hence, dynamic calibration is the logical successor to static calibration. However, this approach is new and standards for dynamic calibration still have to be developed.

Project meeting of NMIs in EMRP IND 09 at PTB, Braunschweig, March 2014.

In the field of force transducers, this applies mainly to aerospace and materials testing (e.g. in material testing machines). In the field of torque, automotive and shipbuilding applications are of interest. Here, in-line torque measurement is required, i.e. measurement directly in the drive train of ships. More stringent regulations (e.g. for emission limits) require substantially increased accuracy of torque measurement. Eventually, measurement of both rotational speed and power must be certified.

NMIs, too, were facing these challenging requirements from industry. As a result, attempts have been made to develop the required calibration and traceability infrastructure within NMIs. A major step has been implemented in the framework of EMRP (*European Metrology Research Project*) and EURAMET, the *European Association of National Metrology Institutes*.

HBM booth at the XX IMEKO World Congress in Busan, Korea.

Besides the project entitled IND09 *Traceable Dynamic Measurement of Mechanical Quantities*, I want to write about another project entitled IND16 *Metrology for Ultrafast Electronics and High-Speed Communications* that paved the way for this new approach. In any case, the project IND09 in particular has established a metrological infrastructure for traceable dynamic calibration of the considered quantities at the NMI level.

To cope with the new challenges facing metrology – within the framework of EURAMET – good ways to organize research cooperation with industry were contemplated. HBM, like other industrial providers, regularly takes part in IMEKO events. This covers not only the IMEKO World Congress, but also events of technical committees and several joint meetings. So it was no wonder that HBM was among the first to know when EURAMET started the so-called EMRP calls.

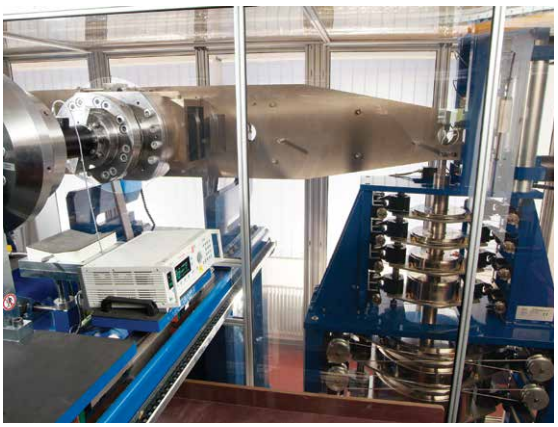

Torque calibration machine at HBM.

Force calibration machine at HBM.

What made the topic of JRP IND09 *Traceable Dynamic Measurement of Mechanical Quantities* outstanding was its vision. Although static calibration still seems to be prevailing in real-life applications, the automotive industry, in particular, is very interested in dynamic calibration research with a focus on mechanical quantities. In our experience, it is always crucial to such projects that not only measurement providers be interested but also "end users". In our case, these were automotive companies and, luckily, Volkswagen AG and Dr. Ing. h.c. F. Porsche AG joined the project as collaborators. Also, under the supervision of mainly PTB, NPL, LNE but also MIKES all initial project partners attached highest importance to asking their end users to contribute support letters to the project. In the end, approximately twenty parties supported the project.

3 Fruitful Dynamic Workshops

A great milestone in the project was the international workshop on *Challenges in Metrology for Dynamical Measurement* taking place at the BIPM (Bureau International des Poids et Mesures) near Paris in November 2012. The event was headed up by Dr. Takashi Usuda and Dr. Thomas Bruns. It was on their initiative that HBM was invited to give one of the main lectures. The workshop was meant to cover talks from both industry and NMI experts, including room for discussion.

The workshop opened with two papers, the first from Dr. Tatsuo Fujikawa of Japan Automotive Research Institute entitled *Requested Reliability of Dynamic Mechanical Measurement in Mobility from Automotive to Humanoid Robot* and the second by HBM (presented by Dr. André Schäfer) entitled *Challenges in Dynamic Torque and Force Measurement with Special Regard to Industrial Demands*. Subsequent presentations, e.g. by Rolls-Royce, UK, picked up on the same topics: "… reduced safety factors demand improvements of measuring uncertainty". Another industry speaker was from Volkswagen do Brasil. The presentations are available for downloading from the BIPM server [3].

The HBM presentation pointed out that foil type strain gauge transducers are most accurate for torque and force measurement and that using measuring bodies from steel and titanium allows measurement of very high force and torque values. HBM described the advantages of offering complete measuring chains to the user. HBM pointed out that, eventually, the dynamic behavior of the complete application system needs to be described while good knowledge of the dynamic behavior of the components (transducers, DAQ units) is the first essential step in the right direction. Subsequently, these components were specified in the project's [4] different work packages. Major conclusions of the workshop were that measuring chains implemented at national level as well as reference transducers have to be as effective as possible and, at industrial level, above all affordable. We were proud to be able to contribute to an overall picture that was created for the first time ever.

The event attracted an international audience and participants developed task lists and further discussed these issues in breakout sessions, contributing to the conclusions drawn at the workshop.To name only a few of the approximately 60 participants from 25 countries' NIMs: France (LNE), China (NIM), United Kingdom (NPL), Germany (PTB), USA (NIST), Japan (AIST), Italy (IMGC), Netherlands (VSL), Spain (CEM), Sweden (SP), Seychelles (NML), Kenya (KBS), Bosnia Herzegowina (IMBIH), Korea (KRISS), Taiwan (ITRI-CMS), Chile (IDIC), Mexico (CENAM), Singapore (NMC), Poland (GUM), Malaysia (SIRIM), Austria (BEV), Switzerland (METAS), Ukraine (Urkme), Egypt (NIS) and Brazil (INMETRO).

In the further course of the project a *Workshop on Analysis of Dynamic Measurements* took place in Torino, Italy in early 2014. It focused not only on the analysis of dynamic measurements, but also on applications. To name only one presentation, *Analysis of Shock Force Measurements for the Model-based Dynamic Calibration* [5] has shown that the results gained from the model-based dynamic calibration of market-relevant (and most of them HBM) force transducers are quite encouraging.

4 Progress Through Exchange of Information

Of course, experts from HBM went to Braunschweig for meetings and experiments in the specific fields during the project. Still, what I want to highlight here is the visit of a PTB working

Participants of the "8th Workshop on Analysis of Dynamic Measurements" May 2014 in Turin, Italy.

group to HBM. HBM's company culture is centered around the concept of dialog for stimulating new approaches and breaking new ground. New impulses come, not only from customers. Moreover, in our endeavor to be innovative we are open to rethinking fundamental aspects. For this reason, it was very much welcomed that the PTB project working group made it possible to come to HBM. More than 20 people, mainly from HBM's R&D department, followed our guests' presentations with keen interest. And, indeed, who could better convey the idea of dynamic calibration than the presentations of our guests Dr. Thomas Bruns, Dr. Michael Kobusch and Dipl.-Ing. (FH) Leonard Klaus? The illustration of this new dimension has been very well received by HBM's developing engineers. HBM project participants received lots of positive feedback over the following months. And for the guests, too, it was interesting to see the laboratories and production lines in our factory. Bearing in mind the new approach, we were able to consider the possible outcome and what will be possible in future.

The second day of the visit focused on specific activities and detailed discussions with our experts for force transducers and torque transducers. Here, design ideas and phenomena were discussed.

Also the resulting approaches for analogue and digital data acquisition items of the talks were indeed very concrete. It can be said that they were completely dedicated to the question of how further requirements can be implemented.

HBM T40B as an example of investigated torque transducers in the project.

The greatest progress made in the project was in the field of data acquisition, since PTB is in need of suitable equipment as a basis for proper investigations at the NMI level for carrying out the work packages of the project. Thus the measurement manufacturer, participating as a collaborator in this project, not only had to come up with suitable sensors, but also conditioning amplifiers [6]. It is a fact that all sensors have to be connected to some kind of conditioning amplifier for further processing or display (a *measuring chain*). To ensure traceability of such a measuring chain and also to make its components exchangeable, it is essential to characterize each of the components of a measuring chain (sensor and conditioning amplifier) independently.

It has been shown that conditioning amplifiers need to provide an even, i.e. flat, frequency response (up to a certain cut-off frequency). On the other hand, the industry requires that DAQ systems fit into an increasingly digital environment. However, such commercially available digital conditioning amplifiers do not have a flat frequency response.

HBM U9B as an example of investigated force transducers in the project.

Thus, as a result of the talks, HBM created a DAQ system with an even frequency response that can claim to be dynamically suitable. To achieve this objective, the digital filter functions of an adequate module have been optimized. The MX410B module – a four-channel highly dynamic universal amplifier of the QuantumX DAQ series – meets this requirement and thus proved to be suitable for dynamic calibration. MX410B is a conditioning amplifier that works with direct current (DC) and 4.8 kHz carrier frequency (CF) while at the same time being fast and universal. The full bridge configuration plays an important role for the mechanical quantities considered here such as force, torque and pressure. The module can either be used with DC excitation for maximum dynamics or with distortion-immune carrier-frequency excitation. The module described above thus could fulfil the requirements of the NMIs participating in the project.

HBM QuantumX MX410B, a versatile and dynamically suitable digital conditioning amplifier.

Needed frequency response of a bridge amplifier.

5 Making Research Results Known Worldwide

One important goal of EMRP is to facilitate closer integration of national research programs and to disseminate the newly gathered knowledge, ensuring collaboration between the National Measurement Institutes as well as with industry, thus reducing redundancy and increasing impact. To put it succinctly: The overall goal is to accelerate innovation in Europe.

Today, the internet is a powerful tool for reaching this goal. Therefore, the project consortium has thought about how to transfer this knowledge to an international audience. In the framework of the project, a *Best Practice Guide* has been made available on the website [8] of IND09 *Traceable Dynamic Measurement of Mechanical Quantities* to everyone, on an international basis.

Furthermore, ongoing efforts toward setting up DKD guidelines in Germany, which are currently taken by the DKD Technical Committee *Force & acceleration* played an important role, too. Documents such as *Dynamic Calibration of Uniaxially Stressed Force Measuring Instruments and testing Machines* as well as *Calibration of Measuring Amplifiers for the Dynamic Measurement of Kinematic and Mechanical Variables*, which are going to be implemented in the DKD – R 3-2 Directive, have been worked out in collaboration with HBM. Of course, one day, the development of methods, technologies and standards for these important applications will be required and finally a specific GUM supplement will have to be created.

In the meantime, this topic has been explored in other events organized by HBM, e.g. the torque seminar at MPA (State Material Testing Institute) [7] or our in-house event *HBM@home*, both held in Darmstadt, Germany. Talks presented at these

Lecturers at the torque seminar at MPA (State Material Testing Institute) in Darmstadt.

events made contributions to better traceability from the NMI level to secondary calibration laboratories and further down, so far only established under static conditions. Some of the attendees, from secondary calibration laboratories as well as from industry expressed their great interest in the topic by very detailed questions. For this reason, we will continue to disseminate our knowledge on the new approach, as dynamic traceability, especially for mechanical values, as well as traceability of high nominal force and torque values is a requirement for further successful developments in industry.

Simposio de Metrologia, Queretaro, Mexico, October 2014.

The latest proof of the importance was shown at the *Simposio de Metrologia* in Queretaro, Mexico on the occasion of the 20th anniversary of Mexico's NMI, CENAM in October 2014, where the topic of dynamic calibration was dealt with extensively [9, 10].

6 Conclusions

Traceable dynamic measurements were first required by the automotive industry. However, measurements are performed under dynamic conditions in other applications, too, that are served by our company, such as aerospace, production, transport or process control. In addition, increasingly complex measurement configura-

tions require characterization and implementation of mechanical multi-component measurements. High-speed data acquisition and modelling are necessary to develop advanced dynamic and/or multi-component measurements. Our customers increasingly demand traceability for their dynamic measurements and a clear representation of the corresponding measurement uncertainty.

The development of methods, technologies and standards is required for these important applications. As a collaborator in the EMRP project *Traceable Dynamic Measurement of Mechanical Quantities* [8], we can now evaluate, that this topic is subject to an increasing worldwide interest.

Although encouraging progress has been made in the project, successful exploitation at the industry level still is challenging. One reason for this is the lack of generic mathematical and statistical methods that can be applied effectively and with confidence by industrial end users, in particular, in the reliable evaluation of uncertainties. This lack may still present a barrier for the application and further development of dynamic metrology in industry. For this reason we think further investigations will be necessary, such as stiffness investigations of torque disk design vs. response characteristics or the development of traceability of a dynamic bridge standard for carrier frequency.

Combining dynamic behavior and larger structures could present another challenge. An example of this is wind energy generation. For torque measurement, the kilonewton metre range is by far insufficient, meganewton metre values are rather required, and still conditions are "dynamic"! Therefore, we strive to make further progress in this field, either by joining new projects or through our own investigations.

We are well aware of the fact that the uncertainties of measurement which can be achieved with dynamic calibration, will – for the time being or, in principle, even for all of time – be markedly more significant than those already attained with static measurements today. It is essential that the expectations raised remain realistic, while at the same time reflecting the industry's requirements. Yet, what we offer is – compared to today's ignorance of these influences – real progress and closer to the "truth".

Users in industry are primarily interested in how mechanical quantities act on the test specimen, to what extent measuring body, electronics, and suspension affect the actual loading, and how this has to be accounted for. The "dynamic dimension" is definitely one of the major emerging fields in the industrial metrology of our century and this project has helped to close the gap between the present and future demands of industry and what NMIs and suppliers can offer.

References

[1] C. Rohrbach et al., *Handbook of Electrical Measurement of Mechanical Quantities*, VDI publishing house, Düsseldorf, Germany, pp. 165 ff., 1967.

[2] J. Andrae, W. Nold and G.Wegener, *Traceability of Rotating Torque Transducers Calibrated under Non-Rotating Operating Conditions*, XVII IMEKO World Congress, Dubrovnik, Croatia, 2003.

[3] A. Schäfer, *Challenges in Dynamic Torque and Force Measurement with Special Regard to Industrial Demands*, BIPM Workshop on Challenges in Metrology for Dynamic Measurements, 2012, http://www.bipm.org/ws/BIPM/DYNAMIC/Allowed/Challenges_2012/BIPM_Dynamic_WS_2012_Talk_02_Schafer.pdf (Retrieved: 2015-08-11).

[4] C. Bartoli, M. F. Beug, T. Bruns, S. Eichstädt, T. Esward, L. Klaus, A. Knott, M. Kobusch and C. Schlegel, *Dynamic Calibration of Force, Torque and Pressure Sensors*, IMEKO 22nd TC3, 12th TC5 and 3rd TC22 International Conferences, Cape Town, South Africa, 2014.

[5] M. Kobusch, S. Eichstädt, L. Klaus and T. Bruns, *Analysis of Shock Force Measurements for the Model-based Dynamic Calibration*, 8th International Workshop on Analysis of Dynamic Measurements, Torino, Italy, 2014. http://www.inrim.it/ADM2014/slides/M.Kobusch.pdf (Retrieved: 2015-08-11).

[6] H. Volkers and T. Bruns, *The Influence of Source Impedance on Charge Amplifiers*, XX IMEKO World Congress, Busan, Rep. of Korea, 2012, http://www.imeko.org/publications/wc-2012/IMEKO-WC-2012-TC22-O6.pdf (Retrieved: 2015-08-11).

[7] A. Schäfer, *Entwicklungen zur statischen und dynamischen Messung von Drehmomenten* (*in English: Development Results for Static and Dynamic Torque Measurement*), Werkstofftechnisches Kolloquium Drehmoment am 22. Juli 2014 in der MPA Darmstadt, TU Darmstadt, Germany, 2014.

[8] Project Home Page of EMRP Project IND09 https://www.ptb.de/emrp/ind09.html (Retrieved: 2015-08-11).

[9] R. Hernández, *Retos en la medición dinámica de fuerza y par torsional enfocado a la industria* (*in English: Challenges in the Dynamic Measurement of Force and Torque for Industry*), Oral presentation by MB Instrumentos S.A., HBM distributor at Simposio de Metrología, Queretaro, Mexico, 2014, http://www.cenam.mx/memorias/doctos/SM2014-018.pdf (Retrieved: 2015-08-31).

[10] M. Kobusch, C. Bartoli, M. F. Beug, T. Bruns, S. Eichstädt, T. Esward, L. Klaus, A. Knott, N. Medina and C. Schlegel, *Proyecto de investigación europeo para la medición dinámica de magnitudes mecánicas*, (*in English: European Research Project for the Dynamic Measurement of Mechanical Quantities*); Simposio de Metrología, Queretaro, Mexico, 2014.

Standards and Software to Maximize End-User Uptake of NMI Calibrations of Dynamic Force, Torque and Pressure Sensors: a Follow-Up EMPIR Project to EMRP IND09 "Dynamic"

Sascha Eichstädt*, PTB, and Trevor Esward, NPL

* Dr. Sascha Eichstädt, Working Group "Data Analysis and Measurement Uncertainty", PTB, e-mail: sascha.eichstaedt@ptb.de

The aim of this new project is to maximize uptake by industry end users and the Joint Committee for Guides in Metrology (JCGM) of outputs of EMRP JRP IND09 (*Traceable dynamic measurement of mechanical quantities*) by providing concrete, specific and directed advice on how to make best use of the results of dynamic calibrations provided by NMIs.

The project's primary supporter is Rolls-Royce who recognize that dynamic measurements are a key class of problems for high-value manufacturing and are providing data from measurements of unsteady pressure and vibration for the project team to demonstrate the methods developed in EMRP project IND09 in action.

Many applications of the measurement of quantities such as force, torque and pressure are dynamic, i.e. the measurand shows a strong variation over time. Transducers are in most cases calibrated by static procedures owing to a lack of commonly accepted procedures or documentary standards for the dynamic calibration of mechanical sensors. However, it is well known that mechanical sensors exhibit distinctive dynamic behaviour that shows an increasing deviation from static sensitivity characteristics as frequency increases. This lack of dynamic calibration standards also applies to the electrical conditioning components of the measurement chain.

The key output of JRP IND09 was the establishment of primary and secondary NMI-level traceability for the mechanical quantities; dynamic force, dynamic torque and dynamic pressure. However, effective dissemination of dynamic calibrations requires specific advice to be provided to industrial end users on how to use calibration results to correct measurements for dynamic effects and to demonstrate compliance with the *Guide to the expression of uncertainty in measurement*. Although JRP IND09 (i) developed general dynamic models for the complete calibration measurement chain, (ii) developed procedures for uncertainty evaluation in line with uncertainty evaluation for static measurements, and (iii) established general procedures for correcting measurements for dynamic effects, these were not able to be embodied in documentary standards and international guidance documents or in software that can be used in industrial applications to correct measurements and provide GUM-compliant uncertainty evaluations during the lifetime of the project.

Calibration certificates and associated information provided for dynamic quantities by NMIs and accredited calibration laboratories can take several forms, such as parameterized models of the sensors and measuring systems that are calibrated, or frequency response data that describes the amplitude and phase response of the calibrated system as a function of frequency. In addition, sensors alone may be calibrated, so that the end user has to understand how the remainder of the measuring system (amplifiers, filters, digital acquisition systems) affects the performance of the calibrated system.

The calibration methods may also be based on a variety of input signals, sine waves, chirps, steps and impulses, and the choice of signal determines what calibration information may be obtainable and how it may be used. Therefore, industrial end users require (i) guidance on what calibration information to request from NMIs and accredited calibration laboratories, (ii) guidance on how to use this information in their own dynamic measurement applications to ensure compliance with the GUM, and (iii) software that demonstrates the guidance in action.

The specific technical objectives of this project are concerned with providing detailed practical guidance in measurement uncertainty evaluation for industrial end users of the outputs from JRP IND09:

- To provide written advice and guidance to end users, that demonstrates (by means of case studies applied to end-user data) methods to evaluate reliable estimates of dynamic mechanical quantities and their associated uncertainties, taking into account the various forms that calibration results may take as well as correlation effects.

- To make publicly available, validated and tested software for industrial end users to implement the methods described in point 1 above.

- The project will undertake two activities, one associated with each of the project's objectives.

- The preparation and submission of a paper to Metrologia (the main international metrology journal) that describes the application of the methods developed in JRP IND09 to industrial end-user data made available by two key JRP IND09 stakeholders, Rolls-Royce plc and Hottinger Baldwin Messtechnik GmbH (HBM). The data will be for quantities studied in JRP IND09 (dynamic force, torque and pressure). The Metrologia paper will also be used as the basis for input to JCGM Document 103 on building and using measurement models and to Document 110 giving examples of uncertainty evaluations in metrology. Both JCGM documents are currently in the early stages of preparation.

- The production, validation and testing of software that demonstrates the methods developed in JRP IND09 in action on end-user data as well as the production of case study material for inclusion in the publications/contributions in the first activity. The software will be made available for public downloading, therefore marketing and end-user awareness activities will be undertaken by means of targeted end-user emails and the use of the PTB and NPL public websites to advertise the software.

These activities align directly with the identified needs of the end-user, who requires specific guidance on how to apply the outputs of JRP IND09: to their own measurements of dynamic effects in engines, and to their selection of suitable sensors so as to establish confidence in their measurement results; to be able to show that they comply with best practice in uncertainty evaluation in accordance with the GUM; and to understand how the deconvolution and correction algorithms needed for this purpose can be embodied in validated software.

The project will also create impact by enabling efficient application of the methods developed in JRP IND09 by disseminating software that demonstrates the methods in action on industrially relevant example data, to industry end users and through the public websites of NPL and PTB.

In the longer term, the outputs of the project will assist high-value manufacturing in the optimization of products and processes where dynamic measurements are necessary. To quote Rolls-Royce itself, "As companies strive to reduce margins even further to optimize performance, costs and reliability, it becomes more important to quantify the uncertainties involved rigorously and to be able to demonstrate metrological traceability of the resulting data".

Figure 1 shows the effect of ignoring dynamic effects. It shows how the use of a statically calibrated sensor produces erroneous results, which becomes evident when compared with the results obtained by a dynamically calibrated sensor. The project will ensure that end users are able to correct measurements for dynamic effects and thus produce good estimates of the underlying dynamic signal.

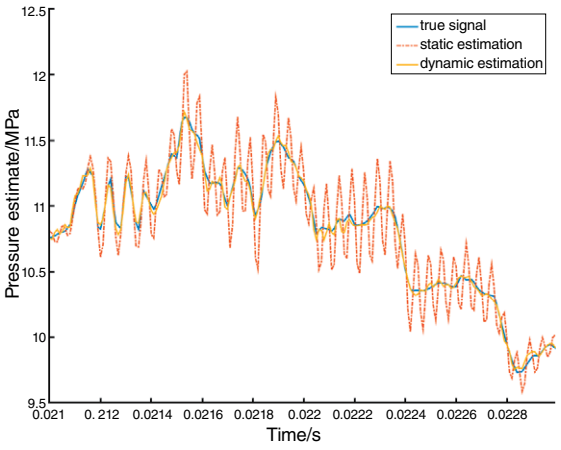

Figure 1:
Estimating the value of a dynamic signal: effect of ignoring the dynamic properties of a measuring system compared with taking dynamic effects into account.

Flow Cytometry

Reference Procedure for the Measurement of Stem Cell Concentrations in Apheresis Products

Jörg Neukammer*[1], Martin Kammel[1], Jana Höckner[2], Andreas Kummrow[1], Andreas Ruf[2]

[1]Physikalisch-Technische Bundesanstalt, [2]Klinikum Karlsruhe

* Dr. rer. nat. Jörg Neukammer, Working Group "Flow Cytometry and Microscopy", PTB, e-mail: joerg.neukammer@ptb.de

In May 2015, the original version of this article "Referenzverfahren zur Messung von Stammzellkonzentrationen" was published in the special section on flow cytometry in BIO*spektrum* 03.15, 294–297, ISSN 0947-0867, DOI: 10.1007/s12268-015-0577-8, © Springer-Verlag 2015.

Reference measurement procedures are indispensable for the reliable determination of blood cell concentrations since medical diagnosis, the initiation of a therapy, and the control of blood products are often based on concentration limits of specific cell subpopulations. We have developed a reference procedure for the direct determination of CD34⁺ cell concentrations. In the same measurement, the two established routine protocols, i.e. the relative enumeration with respect to calibration particles or to leukocytes, are simultaneously applied.

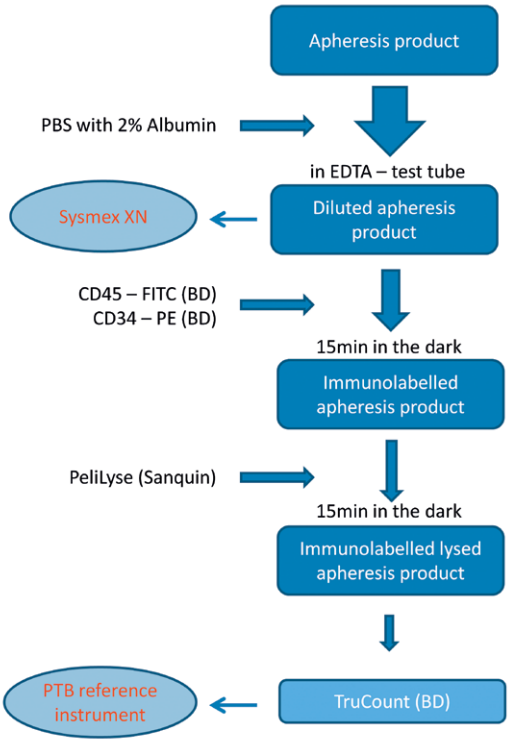

Figure 1:
Sample preparation for the determination of the CD34⁺ cell concentration with PTB's reference instrument. For direct comparison with the one-platform method, the sample was filled into a tube containing TruCount™ calibrator particles; for the assessment according to the two-platform method, the leukocyte concentrations are required which have previously been measured with a hematology analyzer (Sysmex XN).

The transplantation of haematopoietic stem cells is an increasingly frequent method of treating severe diseases. The concentration of CD34+ cells is measured as indicator for the haematopoietic stem cells collected by peripheral blood stem cell harvest. To achieve successful treatment, a dose of at least 4×10^6 viable CD34⁺ cells per kg body weight of the recipient is aimed at for allogenic transplantations [1]. In this context, flow cytometric cell counting is indispensable to determine the CD34⁺ cell dose of a stem cell product and, thus, for the qualification of the products and for their quality assurance. Reference measurement procedures allow the assessment of routine procedures. In the following, we will describe the application of the reference measurement procedure for the direct determination of the CD34⁺ cell concentration. The samples were prepared in such a way that the results of the two routine procedures, which are designated as the one-platform and the two-platform method, are both obtained from the data measured with the reference instrument.

Routine Procedure: One-platform and Two-platform Method

A specific immunological staining with the antibodies against CD34 and CD45 allows the identification of CD34⁺ cells [2] and leukocytes. The relative measurement of CD34⁺ cells compared to the number of leukocytes, one of the routine procedures used, is designated as the two-platform method since, in addition to an optical flow cytometer, a further platform (usually a haematology analyzer) is required. In contrast to this, the one-platform method is based on fluorescent particles as calibrators which are added to the measurement suspension. The number of CD34⁺ cells is determined relative to the number of these fluorescent

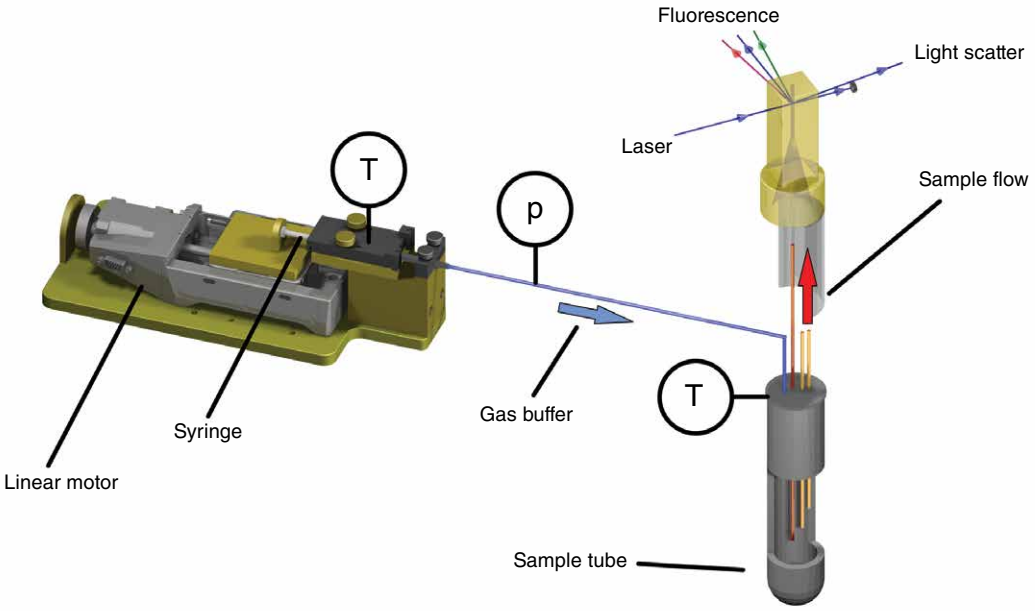

Figure 2:
Exact volume dosing by means of a gravimetrically calibrated syringe. The syringe plunger generates an increased pressure of the air cushion onto the sample which is, in turn, injected into the flow channel. Temperature sensors (T) and pressure sensors (p) are used to ensure that no changes in the steady-state conditions occur during the measurement.

particles. To derive the $CD34^+$ cell concentration in the case of the two-platform method, the leukocyte concentration must be known and in the case of the one-platform method, the concentration of the calibrator is needed.

Preparation for the Comparison of the Reference Procedure with the Routine Procedures

In order to measure concentrations with the reference procedure and with the two routine procedures simultaneously, first of all, the leukocyte concentration needed for the two-platform method was determined by a haematology analyser. For this purpose, the apheresis product was appropriately diluted (see figure 1). For staining, the pre-diluted apheresis product is incubated for 15 minutes with the antibodies against CD34 and CD45. The fluorochromes used were fluorescein isothiocyanate (FITC) and phycoerythrin (PE). After staining, the erythrocytes were lysed. For application of the one-platform method, the samples were filled into TruCount™ tubes containing a known number of calibrator particles before being measured with PTB's reference instrument. The subsequent measurement yields the concentration of the $CD34^+$ cells from (1) their direct counting and from the determination of the sample volume, (2) from their relative number compared to the number of CD45-positive leukocytes (the two-platform method), and (3) from their number relative to the number of the calibrator particles (the one-platform method).

Metrological Traceability with Reference Procedures

Compared to routine procedures, reference measurement procedures provide higher measurement accuracy as well as, i.e. measured values that are as close as possible to the true quantity value. Since they are more time-consuming, they are reserved for certain applications such as the determination of target values in round robin tests for external quality assurance in laboratory medicine [3]. One example is the determination of the concentration of red blood cells [4], for which the reference measurement procedure is described in a national standard [5]. Reference measurement procedures are also used to assign reference values to calibrators and to ensure traceability to (derived) SI units as described in ISO 17511 [6]. The traceability chain includes calibrators and a reliable internal quality assurance on the part of the clinical users. Round robin tests and comparisons of reference measurement values with values determined in clinical routine thus allow the whole traceability chain to be validated – provided that the end user achieves the value of the reference measurement procedure within the defined evaluation limits [3].

Reference Measuring Instrument

Currently, there are no commercial flow cytometers or haematology analysers available by which the reference measurement values can be determined. The reference flow cytometers [4] developed at PTB for the determination of target values for round robin tests with regard to the Complete Blood Count (CBC) and the reference procedure which is based on a dilution series are not suited for use in a clinical laboratory. To use reference measurement procedures also in routine applications, a commercial flow cytometer (Partec CyFlow ML) has been equipped with the sample dosing device depicted in figure 2. The volume is measured by means of a linear motor-driven syringe which is gravimetrically calibrated [7].

The increase in pressure due to the movement of the piston of the syringe causes the sample to be injected into the flow cell of the optical flow cytometer through a cannula. The pressure p and the temperature T of the gas buffer are recorded during the measurement. For the volume determination, a relative measurement uncertainty of smaller than 0.25 % has been achieved when injecting 200 µL. Another modification affects the direct connection between the sample and the flow cell using a platinum/iridium cannula. In routine instruments, tubings are used which prevent the accurate measurement of the volume and may lead to haemolysis and losses due to adhesion.

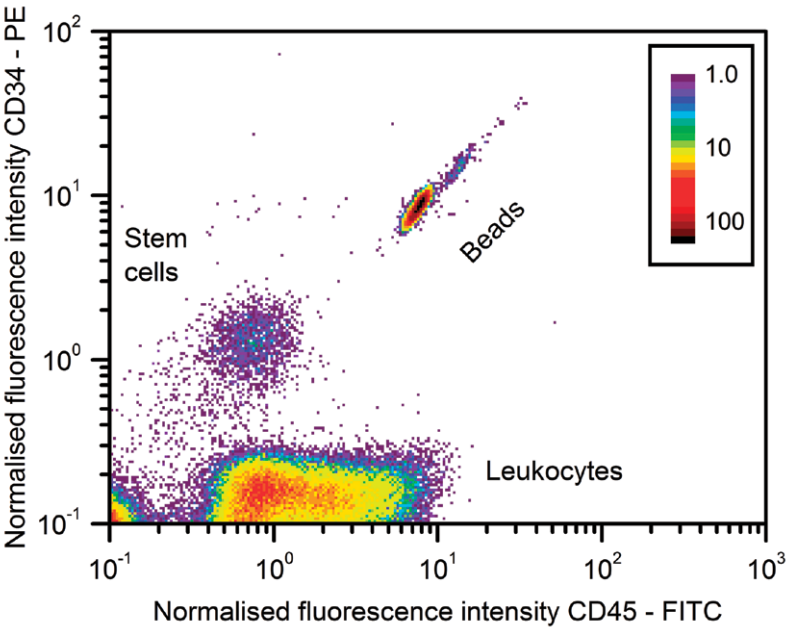

Figure 3:
Fluorescence scatter diagram for the counting of the CD34⁺ cells. At the same time, the number of leukocytes and the number of calibrator particles are registered. In this way, the results of the direct reference measurement can be compared with the relative measurements of the one-platform and of the two-platform method.

Results and Discussion

Figure 3 shows a typical result of a measurement of CD34⁺ cells. In the fluorescence scatter diagram, the normalized intensity of the CD34-PE fluorescence is plotted against the CD45-FITC fluorescence. The figure shows three clusters that correspond to the CD34⁺ cells, the leukocytes and the calibrator beads, respectively. The value obtained with the reference method for the concentration C_{RMV}= (245 ± 6) µL^{-1} results from the number of CD34⁺ cells and from the volume measurements. From the relative number of leukocytes, we obtain the value for the two-platform method C_{2P} = (258 ± 46) µL^{-1}. The concentration of C_{1P} = (238 ± 12) µL^{-1}, based on the one-platform method, follows from the ratio of the number of CD34⁺ cells to the number of calibrator particles. The results are in good agreement with each other.

The measurement uncertainties, however, differ drastically. In the case of the reference method, the uncertainty of 2.5 % is determined by the accuracy of the volume measurement and by the counting statistics. In the case of the two-platform method, the measurement uncertainties of the leukocyte measurements contribute considerably to the total uncertainty and, in the worst case, amount to 18 %, since such deviations from the target values for leukocyte measurements are admissible in external quality assurance [3]. In the case of the one-platform method, the measurement uncertainty of the number of calibrator beads adds to the statistical uncertainties. For the batch of TruCount™ tubes used, we determined a contribution caused by the calibrator of 2.1 %.

Our results demonstrate the use of a reference procedure for CD34⁺ cell counting in a clinical laboratory. When measuring the volume directly, the measurement uncertainties were lower compared to relative measurements based on the one-platform or the two-platform method. We are currently carrying out investigations comparing the reference method with the established one-platform and two-platform methods on fresh and on cryogenically preserved apheresis products using different calibrators. In addition, the applicability of the results to routine devices of various manufacturers is also tested within the scope of these experiments. This aims to quantify the measurement uncertainties and to determine the deviations from the reference measurement value in the clinically relevant concentration range, in order to validate the best-suited method for routine measurements.

Acknowledgements

We would like to thank Ms. Nicole Bock and Ms. Dagmar Oehmichen for their support in carrying out the experiments. These activities were funded by the BMWi promotion programme "Transfer of Research & Development (R & D) by means of standardization" and by the European Metrology Research Programme (EMRP) SIB-54, 2012 "BioSITrace". The EMRP is jointly funded by the EMRP participating countries within EURAMET and the European Union.

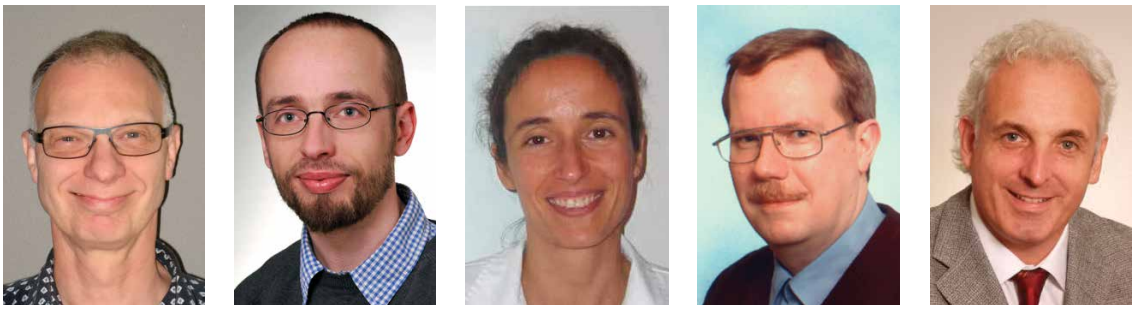

Jörg Neukammer, Martin Kammel, Jana Höckner, Andreas Kummrow, Andreas Ruf (from left to right)
At the Physikalisch-Technische Bundesanstalt, reference measurement procedures for the determination of the concentration of cells in body fluids are developed in the Working Group "Flow Cytometry and Microscopy" (Head of WG: Dr. Jörg Neukammer). The investigations on the determination of the $CD34^+$ cell concentrations were carried out in the Department for Blood Transfusion and Haematostaseology at Klinikum Karlsruhe (Head of Department: Associate Professor Dr. med. Andreas Ruf).

References

[1] Bundesärztekammer (2014) Richtlinie zur Herstellung und Anwendung von hämatopoetischen Stammzellzubereitungen. Dtsch Arztebl 111, doi: 10.3238/arztebl.2014.rl_haematop_sz01

[2] Sutherland DR, Anderson L, Keeney M et al. (1996) The ISHAGE guidelines for CD34+ cell determination by flow cytometry. J Hematotherapy 5: 213–226

[3] Bundesärztekammer (2014) Richtlinie der Bundesärztekammer zur Qualitätssicherung laboratoriumsmedizinischer Untersuchungen. Dtsch Arztebl 111: A1583–A1618

[4] Kammel M, Kummrow A, Neukammer J (2012) Reference measurement procedures for the accurate determination of cell concentrations: present status and future developments. J Lab Med 36: 25–35

[5] Deutsches Institut für Normung 1994 Haematology; determination of the concentration of blood corpuscles in blood; determination of the concentration of erythrocytes; reference method. DIN 58932-3

[6] Deutsches Institut für Normung 2003 In vitro diagnostic medical devices. Measurement of quantities in biological samples. Metrological traceability of values assigned to calibrators and control materials EN ISO 17511

[7] Reitz S, Kummrow A, Kammel M et al. (2010) Determination of micro-litre volumes with high accuracy for flow cytometric blood cell counting. Meas Sci Technol 21: 074006

Correspondence addresses:

Dr. rer. nat. Jörg Neukammer
Head of Working Group
"Flow Cytometry and Microscopy"
Department "Medical Physics and Metrological Information Technology"
Physikalisch-Technische Bundesanstalt
Abbestraße 2–12
D-10587 Berlin
Phone: +49 (0)30 3481-7241
Fax: +49 (0)30 3481-7505
joerg.neukammer@ptb.de

Associate Professor Dr. med. Andreas Ruf
Medical Director of the Department for Transfusion Medicine and Haemostaseology
Städtisches Klinikum Karlsruhe gGmbH
Moltkestraße 90
D-76133 Karlsruhe
Phone: +49 (0)721 974-1701
Fax: +49 (0)721 974-1709
andreas.ruf@klinikum-karlsruhe.de

PTB mitteilungen

Imprint

The PTB-Mitteilungen are the metrological specialist journal and the official information bulletin of the Physikalisch-Technische Bundesanstalt. As a specialist journal the PTB-Mitteilungen publish original scientific contributions and general articles on metrological subjects from the areas of activities of the PTB. The individual volumes are focused on one subject. The Mitteilungen have a long tradition dating back to the beginnings of the Physikalisch-Technische Reichsanstalt (founded in 1887).

Publisher
Fachverlag NW in der
Carl Schünemann Verlag GmbH
Zweite Schlachtpforte 7
28195 Bremen
Web: www.schuenemann.de
Email: info@schuenemann-verlag.de

Editor
Physikalisch-Technische Bundesanstalt (PTB),
Braunschweig and Berlin
Postal address:
Postfach 33 45,
38023 Braunschweig
Delivery address:
Bundesallee 100,
38116 Braunschweig

Editorial Staff/Layout
Press- and Information Office, PTB
Sabine Siems
Dr. Dr. Jens Simon (Editor in Chief)
Dr. Thomas Bruns
Dr. Michael Kobusch
(Scientific Editors)
Phone: (05 31) 592-82 02
Fax: (05 31) 592-30 08
Email: sabine.siems@ptb.de

Reader and Subscription Service
Karin Drewes
Phone: (0421) 369 03-56
Fax: (0421) 369 03-63
EMail: drewes@schuenemann-verlag.de

Anzeigenservice
Karin Drewes
Phone: (0421) 369 03-56
Fax: (0421) 369 03-63
Email: drewes@schuenemann-verlag.de

Frequency of publication and prices
The PTB-Mitteilungen are published four times each year. An annual subscription costs € 39.00, one issue costs € 12.00, plus postage costs. The journal can be obtained from bookshops or from the publisher. Cancellations of orders must be made to the publisher in writing at least three months before the end of a calendar year.

Printed in Germany ISSN 0030-834X

The technical articles from this issue of the PTB-Mitteilungen are also available online at:
doi: 10.7795/310.20150299

Bundesministerium
für Wirtschaft
und Energie

The Physikalisch-Technische Bundesanstalt, Germany's national metrology institute, is a scientific and technical higher federal authority falling within the competence of the Federal Ministry for Economic Affairs and Energy.

The Physikalisch-Technische Bundesanstalt, Germany's national metrology institute, is a scientific and technical higher federal authority falling within the competence of the Federal Ministry for Economic Affairs and Energy.

Physikalisch-Technische Bundesanstalt
Braunschweig and Berlin
National Metrology Institute

Bundesallee 100
38116 Braunschweig, Germany

Press and Information Office

Phone: 0531 592-3006
Fax: 0531 592-3008
Email: presse@ptb.de
www.ptb.de